MARTIN-LUTHER-UNIVERSITÄT
HALLE-WITTENBERG

# Advancing Anodic Electro-Fermentation

## Insights into Energy Management, Substrate Utilization, and Redox Mediation in *Pseudomonas putida* within a Bio-electrochemical System

Dissertation

zur Erlangung des Doktorgrades der Naturwissenschaften (Dr. rer. nat.)

der

Naturwissenschaftlichen Fakultät I - Institut für Biochemie und Biotechnologie

der Martin-Luther-Universität Halle-Wittenberg,

vorgelegt

von Frau Laura Pause

Verteidigt am 24.06.2025

Gutachter*innen:
Prof. Dr Jens O. Krömer
Prof. Dr. Bruno Bühler
Prof. Dr. Miriam Agler-Rosenbaum

# Acknowledgments

This thesis represents not only my research but also the culmination of years of guidance, collaboration, and encouragement. I am deeply grateful to everyone who has contributed to this journey in various ways.

Firstly, I would like to express my sincere gratitude to my doctoral advisor, Prof. Jens O. Krömer, for allowing me to be a part of your research group and for your guidance and mentorship throughout this project. Your expertise and encouragement helped me grow as a researcher and pushed me to achieve this milestone.

I would also like to extend my heartfelt thanks to Dr. Bin Lai for your insightful feedback and collaborative spirit. Your diverse perspectives helped shape the direction of this research and tackle every problem that arose.

I am particularly grateful to the department heads who guided our research environment during a period of restructuring. Throughout my PhD journey, I was fortunate to be part of three different departments. I sincerely thank Prof. Andreas Schmid for fostering an engaging and collaborative start to my research in SOMA, Prof. Hauke Harms for steering the UMB department through the period of transition, and Prof. Katja Bühler and Prof. Falk Harnisch for their leadership and commitment to strengthening the research culture during the final stages of my PhD in MIBITECH. Your dedication and efforts ensured I could continue my work seamlessly despite the institutional changes.

I would also like to thank Prof. Bruno Bühler and Prof. Miriam A. Rosenbaum for agreeing to review my thesis.

Special thanks go to my collaborators. I am especially thankful to Dr. (!) Anna Weimer for being the best collaboration partner I could wish for. Sharing the various hurdles of this project made it so much easier to stay on track. The time we worked together in the lab in Saarbrücken was so much fun and gave me fresh motivation even beyond our time together. Furthermore, I would like to thank Miriam A. Rosenbaum, Dr. Santiago Boto and Dr. Christine Vogler for the coordination of our SPP group and the organisation of various events with fellow researchers. These meetings were always a spark of inspiration to me.

I am also immensely grateful for the friendship and support from my colleagues, who made long days in the lab so much more enjoyable. Especially my ducklings Nina, Mahir, and Tilman, my office mate Hans, and the ice bathing, coffee/lunch break, volleyball, table tennis, and table soccer crews made my PhD time wonderful and helped me to maintain a healthy work-life-balance. I'm so thankful to have found so many amazing people in my workplace.

I would also like to acknowledge the technical and administrative staff at SOMA, UMB, and MIBITECH for their expertise and assistance, whether troubleshooting daily lab problems or ensuring a smooth research environment.

Last but not least, a very special thanks to my family and friends for their love, support, and encouragement. To my parents, Carsta and Ulrich, the home and upbringing you've provided for me were the base for everything I've achieved, and your support in every phase of my life means everything to me.

# Content

## Summary

One of the most urgent challenges of our time is tackling the increasingly severe changes in the climate of the earth. The transition from a fossil fuel-based economy towards more sustainable alternatives is essential to address this global crisis. One strategy on the path to a greener future is the replacement of traditional chemical production processes with the synthesis of valuable products by microbial systems. These biotechnological production processes have significantly lower environmental footprints, but their success depends strongly on the choice of the right microbial hosts. An ideal host needs to fulfill several characteristics, like efficient substrate utilization, robust metabolic performance, and resilience to environmental stresses. *Pseudomonas putida* (*P. putida*) has emerged as a highly promising candidate due to its versatile metabolism and remarkable stress tolerance. This microorganism can process a wide range of substrates and withstand exposure to solvents, heavy metals, organic pollutants, and other environmental stressors—making it an ideal workhorse for industrial applications.

However, the obligate aerobic nature of *P. putida* presents a significant limitation for large-scale biotechnological processes. The dependency on oxygen does not only increases operational costs but also restricts reactor scalability. Overcoming this limitation is crucial for unlocking the full potential of *P. putida* in sustainable bioprocesses. An innovative approach to address this challenge is anodic electro-fermentation via bio-electrochemical systems (BES). This technology replaces the terminal electron acceptor oxygen with an electrode (anode) under anaerobic conditions, enabling efficient substrate conversion with reduced energy input. BES offers a cost-effective and scalable solution for industrial biotechnology.

The first part of this thesis investigates anaerobic glucose uptake in *P. putida* KT2440 within a BES. The research focused on how *P. putida* survives and metabolizes glucose under anode-driven anaerobic conditions provided by the BES. *P. putida* possesses three native glucose uptake pathways, each with distinct energy and redox requirements. Gene deletion mutants were utilized to isolate individual uptake pathways and understand their contributions under electro-fermentative conditions. The findings revealed that while these mutants displayed significant differences in sugar consumption, current output, and product formation, the stoichiometry of glucose uptake was not a limiting factor. Interestingly, approximately half of the acetate produced in the cytoplasm originated from carbon present in the inoculation biomass rather than the substrate. These results suggest that the low carbon turnover rates in BES are likely due to energy limitations or a yet-to-be-identified oxygen-dependent regulatory mechanism rather than constraints in glucose uptake pathways.

Building on these findings, a systems biology approach was employed in subsequent experiments to unravel the metabolic and physiological adaptations of *P. putida* in BES. Using multi-omics analyses led to identifying critical pathways and regulatory mechanisms involved in the adaptation of the bacterium to anoxic and anode-driven conditions. Notably, the bacterium reorganizes its carbon fluxes, enhances β-oxidation, and utilizes alternative ATP and NAD(P)H generation pathways to address energy limitations. A key discovery was the involvement of polyphosphate (polyP), an energy storage compound, in supporting energy metabolism under BES conditions. The upregulation of exopolyphosphatase during the later stages of BES indicated the role of polyP in energy management. Advanced analytical techniques, including scanning electron microscopy, energy-dispersive X-ray spectroscopy, and Raman spectroscopy, provided compelling evidence for polyP utilization during BES fermentation to compensate for energy deficiencies.

Additional experiments explored the role of redox mediators in facilitating electron transfer from *P. putida* to the anode. This research compared the BES performance of *P. putida* using both an artificial and a natural redox mediator. The artificial mediator ferricyanide (FeCN) exhibited superior electron transfer rates and faster substrate-to-product turnover, making it an excellent choice for processes requiring rapid product formation. However, the use of an externally added mediator increases operational costs and necessitates recycling, which limits its feasibility for large-scale or resource-constrained applications. In contrast, the natural mediator phenazine-1-carboxylic acid (PCA), produced endogenously by a genetically engineered strain of *P. putida*, offered a more sustainable and cost-effective solution for processes where slower but more stable fermentation is acceptable. However, the need to supplement antibiotics to maintain PCA production is a significant drawback and limits both sustainability and process efficiency. It is, therefore, essential to find a balance between efficiency, costs, and sustainability when it comes to selecting mediators for BES applications.

The second part of the study evaluated quinone-based redox mediators, including 1,4-benzoquinone (BQ), duroquinone (DQ), and anthraquinone-2,6-disulfonate (AQDS), for their potential in BES applications. Among the tested mediators, BQ demonstrated the highest electron transfer rates and superior substrate conversion rates. However, its low stability limits its use in continuous BES processes. In contrast, DQ and AQDS were more stable, but their redox potentials were found to be incompatible with the electron transfer chain of *P. putida*, resulting in poor BES performance. These results emphasize the importance of tailoring redox mediator properties to align with the specific requirements of BES systems and the metabolic characteristics of the microbial host. However, the accelerated metabolic rates observed in *P. putida* with BQ demonstrated the great potential of anodic electro-fermentation with this versatile microbe.

This thesis provides valuable insights into the changed physiology as well as survival strategies of *P. putida* under anaerobic and anode-driven conditions in a BES. Open questions related to substrate utilization, electron transfer, and energy limitations during anodic electro-fermentation were addressed, and the gained insights will help advancing BES as a cost-effective and scalable solution for sustainable biotechnological production.

# Zusammenfassung

Eine der dringendsten Herausforderungen unserer Zeit ist die Bewältigung der zunehmend drastischen Veränderungen des Erdklimas. Der Übergang von einer auf fossilen Brennstoffen basierenden Wirtschaft zu nachhaltigen Alternativen ist von entscheidender Bedeutung, um diese globale Krise zu entschärfen. Unter den Strategien, die diesen Übergang vorantreiben, ragen biotechnologische Produktionsprozesse als Eckpfeiler einer grüneren Zukunft heraus. In einem solchen nachhaltigen Rahmen würde die herkömmliche chemische Produktion durch biotechnologische Systeme ersetzt, die Mikroorganismen zur Synthese wertvoller Produkte mit deutlich geringeren Umweltauswirkungen nutzen.

Der Erfolg der Biotechnologie hängt stark von der Auswahl der richtigen mikrobiellen Wirte ab. Diese Wirte müssen bestimmte Eigenschaften aufweisen, darunter eine effiziente Substratnutzung, robuste Stoffwechselfähigkeiten und Widerstandsfähigkeit gegenüber Umweltbelastungen.
*Pseudomonas putida* (*P. putida*) hat sich aufgrund seines vielseitigen Stoffwechsels, der es ihm ermöglicht, eine breite Palette von Substraten zu verarbeiten, und seiner bemerkenswerten Robustheit als vielversprechender Kandidat erwiesen. Dieses Bakterium zeigt eine außerordentliche Toleranz gegenüber Lösungsmitteln, Schwermetallen, organischen Schadstoffen und anderen Umweltbelastungen, was es zu einem idealen Kandidaten für industrielle Anwendungen macht.

Eine wesentliche Einschränkung von *P. putida* ist jedoch seine obligate aerobe Natur, die für biotechnologische Prozesse im großen Maßstab eine Herausforderung darstellt. Die Abhängigkeit von Sauerstoff erhöht nicht nur die Betriebskosten, sondern schränkt auch die Skalierbarkeit von Reaktoren ein. Diese Einschränkung muss unbedingt behoben werden, um das volle Potenzial des Bakteriums für nachhaltige Bioprozesse zu erschließen. Eine innovative Lösung ist der Einsatz der anodischen Elektrofermentation über bioelektrochemische Systeme (BES). Diese Technologie bietet einen alternativen terminalen Elektronenakzeptor, der den Sauerstoff unter anaeroben Bedingungen durch eine Elektrode (Anode) ersetzt. Die BES-Technologie ermöglicht eine effiziente Substratumwandlung mit geringerem Energieaufwand und bietet eine kostengünstige und skalierbare Lösung für die industrielle Biotechnologie.

Im ersten Teil dieser Arbeit wurde die anaerobe Glukoseaufnahme in *P. putida* KT2440 in einer BES untersucht. Es wurde untersucht, wie *P. putida* unter anaeroben und anodengetriebenen Bedingungen im BES überlebt und Glucose zu Produkten umsetzt. Das Bakterium verfügt über drei native Glukoseaufnahmewege mit unterschiedlichen Energie- und Redoxanforderungen. Es wurden Gen-Deletionsmutanten verwendet, um die Nutzung der einzelnen Aufnahmewege zu erzwingen und ihre

Beiträge unter elektrofermentativen Bedingungen zu verstehen. Die Ergebnisse zeigten, dass diese Mutanten zwar signifikante Unterschiede im Zuckerverbrauch, in der Stromproduktion und in der Produktbildung aufwiesen, die Stöchiometrie der Glukoseaufnahme jedoch kein limitierender Faktor war. Etwa die Hälfte des im Zytoplasma produzierten Acetats stammte aus dem in der Inokulationsbiomasse vorhandenen Kohlenstoff und nicht aus dem Substrat. Diese Ergebnisse deuten darauf hin, dass die niedrigen Kohlenstoff-Umsatzraten in BES eher auf Energiebeschränkungen oder einen noch zu identifizierenden sauerstoffabhängigen Regulierungsmechanismus zurückzuführen sind als auf Beschränkungen im Zusammenhang mit den Glukose-Aufnahmewegen.

Aufbauend auf diesen grundlegenden Erkenntnissen konzentrierten sich die nachfolgenden Experimente darauf, die metabolischen und physiologischen Anpassungen von *P. putida* in BES mit Hilfe eines systembiologischen Ansatzes zu entschlüsseln. Durch Multi-omics-Analysen wurden kritische Stoffwechselwege und Regulationsmechanismen identifiziert, die Aufschluss darüber geben, wie sich das Bakterium an anoxische und anodengesteuerte Bedingungen anpasst. Insbesondere reorganisiert das Bakterium seine Kohlenstoffflüsse, verstärkt die β-Oxidation und nutzt alternative ATP- und NAD(P)H-Erzeugungswege, um Energiebeschränkungen zu überwinden. Eine entscheidende Entdeckung war die Beteiligung von Polyphosphat (polyP), einer Energiespeicherverbindung, an der Unterstützung des Energiestoffwechsels unter BES-Bedingungen. Die Hochregulierung des Proteins Exopolyphosphatase in den späteren Stadien der anodischen Elektrofermentation deutete auf die Bedeutung von polyP im Energiemanagement hin. Fortgeschrittene Techniken wie Rasterelektronenmikroskopie, energiedispersive Röntgenspektroskopie und Raman-Spektroskopie bestätigten die Nutzung von PolyP während der BES-Fermentation als Mechanismus zum Ausgleich des Energiemangels.

Weitere Experimente untersuchten die Rolle von Redox-Mediatoren für den Elektronentransfer von *P. putida* zur Anode. Im ersten Teil dieser Untersuchung wurde die BES-Performance von *P. putida*, unter Verwendung eines künstlichen und eines natürlichen Redox-Mediators, direkt verglichen. Der künstliche Mediator Ferricyanid (FeCN) zeigte überlegene Elektronentransferraten und einen schnelleren Substrat-zu-Produkt-Umsatz, was ihn zu einer hervorragenden Wahl für Prozesse macht, die eine schnelle Produktbildung erfordern. Die Abhängigkeit von einem extern hinzugefügten Mediator führt jedoch zu zusätzlichen Kosten und macht ein Recycling des Mediators erforderlich, was seine Einsatzbarkeit bei groß angelegten oder ressourcenbeschränkten Anwendungen erschwert. Im Gegensatz dazu bot der natürliche Mediator Phenazin-1-Carbonsäure (PCA), der von einem gentechnisch veränderten Stamm von *P. putida* endogen produziert wird, eine nachhaltigere und kostengünstigere Lösung für Prozesse, bei denen eine langsamere, stabile Fermentation akzeptabel ist. Allerdings stellt der Bedarf an Antibiotika zur Aufrechterhaltung der PCA-Produktion einen

erheblichen Nachteil dar, der sowohl die Nachhaltigkeit als auch die Prozesseffizienz beeinträchtigen kann. Diese Ergebnisse unterstreichen die Notwendigkeit, bei der Auswahl von Mediatoren für BES-Anwendungen ein Gleichgewicht zwischen Effizienz, Kosten und Nachhaltigkeit herzustellen.

Im zweiten Teil der Mediator Studie wurden die auf Chinon basierenden Redox-Mediatoren 1,4-Benzochinon (BQ), Durochinon (DQ) und Anthrachinon-2,6-Disulfonat (AQDS) untersucht, um ihr Potenzial für BES-Anwendungen zu bewerten. Der Einsatz von BQ generierte unter den getesteten Mediatoren die beste BES-Performance mit hohen Elektronentransferraten und einer überlegenen Effizienz bei der Substratumwandlung. Seine geringe Stabilität schränkt jedoch seine Anwendbarkeit in kontinuierlichen BES-Prozessen ein. Im Gegensatz dazu wiesen DQ und AQDS eine höhere Stabilität auf. Dennoch waren sie aufgrund ihrer Redoxpotentiale, die mit der Elektronentransferkette von *P. putida* nicht kompatibel waren, ungeeignet, was zu einer schlechten BES-Leistung führte. Diese Ergebnisse unterstreichen, wie wichtig es ist, die Eigenschaften des Redox-Mediators auf die spezifischen Anforderungen von BES-Systemen und die eingesetzten Mikroorganismen abzustimmen, um eine optimale Leistung zu erzielen. Darüber hinaus unterstreichen die beschleunigten Stoffwechselraten von *P. putida*, die mit BQ als Redox-Mediator beobachtet wurden, das vielversprechende Potenzial der anodischen Elektrofermentation mit dieser Mikrobe.

Diese Arbeit trägt zu einem umfassenderen Verständnis darüber bei, wie *P. putida* für die anodische Elektrofermentation nutzbar gemacht werden kann, und bietet Einblicke in metabolische Entwicklungsstrategien und Systemoptimierung. Indem offene Fragen zur Substratnutzung, Elektronentransfer und der Energiebeschränkungen von *P. putida* unter anodengetriebenen und anaeroben Bedingungen geklärt wurden, legt diese Arbeit den Grundstein für die Weiterentwicklung der BES als kosteneffiziente und skalierbare Lösung für eine nachhaltige biotechnologische Produktion.

# Authors Declaration

This dissertation consists of original work conducted by myself and contains no material previously published or written by another person except where due reference has been made in the text. I certify that, to the best of my knowledge, my dissertation does not infringe upon anyone's copyright nor violate any proprietary rights and that any ideas, techniques, quotations, or any other material from the work of other people included in my dissertation, published or otherwise, are fully acknowledged in accordance with the standard referencing practices. The contributions by others to jointly authored works included in this work are duly acknowledged. I have clearly stated the contribution of others to my dissertation as a whole, including data analysis, significant technical procedures, professional editorial advice, and any other original research work used or reported in my work. I declare that this is a true copy of my dissertation, including any final revisions, as approved by my doctorate committee and Martin-Luther-University Halle-Wittenberg, and that this dissertation has not been submitted for a higher degree to any other university or institution. The content of this dissertation is the result of works I have conducted since the commencement of my research higher degree candidature and does not include a substantial part of work that has been submitted to qualify for the award of any other degree or diploma in any university or other tertiary institution.

I acknowledge that an electronic copy of my dissertation must be lodged with the University Library and, subject to the policy and procedures of Martin-Luther-University Halle-Wittenberg, the dissertation be made available for research and study in accordance with the German Copyright Act (Urheberrechtsgesetz, or UrhG) unless a period of embargo has been approved by Martin-Luther-University Halle-Wittenberg. I acknowledge that the copyright of all material contained in my dissertation resides with the copyright holder(s) of that material. Where appropriate I have obtained copyright permission from the copyright holder to reproduce material in this dissertation.

I am aware that the use of machine-generated content does not guarantee its quality and accuracy. I, therefore, affirm that I have only used generating AI tools as an aid and that my own intellectual and creative contribution predominates in this work. I am fully responsible for the adoption of any machine-generated content I have used. I confirm that I have listed all AI-supported tools used and have explained and reflected on their use.

The following AI-supported tools were used to create this thesis:
DeepL for translation assistance, ChatGPT for improvement of text structure, language, and writing style, Consensus for literature research, Grammerly for proofreading and improvement of grammar and spelling

_____

Leipzig, 15.01.2025

# Publication List and Authors' Contribution

Parts of this thesis were published:

1. **Pause, L.**; Weimer, A.; Wirth, N. T.; Nguyen, A. V.; Lenz, C.; Kohlstedt, M.; Wittmann, C.; Nikel, P. I.; Lai, B.; Krömer, J. O. (2024). Anaerobic glucose uptake in *Pseudomonas putida* KT2440 in a bioelectrochemical system. *Microbial biotechnology*. 17. e14375. 10.1111/1751-7915.14375.

LP conducted all bio-electrochemical cultivations and led the data curation and formal analysis. NW carried out genetic engineering and supplied the three KO mutants. AVN conducted the aerobic growth experiments. LP and CL carried out $^{13}C$ labeling measurements via IC-MS. AW conducted the $^{13}C$ labeling measurements via GC-MS. JOK supplied the flux balance analysis. BL and JOK led the visualization. JOK, BL, PIN, and CW conceptualized the project. MK supported with methodology and administration. LP and BL wrote the first draft of the manuscript. All authors reviewed and approved the final manuscript. JK and CW secured funding.

2. Weimer, A.; **Pause, L.**; Ries, F.; Kohlstedt, M.; Adrian, L.; Krömer, J.; Lai, B.; Wittmann, C. (2024). Systems biology of electrogenic *Pseudomonas putida* - multi-omics insights and metabolic engineering for enhanced 2-ketogluconate production. *Microbial cell factories*. 23. 246. 10.1186/s12934-024-02509-8.

LP and AW conducted the bio-electrochemical cultivation for proteome and transcriptome sampling and energy metabolite measurements. The other BES cultivations were done by AW. LP and AW performed the energy metabolite measurements. AW carried out genetic engineering, as well as the remaining intracellular and extracellular analytics and transcriptome analysis. LP performed proteome analysis and data processing. AW and FR conducted polysome profiling and processed and combined the -omics data. AW and MK processed the metabolome data. AW and CW wrote the first draft of the manuscript and prepared all figures. All authors reviewed and approved the final manuscript. BL, JK, and CW conceived and structured the work. JK and CW secured funding.

# List of Abbreviations

| | |
|---|---|
| $^{13}C$ | carbon-13 isotope |
| 2-KG | 2-ketogluconate |
| 2kgaT | 2-ketogluconate transporter |
| ADP | adenosine diphosphate |
| AQDS | anthraquinone-2,6-disulfonate |
| ATP | adenosine triphosphate |
| BES | bio-electrochemical system |
| BQ | 1.4-benzoquinone |
| CaO buffer | sodium cacodylate buffer |
| CoA | coenzyme A |
| DQ | duroquinone |
| ED-EMP cycle | Entner-Doudoroff-Embden-Meyer-Parnas Cycle |
| EDX | energy-dispersive X-ray spectroscopy |
| ETC | electron transport chain |
| $FADH_2$ | flavin adenine dinucleotide |
| FC | foldchange |
| FeCN | ferricyanide |
| GC | gas chromatography |
| glaT | gluconate transporter |
| glcT | glucose transporter |
| HPLC | high-performance liquid chromatography |
| IC | ion chromatography |
| KO | knock out mutant |
| LB | lysogeny broth |
| $Log_2(FC)$ | $Log_2$ fold change |
| MS | mass spectrometry |
| $NAD^+$/NADH | nicotinamide adenine dinucleotide |
| $NADP^+$/NADPH | nicotinamide adenine dinucleotide phosphate (oxidized/reduced) |
| $OD_{420}$ | optical density at 420 nm |

| | |
|---|---|
| $OD_{600}$ | optical density at 600 nm |
| PCA | phenazine-1-carboxylic acid |
| polyP | polyphosphate |
| $PQQH_2$ | pyrroloquinoline quinol |
| p-value | probabilitas (lat. probability) value |
| RE | reference electrode |
| RI | refractive index |
| rpm | revolutions per minute |
| RT | room temperature |
| SEM | scanning electron microscopy |
| SHE | standard hydrogen electrode |
| sp. | species |
| TTN | total turnover number |
| UV-Vis | ultraviolet-visible light |
| WT | wild-type |

# 1. Introduction

## 1.1 Microbial Electrochemical Biotechnology

The interdisciplinary field of microbial electrochemical biotechnology integrates methods and principles from microbiology, electrochemistry, and engineering to investigate the interactions between microorganisms and electrically conductive materials (Schröder*, et al.* 2015). Through extracellular electron transfer, microbial cells can exchange electrons with external electrodes, a process that is particularly significant for developing sustainable technologies to address global energy and environmental challenges. Key applications of microbial electrochemistry include generating electrical power coupled with wastewater treatment (Santoro et al., 2017), producing biofuels or valuable chemicals (Chu et al., 2020), and developing biosensors (Zhai & Dong, 2022).

Bio-electrochemical systems (BES) and electroactive microbes are fundamental to microbial electrochemical biotechnology. In BES, the anode functions as the electron acceptor through oxidation, while the cathode serves as the electron donor through reduction. Electroactive microorganisms can be cultivated on either side of the BES, depending on the goal of the process.

Pioneering research in microbial electrochemical biotechnology began with Potter in 1911, who first measured the electric potential generated by *Escherichia coli* and *Saccharomyces cerevisiae* in a galvanic cell (Potter 1911). Although the output signals were minimal, this initial microbial fuel cell marked the inception of extensive research into microbial electrochemical biotechnology. Microbial fuel cells offer the potential to convert organic wastes into electrical energy by exploiting microbial metabolism. In 1931, Cohen enhanced the generated potential by connecting multiple of these systems in series, creating the first microbial fuel cell stack that generated 2 mA and 35 V (Cohen 1931).

Despite significant advancements, implementing this technology in real-world applications has consistently faced challenges. The primary bottleneck is the oxygen reduction reaction at the cathode, which is hindered by high over-potential and low kinetics (Rismani-Yazdi*, et al.* 2008). Additionally, microbial fuel cells exhibit lower energy output compared to chemical fuel cells and encounter complex and variable conditions when processing real industrial waste streams (Pandey*, et al.* 2016). Furthermore, the kinetics of electroactive bacteria, extracellular electron transfer mechanisms, and biofilm formation on electrodes are not fully understood (Read*, et al.* 2010; Kiely*, et al.* 2011; Dennis*, et al.* 2016).

However, recent developments indicate the potential for commercializing microbial fuel cell technology. Progress in pilot-scale microbial fuel cells, mainly through innovations like modular unit stacking, has demonstrated promise for real-world applications (Hiegemann*, et al.* 2016; Ge; He 2016;

Liang*, et al.* 2018; Lu*, et al.* 2017; Wu*, et al.* 2016). Two ground-breaking examples of microbial fuel cell applications that have successfully transitioned to commercialization are the iMETland system and AQUACYCL. The iMETland project, initiated in 2014 by Abraham Esteve-Núñez, has demonstrated exceptional success in urban wastewater treatment by integrating microbial electrochemical technologies with constructed wetlands (iMETland). This innovative system treats sewage up to ten times faster than conventional methods, generates electricity, and operates without requiring external energy input (Ramírez-Vargas*, et al.* 2019). The concept has been commercialized through a startup called METfilter®, which manages decentralized wastewater treatment systems for small communities across southern Europe (METfilter).

Similarly, AQUACYCL leverages bio-electrochemical wastewater treatment but focuses on industrial high-strength sewage streams. Their system employs a natural microbial consortium capable of processing wastewater streams 7 to 10 times more concentrated than those treatable by traditional methods. AQUACYCL's modular and scalable technology provides a versatile solution for diverse industrial applications, highlighting its adaptability and efficiency (AQUACYCL).

Besides microbial fuel cells, microbial electrochemical biotechnology offers various other technologies, including microbial electrolysis and desalination cells. Microbial electrolysis cells facilitate hydrogen production at the cathode and organic matter oxidation at the anode, requiring less electrical energy than water electrolysis. However, scaling up MECs is challenging due to balancing antagonistic processes at the cathode and anode. Efficient electrolysis requires clean, simple electrolytes with high ionic conductivity and extreme pH values, while microbial processes necessitate complex culture media and neutral pH. Current compromises result in low current densities, which are insufficient for efficient industrial production (Rousseau*, et al.* 2020). Microbial desalination cells combine desalination, wastewater treatment, and electricity generation. Electroactive bacteria oxidize organic matter in wastewater, producing electrons and protons. Electrons generate electric current as they move to the cathode, while protons migrate through an ion-exchange membrane, driving the desalination process. Significant drawbacks include variability in wastewater composition and biofouling of membranes (Zahid*, et al.* 2022).

Another significant application of microbial electrochemical biotechnology is microbial electrosynthesis. Here, carbon dioxide is reduced at the cathode using biocatalysts like acetogenic bacteria to produce valuable chemicals such as acetate, methane, alcohols, organic acids, hydrocarbons, and polymers. In 2015, a broader definition for this technology was proposed, encompassing the production of complex organic matter through electrochemical reactions catalyzed by microbes on both the cathode and anode sides (Schröder*, et al.* 2015). Microbial electrosynthesis is valuable for renewable energy storage, sustainable chemical production, carbon capture, and

bioremediation. However, challenges such as low current density outputs, high overpotentials, and high energy demand persist, making the process expensive. Additionally, ensuring long-term microbial performance and developing cost-effective and durable electrode materials remain critical focus areas (Prévoteau*, et al.* 2020). Opportunities for microbial electrosynthesis improvement include enhancing efficiency through genetically engineered pure cultures with improved electron uptake and metabolic pathways, innovations in material and design, and employing synthetic biology to tailor bacterial strains for optimal adaptation to the applied conditions (Harnisch*, et al.* 2024).

In contrast to microbial electrosynthesis, where the cathode side is used to cultivate microorganisms, in anodic electro-fermentation, the bacteria of interest are grown in the anode chamber of the BES. The aim is to utilize the anode as a terminal electron acceptor for microbial metabolism, regulating redox and energy metabolism to produce value-added products without the need for oxygen. This process will be discussed in detail in the next section.

In summary, microbial electrochemical biotechnology offers promising solutions for sustainable energy and environmental technologies. Continued research and development are essential to overcome existing challenges and fully realize the potential of these innovative systems.

## 1.2 Anodic Electro-Fermentation

The process of energy generation during respiration is called oxidative phosphorylation. Here, electrons travel along an ETC with redox-active proteins from low potentials toward higher potentials. A proton gradient across the membrane builds up due to the thermodynamic energy difference between electron donors and acceptors, which fuels ATP production by the ATP synthase via chemiosmosis (Anraku 1988). Under aerobic conditions, oxygen is the electron acceptor with the highest formal redox potential, leading to the highest energy yields compared to other energy generation strategies.

For biotechnological production, anaerobic processes are often preferred over aerobic ones in specific applications due to their potential for lower operating costs, higher yields, and better volumetric production rates. In aerobic processes, the gas-liquid mass transfer kinetics remains the limiting factor (Weusthuis*, et al.* 2011). The sufficient supply of oxygen requires high energy inputs, which account for up to 20% of all operation costs (Junker*, et al.* 1998) and limits possible reactor sizes (McMillan; Beckham 2017). Additionally, the need for aeration of the bioreactors leads to heat generation and foaming of the medium, necessitating cooling and adding anti-foaming reagents. These measures further increase the costs of aerobic processes (Delvigne; Lecomte 1981). Furthermore, substrate loss through complete oxidation to $CO_2$ in aerobic metabolism and high biomass production lowers product

yields. Redox imbalances caused by insufficient oxygen supply can also result in increased by-product formation (Hannon 2007).

In contrast, anaerobic processes eliminate the need for oxygen supply, significantly reducing energy and equipment costs associated with aeration. Under anaerobic conditions, many organisms channel more substrate into product formation rather than energy production, resulting in higher yields of desired metabolites, such as ethanol or organic acids. Furthermore, the reduced focus on biomass formation in anaerobic pathways can enhance volumetric productivity as more metabolic flux is allocated to product synthesis. However, fermentation and anaerobic respiration have lower energy conservation than aerobic metabolism. Fermentative processes deliver a mix of reduced products (e.g., organic acids like lactate, acetate, and succinate), which are valuable as platform chemicals but often lead to lower yields and titers, as well as more challenging downstream processing (Förster; Gescher 2014). While anaerobic processes have significant advantages in reducing costs and improving product yields in specific contexts, they also have limitations. The lower energy (ATP) yield in anaerobic processes can sometimes constrain microbial growth or productivity. Moreover, not all biotechnological processes are suitable for anaerobic conditions. Many high-value products, such as antibiotics, secondary metabolites, and recombinant proteins, require aerobic conditions for optimal synthesis. Additionally, some microorganisms, such as *P. putida*, are obligate aerobes and cannot function effectively without oxygen.

Anodic electro-fermentation could deliver a solution that combines the advantages of aerobic and anaerobic processes by introducing an anode as a terminal electron acceptor. This approach would diminish the need for oxygen as the terminal electron acceptor in aerobic respiration. At the same time, the anode is non-depletable and, therefore, guarantees continuous product formation and prevents redox imbalances. Compared to aerobic processes, the usage of anodic electro-fermentation results in very high product over substrate yields due to only minor production of by-products, less substrate loss due to biomass formation, and no complete oxidation of substrate to $CO_2$ (Lai*, et al.* 2016b). Not only aerobic bioprocesses but also anaerobic ones can be improved as the anode can help to balance the redox and energy state of anaerobic cells due to the regeneration of co-factors at the anode instead of the production of reduced by-products (Kracke*, et al.* 2015).

Proof of concept studies on the usage of anodic electro-fermentation for the transformation of an aerobic into an anaerobic process were, amongst others, carried out with *Corynebacterium glutamicum* (Vassilev*, et al.* 2018), and *P. putida* (Lai*, et al.* 2016b)However, significant challenges remain before implementation into real-world applications is possible. The most critical steps might be understanding and improving the extracellular electron transfer rate and enhancing the product formation rates.

## 1.3 Electroactive Microorganisms

Physical barriers such as the cytoplasmic membrane and other membrane layers (e.g., peptidoglycan, outer membrane) function as insulators, leading to the evolution of mechanisms that enable bacteria to utilize insoluble electron acceptors outside their membranes. This adaptation is crucial in environments lacking soluble electron acceptors.

Electroactive microorganisms are involved in the extracellular electron transfer in both microbial biofilms and planktonic cells. Direct electron transfer occurs in biofilms, whereas planktonic cells typically engage in mediator-based indirect electron transfer. Pure and mixed cultures participate in indirect electron transfer, with mixed cultures often containing non-electroactive species alongside electroactive ones.

Exoelectrogens oxidize substrates and transfer electrons to an anode, encompassing microorganisms from the Bacteria, Archaea (specifically within the Euryarchaeota phylum), and Eukarya (notably fungal species in the Ascomycota phylum) domains (Suresh*, et al.* 2022). Conversely, electrotrophs capture electrons from a cathode for their metabolism, with representation solely among prokaryotes, including both Bacteria and Archaea (also within the Euryarchaeota phylum) (Logan*, et al.* 2019; Logan; Rabaey 2012). Some microorganisms, such as *Bacillus subtilis*, *Geobacter* sp., *Shewanella* sp., and *Pseudomonas* spp., exhibit either electrogenic or electrotrophic capabilities depending on the environmental conditions (Koch; Harnisch 2016).

### 1.3.1 Exoelectrogens

Exoelectrogens utilize anodes as electron acceptors, producing power ranging from 4.4 to 3900 mW/m² (Logan*, et al.* 2019). The primary groups of exoelectrogens identified to date are gram-negative bacteria within the Gammaproteobacteria and Deltaproteobacteria classes of Proteobacteria, including *Geobacter* and *Shewanella* species. The best-studied electroactive microorganisms are *Shewanella oneidensis* and *Geobacter sulfurreducens*, serving as model organisms for direct extracellular electron transfer mechanisms. *Shewanella* species employ various cytochromes in their outer membrane extensions for electron hopping across insulating spaces (Dohnalkova*, et al.* 2011), while *Geobacter* species use porin-cytochrome trans-outer membrane protein complexes and/or aromatic amino acids enriched conductive nanowires (Kumar*, et al.* 2017). Additionally, *Shewanella* secretes the endogenous redox-mediator riboflavin (Marsili*, et al.* 2008). *Geobacter* species are typically found in biofilms (Sydow*, et al.* 2014), whereas *Shewanella* species can exist as both planktonic cells and biofilms (Fredrickson*, et al.* 2008). Nowadays, the electron transfer mechanisms of various other electroactive microorganisms are also examined but remain mostly unresolved (Zhao*, et al.* 2021).

Previously, gram-positive bacteria were thought incapable of interacting with anodes due to their thicker, non-conductive cell walls (Milliken; May 2007). However, many gram-positive bacteria are now recognized as electroactive (Paquete 2020). Notably, several species within the Firmicutes phylum, such as *Bacillus* (e.g. *Bacillus subtilis* (Nimje*, et al.* 2009)), *Clostridium* (e.g. *Clostridium propionicum*), *Enterococcus* (e.g. *Enterococcus faecalis* (Pankratova*, et al.* 2019)), *Lactobacillus* (e.g. *Lactobacillus plantarum*), and *Lactococcus* (e.g. *Streptococcus lactis*) (Pankratova*, et al.* 2019), can interact with anodes, likely through mediator diffusion across the peptidoglycan layer, conductive cell wall-associated proteins, or the formation of electroactive biofilms.

Exoelectrogenic bacteria are often found in extreme environments, including thermophilic conditions (e.g., *Calditerrivibrio nitroreducens* (Fu*, et al.* 2013) and *Thermincola ferriacetica* (Parameswaran*, et al.* 2013)), acidic pH (e.g., *Acidiphilum* sp. (Malki*, et al.* 2008)), or alkaline pH and high salt concentrations (e.g., *Geoalkalibacter* spp. (Badalamenti*, et al.* 2013) and *Geoglobus ahangari* (Kashefi*, et al.* 2002)). These adaptations enhance the potential for MET development (Chaudhary*, et al.* 2022).

Energy generation in exoelectrogenic microorganisms can be respiratory or fermentative. Respiratory exoelectrogens utilize electron transport through membrane-associated proteins to generate a proton gradient that drives ATP synthase, producing ATP. Fermentative exoelectrogens conserve energy through substrate-level phosphorylation. Respiratory exoelectrogens typically exhibit faster extracellular electron transfer rates per mole and complete substrate oxidation to $CO_2$, while fermentative exoelectrogens produce more oxidized products like organic acids and alcohols (Lovley; Holmes 2022). Similar distinctions apply to electrotrophic microorganisms, which can be classified into respiratory and non-respiratory electron consumers (Choi; Sang 2016).

Exoelectrogenic bacteria are employed in techniques of microbial electrochemical biotechnology, which cultivate electroactive microorganisms on the anode side of BES, including microbial fuel cells, microbial electrolysis cells, microbial desalination cells, and anodic electro-fermentation. Common exoelectrogens used include *G. sulfurreducens*, *S. oneidensis*, *P. aeruginosa* (Yong*, et al.* 2017), genetically engineered *Escherichia coli (Feng, et al. 2018)*, and *Klebsiella pneumoniae* (Zhang*, et al.* 2008). Additionally, *Desulfovibrio* spp. and *Clostridium* spp. are utilized in microbial electrolysis cells for their high hydrogenase activity (Noori*, et al.* 2024). Weaker exoelectrogens, such as *Pseudomonas* spp., *Thaurea* sp., and *Lactobacillus* spp. (Aiyer; Doyle 2022), as well as anaerobic ammonium-oxidizing bacteria like *Candidatus Brocadia* sp. and *Candidatus Scalindua* sp. (Shaw*, et al.* 2020), are also employed. Gram-positive, redox mediator-producing bacteria such as *Lysinibacillus sphaericus* (Nandy*, et al.* 2013) and *Corynebacterium* spp. (Liu*, et al.* 2010) are reported to be used in microbial fuel cells.

### 1.3.2 Electrotrophic Bacteria

Electrotrophic bacteria use cathodes as electron donors, with current consumption ranging from 0.2 to 1000 mA/m² (Logan*, et al.* 2019). Electrotrophs are primarily found within the Proteobacteria (e.g., *Acinetobacter* sp., *Pseudoalteromas* sp., *Branhamella catarrhalis*, *Brevundimonas diminuta*, *Burkholderia cepacia*, *Marinobacter* sp., *Mariprofundus ferrooxydans*, and *Roseobacter* sp. (Debuy*, et al.* 2015)) and Firmicutes (e.g., *Bacillus* sp., *Clostridium* sp., *Sporomusa* sp., and *Staphylococcus carnosus* (Erable*, et al.* 2010)) phyla.

In microbial electrochemical biotechnology, electrotrophs are cultivated on the cathode side. They support hydrogen production in microbial electrolysis cells through $H_2$-producing biofilms, predominantly featuring *Desulfovibrio* sp. and *G. sulfurreducens* (Geelhoed; Stams 2011). Electrotrophs are also used for metal recovery from wastewater, including species such as *Klebsiella pneumoniae* (Bergel*, et al.* 2005), *G. sulfurreducens*, and *S. oneidensis* (Yates*, et al.* 2013). In microbial electrosynthesis, electrotrophic bacteria reduce $CO_2$ to valuable organic molecules, such as acetate, by acetogenic bacteria like *Sporomusa* sp. and *Clostridium* sp. (Nevin*, et al.* 2011), or alcohol by *Ralstonia eutropha* (Li*, et al.* 2012).

## 1.4 Extracellular Electron Transfer

Electroactive bacteria interact with external electrodes through a process known as extracellular electron transfer. This transfer of electrons beyond the cell membrane can occur directly or indirectly (Gralnick; Newman 2007).

Direct electron transfer involves electroactive microbes delivering their terminal electrons directly to the anode after substrate oxidation without using soluble electron shuttles or redox mediators. This process requires the cells to be in direct contact with the electrode surface or to form conductive pili, also known as nanowires. Biofilm formation by electroactive bacteria on the electrode surface facilitates this direct contact, reducing the distance between the electrode and cells. Electron transfer across the cell membrane occurs through redox-active membrane proteins, such as cytochromes, which transfer electrons from a reaction partner with a lower redox potential to one with a higher potential (Seeliger*, et al.* 1998). Most electroactive bacteria utilize multiheme cytochromes to support their electron transfer activities. These cytochromes are cell-bound proteins crucial for intracellular electron transport and respiration. Other proteins involved in electron transfer across the cell surface include porin-cytochrome complexes, cell-surface exposed cytochromes, and other redox proteins like copper and iron-sulfur proteins (Costa*, et al.* 2018b). Conductive pili, or microbial nanowires, provide another mechanism for direct electron transfer. These filamentous structures, first discovered in *Geobacter sulfurreducens* and found in various phyla, exhibit conductivities similar to metals and

enable electron transport without requiring direct cell-electrode proximity (Malvankar; Lovley 2012) and, therefore, can transport electrons across the biofilm. A notable example of direct long-range electron transfer is found in cable bacteria. These electroactive, multicellular microbes form conductive filaments several centimeters long. They connect anoxic and aerobic environments, transferring electrons produced during sulfide oxidation in anaerobic sediment to regions where oxygen or nitrate acts as an electron acceptor (Pfeffer*, et al.* 2012; Nielsen; Risgaard-Petersen 2015).

In contrast, electroactive bacteria that lack proteins for exo-electron transfer are considered weak electrogens (Aiyer; Doyle 2022; Doyle; Marsili 2018). These bacteria rely on external compounds such as redox mediators or electron shuttles to facilitate indirect electron transfer). These compounds can be reduced and oxidized by the microorganism and the electrode and can, therefore, shuttle electrons between them. Redox mediators, though effective in enhancing current densities compared to direct electron transfer, can be environmentally toxic and undermine the sustainability of mediated processes (Roller*, et al.* 1984; Park; Zeikus 2000). In the following section, redox mediators will be discussed in detail.

Some electroactive bacteria employ multiple electron transfer mechanisms, such as pili, in conjunction with biofilm formation, demonstrating the adaptability and complexity of microbial interactions with electrodes (Steidl*, et al.* 2016). Redox mediators have also been measured in the extracellular polymeric substances (EPS) of biofilms, further highlighting the diverse strategies used by electroactive bacteria in electrode interactions (Yang*, et al.* 2012).

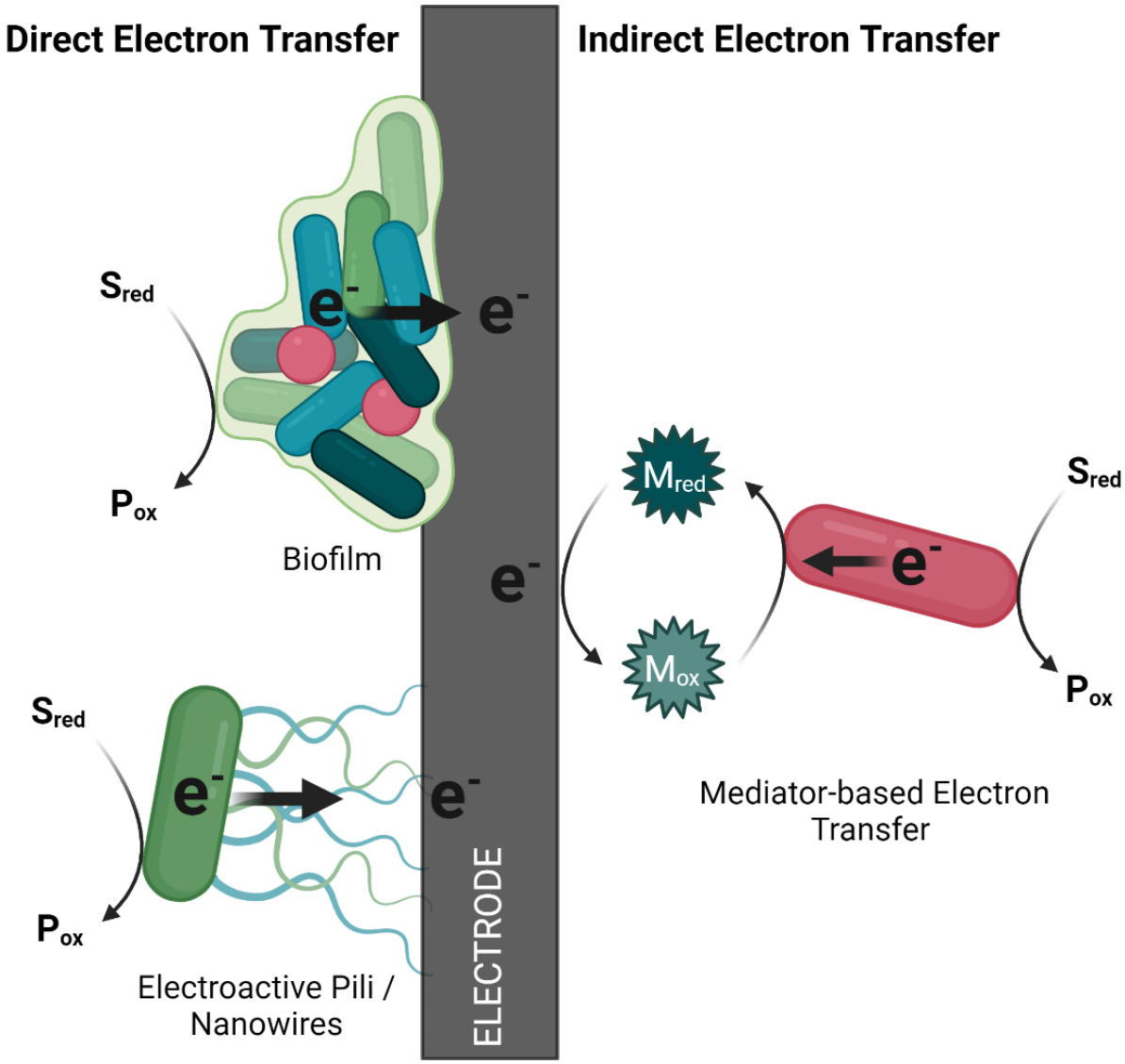


**Figure 1. Extracellular electron transfer mechanisms.** Shown are schematic pictures of direct and indirect electron transfer between an electrode and electroactive microorganisms. Direct electron transfer is possible via biofilm formation or electroactive pili/ nanowires. For Indirect electron transfer, a shuttle substance (redox mediator) is needed. (Created in BioRender.com)

## 1.5 Redox Mediators

As mentioned before, redox mediators are redox-active compounds that can accept and donate electrons from cells and electrodes in multiple cycles and shuttle them between the two entities. They can be either natural (Rabaey*, et al.* 2005) or artificial (Delaney*, et al.* 1984) compounds, also called endogenous and exogenous mediators.

Exogenous or artificial mediators are synthetic compounds that can be added to BES to facilitate or improve the electron shuttling between microbes and electrodes. Research on synthetic redox mediators gained momentum in the 1980s and 1990s, notably through the work of Bennetto (Bennetto

1990). In his work, he focused on the improvement of microbial fuel cells by the usage of various artificial redox mediators, e.g., thionine and resurofine. He was among the first scientists who systematically studied and characterized these electron shuttle compounds (Bennetto*, et al.* 1983). Building on these findings, additional redox mediators were explored. Neutral red was among the first synthetic redox mediators that were extensively studied (Park; Zeikus 1999). Nowadays, a wide range of artificial electron shuttle compounds is known and has been investigated in various BES, including methylene blue, methylene red, thionine, ferricyanide (FeCN), methyl viologen, humic acid analogs, and flavins.

The microorganisms themselves produce endogenous or natural redox mediators. Indications for the existence of such compounds were a wide range of bacteria, which were known to be able to reduce minerals (Turick*, et al.* 2003; Hernandez*, et al.* 2004). Following these hints, the first identified endogenous mediators were pyocyanin and phenazine-1-carboxylic acid (PCA), pigment molecules produced by *Pseudomonas aeruginosa* (Rabaey*, et al.* 2005). Today, several bacteria, such as *Shewanella oneidensis* (Askitosari*, et al.* 2019; Marsili*, et al.* 2008), and *Pseudomonas alcaliphila* (Zhang*, et al.* 2011), are known to produce redox mediators naturally. These bacteria can either be used directly in BES, or their mediator production pathways can be copied via genetic engineering into other strains, e.g. *E. coli* (Feng*, et al.* 2018), and *P. putida* (Askitosari*, et al.* 2019).

Whenever redox mediators are used in BES, several factors must be considered to ensure the efficiency and sustainability of the process (Gemünde*, et al.* 2022; Bedendi*, et al.* 2022). As redox mediators are often toxic to the environment and/or can be costly compounds, effective methods for the removal or recycling of mediators from the BES broth are essential to reduce costs and mitigate environmental impact (Fruehauf*, et al.* 2020). Additionally, the chosen mediator should have good solubility and no negative effects on the survival of the microbe, metabolism, or activity of crucial enzymes within the BES. Furthermore, mediators should exhibit good electrochemical reversibility and stability in both redox states, ensuring efficient electron transfer and prolonged use. The redox potential of the mediator must be compatible with the interaction site, and the cells must be capable of taking up the respective mediator and transferring the electrons at high rates.

The removal of mediators from fermentation broths can make the downstream processing expensive and technically challenging, but it is of high importance, particularly when it comes to using toxic or costly mediators. Redox mediators like menadione and methyl viologen are already in low concentrations highly toxic for organisms (Yonei*, et al.* 1986; Castro*, et al.* 2008). Therefore, removal techniques or biodegradable compounds are needed, but research in this field is scarce. However, techniques from other biotechnological fields, such as membrane or chromatography-based separation, can be adapted for this purpose (Hwang*, et al.* 2013). Additionally, methods from the

textile industry may be useful for removing dye-like mediators from the fermentation broth (Çoruh; Gürkan 2014). Utilizing biodegradable compounds, such as humic substances or analogues thereof, such as anthraquinone-2,6-disulfonate (AQDS) or flavins, can potentially eliminate the need for costly downstream processing (Xin*, et al.* 2020). Immobilizing mediators at electrodes is another strategy to avoid the necessity of downstream removal, though this drastically limits possible reactor volumes (Huang*, et al.* 2017; Kochius*, et al.* 2012).

Mediator stability against chemical, biological, and physical stresses is crucial and can be reflected in the total turnover number (TTN) (Gemünde*, et al.* 2022). As the name suggests, the TTN describes the number of cycles a mediator can be oxidized and reduced before losing its activity. Additionally, to a decrease in activity, mediator molecules can also be lost due to cellular accumulation, differences in membrane permeability between their redox states (e.g. benzyl viologen and methyl viologen (Jones*, et al.* 1976)), permanent adsorption to cell components (e.g. neutral red binds to the cell membrane of gram-negative bacteria (Park; Zeikus 1999)), irreversible attachment to electrodes (e.g. thionine (Allen; Bennetto 1993)), or due to polymerization or semi-reversible redox reactions at the electrodes. Many artificial redox mediators are stable under certain BES conditions, like 2-hydroxy-1,4-naphthoquinone and FeCN (Luo*, et al.* 2017). Continuous feeding can mitigate these issues for unstable mediators but increases costs and toxicity risks. Another more sustainable and cheaper possibility is the usage of microorganisms secreting endogenous mediators, either naturally (e.g. the already earlier mentioned *Pseudomonas aeruginosa*, which produces pyocyanin and phenazine-1-carboxylic acid (PCA) (Hassett*, et al.* 1992)) or through genetic engineering (Askitosari*, et al.* 2019).

These natural redox mediators offer several advantages as they integrate seamlessly into the metabolic processes of the cell. Their high specificity for electron transfer pathways can enhance energy generation, particularly in their native environments. However, these mediators also have several disadvantages. One significant drawback is the additional metabolic burden on the microorganisms and the drainage of carbon, which could otherwise be used for the production of the desired product (Gemünde*, et al.* 2022). Moreover, the use of endogenous mediators is limited to naturally occurring bacteria with the appropriate biosynthetic pathways or to metabolically engineered strains. This restricts the range of species and mediator combinations that can be used. The production of natural mediators is often insufficient, and their effectiveness can change based on environmental conditions (Bosire; Rosenbaum 2017), which potentially reduces the overall efficiency and scalability of BES. Furthermore, natural mediators are prone to degradation over time, leading to a gradual loss of activity (Costa*, et al.* 2018a).

On the other hand, artificial redox mediators can be synthesized in large quantities and can be used consistently and controlled in BES. They are often more stable and can be designed to optimize specific

electrochemical properties, such as redox potential and solubility, which help enhance electron transfer efficiency. However, artificial mediators may have disadvantages, such as cell toxicity, leading to reduced microbial viability and system performance over time. Furthermore, artificial mediators can accumulate or bind irreversibly to cell components or electrodes, resulting in a loss of mediator activity and system inefficiency (Chen*, et al.* 2021). Therefore, while artificial mediators offer greater control and stability, they can introduce additional complexities regarding system sustainability and microbial health.

However, for many electroactive microorganisms, the exact extracellular electron transfers, as well as the redox mediator interaction side, are still not fully understood. For many years, the extracellular electron transfer mechanism of only a few electroactive model organisms, like *S. oneidensis* and *G. sulfurreducens,* relished extensive research. In the past years, more and more insights into the electron transfer mechanisms of other strains have been gained (Zhao*, et al.* 2021). This knowledge is crucial to understanding the interaction between mediator and cells and subsequently improving the BES performance. In general, a redox mediator can only withdraw electrons from a redox-active enzyme in the ETC when it has a more positive standard redox potential than the respective molecular interaction site. For the donation of electrons, in contrast, it needs a more negative standard redox potential compared to the molecular interaction site (Kracke*, et al.* 2015; Bedendi*, et al.* 2022). For example, the redox potential of the artificial redox mediator FeCN is in the right range to most likely withdraw electrons from the cytochrome reductase c in *P. putida* F1 (Lai*, et al.* 2020). As the redox potentials of some mediators (particular organic molecules) can change according to the conditions in the system, e.g. pH, ionic strength, and surrounding lipids (Melin; Hellwig 2020), also the interaction site can change, resulting in changed energy yields in the cell. The ETC of bacteria is typically located on the cytoplasmic membrane. Hence, the uptake of the mediator through the outer membrane of the cells is necessary, either by diffusion or certain transporter systems. This transport can be one of the limiting steps of BES processes, but the uptake pathways for most mediators are still unclear. One of the few examples of an already elucidated mediator transporter is an efflux pump for phenazines in *P. aeruginosa* called MexGHI-OpmD (Sakhtah*, et al.* 2016). For FeCN uptake in *P. putida* KT2440, new findings suggest that TonB-dependent transporter systems might play a role, as they are involved in iron uptake, and FeCN is an iron-containing complex (Noinaj*, et al.* 2010; Nguyen Anh Vu 2024). Neutral red, in turn, can permeate the cell membrane via non-ionic diffusion (Repetto*, et al.* 2008).

## 1.6 *Pseudomonas putida*

*Pseudomonas putida* is a gram-negative, rod-shaped, obligate aerobic bacterium within the class of Gamma proteobacteria (Palleroni 1984). Its natural habitat is soil and water environments, where constantly changing conditions have evolved the metabolism of this microbe to be very versatile (Weimer*, et al.* 2020). Not only can *P. putida* grow on a broad spectrum of substrates (Timmis 2002), but it also tolerates the presence of solvents (Ramos*, et al.* 2002), heavy metals (Bruins*, et al.* 2000), and organic pollutants and is resistant to environmental stresses, like oxidative stress, high salt concentrations, and temperature extremes (Rojo 2010). These properties make *P. putida* an important microbe for environmental biotechnology, especially in the bioremediation of contaminated soil. Due to its promising characteristics and possible application options, extensive research was carried out on the microbe, resulting in genome-scale models (Nogales*, et al.* 2020) and various tools for metabolic engineering and systems-level profiling (Cook*, et al.* 2018; Martínez-García; Lorenzo 2017).

The most commonly used and best-studied strain of *P. putida* is KT2440. This strain emerged from the wild-type mt-2 by the removal of the TOL plasmid (Bagdasarian*, et al.* 1981; Regenhardt*, et al.* 2002). This plasmid enabled the strain to degrade toluene and other possibly harmful aromatic compounds. The removal of this plasmid simplified the genome of the strain, making it more stable and predictable and reducing horizontal gene transfer. KT2440 is classified as a non-pathogenic strain, making it more convenient to be used as a model organism for lab research and industrial application. It is used for bioremediation, bioplastic production, biofuel synthesis, and biotransformation (Nelson*, et al.* 2002). Furthermore, various other strains are used for bioremediation by the utilization of the superb solvent tolerance of the microbe and its ability to withstand stresses. For example, the strain DOT-T1E can degrade different toxic chemical and organic pollutants (Udaondo*, et al.* 2013), CSV86 degrades aromatic compounds (Paliwal*, et al.* 2014), GB-1 can precipitate manganese and is used on heavy-metal contaminated sites (Brouwers*, et al.* 1999), and the strain F1 degrades aromatic hydrocarbons like toluene (Wackett; Gibson 1988). Other strains, in turn, were developed for production purposes, like for example the strain S12 for biofuel and biochemicals production (Wierckx*, et al.* 2005), and CA-3 for the synthesis of bioplastics from polyhydroxyalkanoates (PHAs) (Ward; O'Connor 2005).

### 1.6.1 Glucose Metabolism of *P. putida*

*P. putida* has a versatile glucose metabolism. Its adaptation to thrive under various environmental stresses originates from its efficient mode of energy and reducing power generation. Its glucose metabolism functions primarily via the Entner-Doudoroff pathway and a unique combination of other pathways, resulting in the so-called ED-EMP cycle. This pathway consists of enzymes of the Entner-Doudoroff, Embden-Meyerhof-Parnas, and pentose phosphate pathways (Nikel*, et al.* 2015).

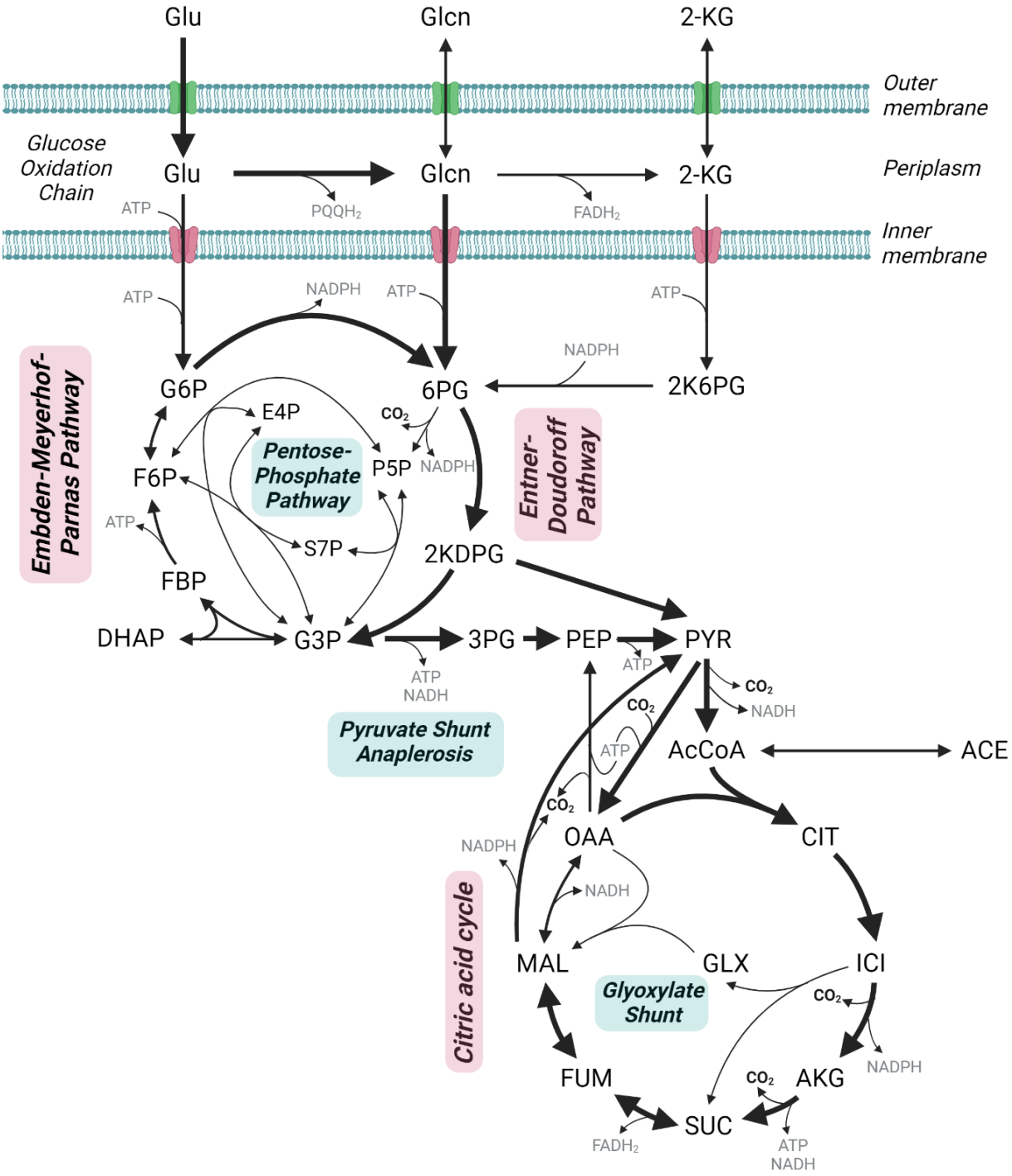


**Figure 2. Central carbon metabolism of *P. putida* KT2440 under aerobic conditions.** The microbe uses the ED-EMP cycle consisting of enzymes of the Entner-Doudoroff, Embden-Meyerhof-Parnas and pentose phosphate pathways to metabolize glucose. Glu – glucose; Glcn – gluconate; 2-KG – 2-ketogluconate; G6P – glucose-6-phosphate ; 6PG – 6-phosphogluconate ; F6P – fructose-6-phosphate; E4P – erythrose-4-phosphate; S7P – sedoheptulose-7-phosphate ; FBP – fructose-1.6-bisphosphate ; 2KDPG – 2-keto-3-deoxy-6-phosphogluconate ; DHAP – dihydroxyacetone phosphate; G3P – glyceraldehyde-3-phosphate ; 3PG – glycerate-3-phosphate ; PEP – phosphoenolpyruvate; PYR – ; AcCoA – acetyl-coenzyme A ; ACE – acetate ; OAA – oxaloacetate ; CIT – citrate; MAL – malate ; GLX – glyoxylate ; ICI – isocitrate ; FUM – fumarate ; SUC – succinate ; AKG – 2-ketoglutarate (Figure modified from Kohlstedt; Wittmann 2019) (Created in BioRender.com)

The glucose metabolism in *P. putida* mainly begins with the transport and subsequent oxidation in the periplasm. Instead of directly transporting the glucose into the cytosol to feed glycolysis, a membrane-bound glucose dehydrogenase enzyme converts glucose to gluconate in the periplasm. Now, a second oxidation step in this periplasmic oxidation chain becomes possible, generating 2-ketogluconate (2-KG) (del Castillo*, et al.* 2007). In each of these oxidation reactions, electrons are released, which contribute to the generation of a proton gradient across the membrane, which fuels ATP generation through ATP synthase (Ebert*, et al.* 2011). However, the main share of glucose is only oxidized once to gluconate, then taken up into the cytosol via a specific transporter and phosphorylated into 6-phosphogluconate. By preferring this uptake pathway, before the direct uptake of glucose, *P. putida* generates a large ATP surplus, as the ATP-binding cassette transporter and following phosphorylation via glucokinase, which is needed for the uptake of glucose, consumes 2 mol of ATP per glucose molecule, while the gluconate uptake only costs one mol of ATP for phosphorylation (Kohlstedt; Wittmann 2019). The 6-phosphogluconate then enters the Entner-Doudoroff pathway, which is the primary route of glucose catabolism in *P. putida*. In most bacteria, the Embden-Meyerhof-Parnas glycolytic pathway is common for glucose metabolism as it is yielding more ATP. However, the Entner-Doudoroff pathway generates a higher amount of NADPH molecules, which are important as reducing agents in many biosynthetic and stress response processes. In summary, the Entner-Doudoroff pathway converts one mol of glucose into two pyruvate molecules, yielding one mol of ATP, one mol of NADH, and one mol of NADPH.

Next to the usage of the Entner-Doudoroff pathway, *P. putida* also uses enzymes of the pentose phosphate pathway and the Embden-Meyerhof-Parnas pathway. The pentose phosphate pathway provides additional NADPH and necessary precursor molecules for biosynthetic reactions like the synthesis of nucleotides and amino acids. On the other hand, the Embden-Meyerhof-Parnas pathway requires the direct uptake of glucose and is, therefore, less energy efficient for *P. putida*. Only approximately 10% of the glucose is taken up via this pathway (Kohlstedt; Wittmann 2019).

Furthermore, a combination of Entner-Doudoroff, Embden-Meyerhof-Parnas, and pentose phosphate pathway enzymes form the ED-EMP cycle, which is used to recycle triose-phosphates from the lower part of the glycolysis and the Entner-Doudoroff pathway back to hexose-phosphates. When grown on glucose, *P. putida* favors this pathway to produce additional NADPH to encounter environmental stress (Nikel*, et al.* 2015).

Another difference from other bacteria is that *P. putida* does not heavily rely on substrate-level phosphorylation for energy production. Instead, the dominant role in ATP generation is played by oxidative phosphorylation, which is driven by the proton gradient created by the periplasmic oxidation chain (del Castillo*, et al.* 2007).

The glucose metabolism is advantageous for *P. putida* since it has a higher energy efficiency due to the conservation of ATP by the usage of periplasmic oxidation and the Entner-Doudoroff pathway, a better redox balance due to large amounts of NADPH being produced, and contributing to higher stress tolerance due to both ATP and NADPH production.

### 1.6.2 Electron Transport Chain of *P. putida*

*P. putida* is typically considered an obligate aerobe and, therefore, requires oxygen for growth and energy production (Schmitz*, et al.* 2015). *P. putida* utilizes a series of membrane-bound protein complexes and electron carriers situated in the cytoplasmic membrane to transfer electrons from metabolic intermediates to oxygen, the terminal electron acceptor (Sweet; Peterson 1981). The electron transport chain (ETC) in bacteria is not as linear as in eukaryotes but may be branched. Enzyme expression depends on oxygen availability. Hence, electrons can take different routes depending on the environmental conditions. Anyways, the protein complexes involved in ETC have increasing redox potentials and, therefore, an increasing affinity for electrons, which determines the direction of the electron flow (Simon*, et al.* 2008). In general, the ETC begins with dehydrogenases, e.g., NADH dehydrogenase and succinate dehydrogenase, which receive electrons from the oxidation of donors like NADH and succinate, respectively. The electrons are then funneled into the quinone pool. From there, the electrons are shuttled by ubiquinone to cytochrome c reductase, which transfers them to the mobile electron carrier cytochrome c. Finally, the electrons reach cytochrome c oxidase, where they reduce oxygen to water. In parallel, the involved protein complexes act as proton pumps, which translocate protons across the membrane, generating a proton motive force that drives ATP synthesis via ATP synthase. This process of energy generation is termed oxidative phosphorylation.

The ETC of *P. putida* is uniquely adaptable to varying oxygen levels, for example, by the expression of alternative terminal oxidases such as cytochrome bo3 and cytochrome bd (Belda*, et al.* 2016; Morales*, et al.* 2006; Sevilla*, et al.* 2013). Under anaerobic or micro-oxic conditions, *P. putida* can even switch to alternative terminal electron acceptors like nitrate to survive and maintain metabolic activity (Carter*, et al.* 1995). This versatility enables the bacterium to survive in diverse environments, making *P. putida* an excellent candidate for anodic electro-fermentation. However, growth and optimal metabolism require oxygen and is therefore considered an obligate aerobe anyway.

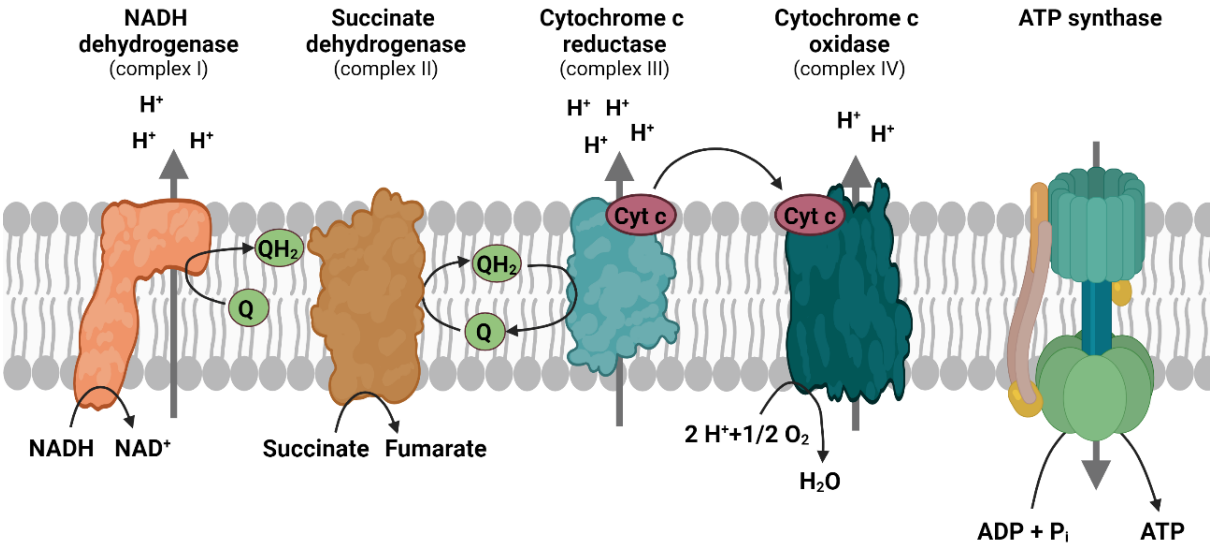


**Figure 3. Electron transport chain of *P. putida*.** Electrons enter the ETC via oxidation of electron donor molecules at different dehydrogenases, e.g., NADH and succinate dehydrogenase. The electrons pass the quinone pool and are transferred to cytochrome c at the cytochrome c reductase. Ultimately, cytochrome c shuttles them to the cytochrome c oxidase, where oxygen is reduced to water. The proton motion force, which is built up by the enzymes of the ETC that are proton pumps simultaneously, is used to fuel ATP synthesis by ATP synthase. (Created in BioRender.com)

### 1.6.3 Anodic Electro-Fermentation with *P. putida*

*P. putida* is a very promising host for various biotechnological production processes, but its obligate aerobic nature limits its efficient use in large-scale bioreactors. The input of oxygen into bioreactors is always a challenge. Heat and foam generation in these systems require special measures that increase the costs and limit the possible reactor sizes. In the past, many efforts were invested to genetically engineer *P. putida* towards anaerobic metabolism (Kampers*, et al.* 2019), but the complexity of its metabolism makes this a very challenging task. An extensive *in silico* analysis combining the comparison of the genomes of over 1,500 *Pseudomonas* strains, genome-scale modeling, and transcriptomics data identified 49 genes with known functions, 8 genes of unknown functions, and three vitamins that must be added externally, as necessary, to enable anaerobic respiration in *P. putida* (Kampers*, et al.* 2021). Microbial electrochemistry delivers an alternative approach to solving the problem. The solution is anodic electro-fermentation (see 1.2 Anodic Electro-Fermentation), a BES in which the cells can transfer their terminal electrons to an anode instead of oxygen.

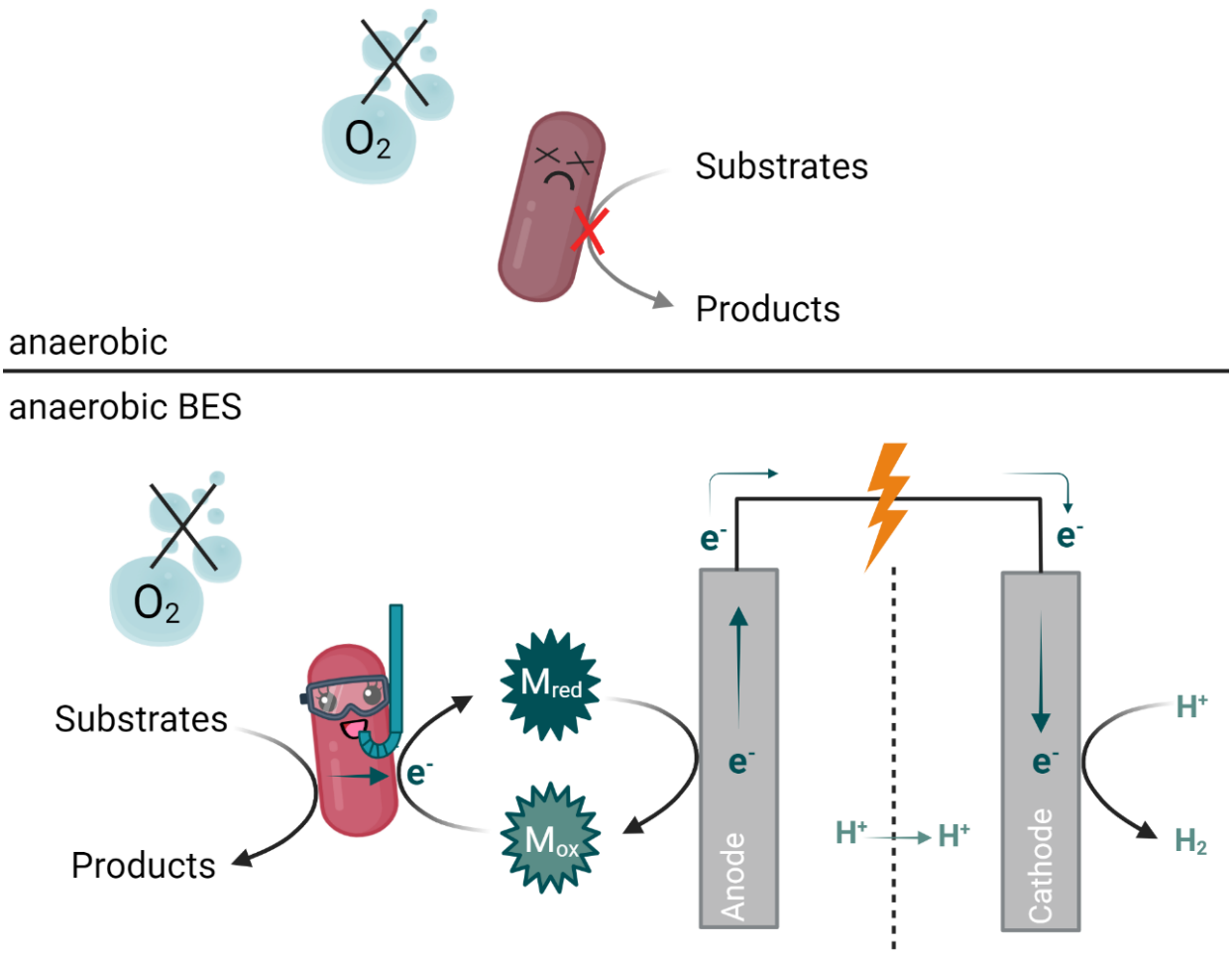


**Figure 4. Schematic illustration of the concept of anodic electro-fermentation with *P. putida*.** Under normal conditions, the obligate aerobic microorganism *P. putida* cannot survive when oxygen is depleted. The provision of an anode as terminal electron acceptor, however, enables them to survive under anaerobic conditions and metabolize substrates into products. An artificial redox mediator has to be supplied as electron shuttle between the electrode and the exoelectrogenic bacterium. Electrons travel to the cathode from the anode and produce a current output signal. At the cathode a counter reaction takes place. (Figure modified from Vassilev*, et al.* 2021) (Created in BioRender.com)

Already in 1984, it was shown that *P. putida* can survive under anaerobic conditions in a microbial fuel cell supplying an electrode as an inexhaustible terminal electron acceptor (Roller*, et al.* 1984). Additionally, this method enables the electrochemical control of the redox and carbon metabolism of the microbe towards the generation of a product of interest. Several studies have demonstrated the potential of *P. putida* in anodic electro-fermentation to improve the yield of value-added chemicals (Schmitz*, et al.* 2015; Hintermayer*, et al.* 2016; Askitosari*, et al.* 2019; Lai*, et al.* 2016b).

A major task for anodic electro-fermentation involves setting up an effective extracellular electron transfer from the microorganism to the anode while integrating it with the central carbon metabolism. The usage of a fitting redox mediator is essential for *P. putida* to enable the transfer of electrons to the anode. As a result of the absence of fermentative pathways in the obligate aerobe and the redox

balance on the external electron sink, anodic electro-fermentation processes lead to remarkably high product over substrate yields. For example, if glucose is used as the sole carbon source, the organic acid 2-KG is produced with a yield of over 90% with only very minor by-product generation (Lai*, et al.* 2016b).

However, despite the high yields, this process with *P. putida* is a very slow process, with substrate uptake and product formation rates far lower than those of aerobic processes in *P. putida*. Furthermore, as of this date, bacterial growth has not been achieved under anaerobic and anode-driven conditions. Recent advancements in metabolic engineering have shown promising potential in overcoming some of these limitations. In 2018, Yu et al. demonstrated that targeted genetic modifications could substantially improve the productivity of *P. putida* in anaerobic and anode-driven conditions. By overexpressing glucose dehydrogenase, an enzyme involved in the oxidation of glucose to gluconate via the periplasmic oxidation chain, both the electron transfer rate and 2-KG productivity were increased by 327% and 644%, respectively (Yu et al. 2018). Such findings indicate that strategic metabolic interventions can enhance the performance of anodic electro-fermentation systems and potentially make them more competitive with traditional aerobic processes.

Looking forward, the integration of multi-omics approaches, such as proteomics and transcriptomics, may uncover additional target genes that can be engineered to optimize electron transfer and improve overall system performance. Further exploration into the role of key metabolites, such as polyphosphate (polyP), and the development of novel redox mediators may help address the current bottlenecks in substrate consumption and growth rates, paving the way for more efficient applications of anodic electro-fermentation with *P. putida*.

## Scope of the Thesis

This thesis aims to provide an in-depth understanding of the physiology of *Pseudomonas putida* in a bio-electrochemical system (BES), particularly under anodic electro-fermentation conditions. *P. putida*, an obligate aerobe, has the remarkable ability to survive under anaerobic conditions as an exoelectrogen, where an anode serves as the terminal electron acceptor instead of oxygen. Anodic electro-fermentation can lead to exceptionally high product yields from substrates due to the absence of fermentative pathways when applied to aerobic bacteria. For instance, the wild-type strain of *P. putida* achieves a yield of over 90% of 2-KG from glucose. However, despite these promising yields, substrate consumption and product formation rates remain significantly low, and the underlying metabolic processes in such systems are still poorly understood.

The scope of this research focuses on unraveling the key physiological limitations within the BES, particularly investigating the carbon uptake pathway across the periplasmic membrane. This exploration aims to identify which factors limit glucose uptake rates, thereby constraining system efficiency. A multi-omics approach, encompassing systems biology techniques such as transcriptomics, proteomics, and metabolomics, was employed to compare the physiology of *P. putida* in the BES with that under standard aerobic conditions. This comparative analysis aims to pinpoint target genes for future genetic engineering, facilitating the construction of mutants with enhanced BES performance.

Furthermore, energy generation, which is a limiting factor in the anaerobic and anode-driven conditions of BES, was closely studied through the investigation of polyP as a key energy storage compound. Lastly, the role of redox mediators in facilitating efficient electron transfer was critically evaluated. This thesis reaffirms the importance of selecting an appropriate redox mediator for optimal exoelectrogenic performance. A comparative analysis of natural and artificial mediators, along with a broader comparison of various artificial redox mediators, was conducted to assess their potential to improve system efficiency.

The findings from this thesis provide key insights into the metabolic and physiological constraints of *P. putida* in BES and suggest strategies for improving the sustainability and efficiency of anodic electro-fermentation for industrial applications.

# 2. Materials and Methods

## 2.1 Chemicals

Chemicals used in this dissertation were purchased at the highest purity from Sigma-Aldrich (Steinheim, Germany), Merck (Darmstadt, Germany), or Carl-Roth GmbH (Karlsruhe, Germany) unless otherwise indicated. Ultrapure water, generated by a Milli-Q purification system (Millipore, Merck), was used for all experiments. The MilliQ system combines filtration methods, including ion exchange, reverse osmosis, and ultrafiltration, to remove ions, organic molecules, and microorganisms.

## 2.2 Bacterial Strains

Table 1 lists all bacterial strains used in this dissertation. Dr. Nikolas Wirth and Prof. Pablo Nikel from the Technical University of Denmark engineered and kindly provided the three gene deletion mutants KT-G, KT-GL, and KT-KG. Prof. Miriam Rosenbaum from Leibniz Institute for Natural Product Research and Infection Biology Hans Knöll Institute in Jena kindly shared the strains KT-PCA and KT-control.

**Table 1: Bacterial strains**

| *P. putida* strains | Genotype | Description | Source |
|---|---|---|---|
| **KT2440 WT** | Wild-type strain | Derivative of strain mt-2, cured from the pWWO catabolic plasmid | (Bagdasarian, Lurz et al. 1981) |
| **KT-G** | *P. putida* KT2440 Δ*gcd* | In-frame gene deletion mutant of glucose dehydrogenase (*gcd*, *PP_1444*); streamlined for cross-membrane transportation pathway via glucose | (Sánchez-Pascuala, Fernández-Cabezón et al. 2019) |
| **KT-GL** | *P. putida* KT2440 Δ*glk* Δ*gtsABCD* Δ*gad* | In-frame gene deletion mutant of glucose ABC transporter (*gtsABCD*, *PP_1015-PP_1018*), glucokinase (*glk*, *PP_1011*), and gluconate dehydrogenase (*gad*, *PP_3382-PP_3384*); streamlined for cross-membrane transportation pathway via gluconate | (Pause*, et al.* 2024) |
| **KT-KG** | *P. putida* KT2440 Δ*glk* Δ*gtsABCD* Δ*gnuK* Δ*gntT* Δ*PP_0652* | In-frame gene deletion mutant of glucose ABC transporter (*gtsABCD*, *PP_1015-PP_1018*), glucokinase (*glk*, *PP_1011*), gluconate transporters (*gntT*, *PP_3417*, and *PP_0652*) and gluconokinase (*gnuK*, *PP_3416*); streamlined for cross-membrane transportation pathway via 2-ketogluconate | (Pause*, et al.* 2024) |
| **KT-PCA** | *P. putida* KT2440 14.phz2 pBNT | PCA-producing strain with kanamycin resistance | (Askitosari*, et al.* 2019) |
| **KT-control** | *P. putida* KT2440 pBNT | Kanamycin resistant strain | (Askitosari*, et al.* 2019) |

## 2.3 Cultivation of *P. putida*

### 2.3.1 Media

Media stocks for cultivation were prepared according to Table 2. LB media was prepared by solving all ingredients in water, adjusting the pH to 7 (pH electrode, InLab Micro Pro-ISM, Mettler Toledo), and sterilization by autoclaving at 121 °C for 20 min. For DM9 minimal media (Lai*, et al.* 2016b), the basic salts were prepared in 10-fold concentration, the pH adjusted to 7.2 by the addition of NaOH solution and sterilized by autoclaving. Trace elements, calcium chloride, and magnesium sulfate stocks were prepared in 1000-fold concentration, sterilized by filtration (PES, pore size of 0.22 µm, Th. Geyer), and

stored at 4 °C. To obtain the final DM9 media, the 10-fold salt stock solution was added to sterile water in a ratio of 1:10, and the additives and trace element solution were added to a ratio of 1:1000 under sterile conditions. For Delft minimal media (Hartmans*, et al.* 1989)All stock solutions were prepared at a 100-fold concentration. The buffer and nitrogen solution were autoclaved, and the salt solution was filtered for sterilization. The final Delft media was obtained by adding all components to water in a ratio of 1:100, respectively.

**Table 2: Media composition**

| Medium | Stock solutions | Composition |
|---|---|---|
| **LB** | | 10 g/L tryptone, 5 g/L yeast extract, 10 g/L NaCl |
| **DM9** | Salt Stock (10x) | 60 g/L $Na_2HPO_4$, 30 g/L $KH_2PO_4$, 10 g/L $NH_4Cl$ 100 g/L |
| | Magnesium sulfate Stock (1000x) | MgSO4 * 7 $H_2O$ |
| | Calcium chloride Stock (1000x) | 15 g/L $CaCl_2$ * 2 $H_2O$ |
| | Trace Elements Stock (1000x) | 1.5 g/L $FeCl_3$ * 6 $H_2O$, 0.15 g/L $H_3BO_3$, 0.03 g/L $CuSO_4$ * 5 $H_20$, 0.18 g/L KI, .0.12 g/L $MnCl_2$ * 4 $H_2O$, 0.06 g/L $Na_2MoO_4$ * 2 $H_2O$, 0.12 g/L $ZnSO_4$ * 7 $H_2O$, 0.15 g/L $CoCl_2$ * 6 $H_2O$, 12.74 g/L Na EDTA, 0.023 g/L $NiCl_2$ * $H_2O$ |
| **Delft** | Buffer Solution (100x) | 388 g/L $K_2HPO_4$, 163 g/L $NaH_2PO_4$ |
| | Nitrogen Source Stock (100x) | 200 g/L $(NH_4)_2SO_4$ |
| | Salt Solution (100x) | 10 g/L $MgCl_2$ * 6 $H_2O$, 1g/L EDTA, 0.2 g/L $ZnSO_4$* 7 $H_2O$, 0.1 g/L $CaCl_2$ * 7 $H_2O$, 0.02 g/L $Na_2MoO_4$ * 2 $H_2O$, 0.5 g/L $FeSO_4$ * 7 $H_2O$, 0.02 g/L $CuSO_4$ * 5 $H_2O$, 0.1 g/L $MnCl_2$ * 2 $H_2O$, 0.04 g/L $CoCl_2$ * 6 $H_2O$ |

### 2.3.2 Storage of Bacterial Strains

All bacterial strains were kept in cryo-stocks at -80 °C for long-term storage. For the preparation of cryo-stocks, bacterial cell material of each strain was taken from the strain collection, spread on LB agar plates, and incubated at 30 °C (Heratherm™ Microbiological Incubator, Thermo Scientific). For the strains *P. putida* KT-PCA and *P. putida* KT-control, 50 µg/mL kanamycin ($Kan^{50}$) was added to the agar as well as to the liquid media, to ensure the presence of the plasmid. After about 24 h of incubation, a single colony was picked, placed in 3 mL of liquid LB media, and incubated for 7 h in a test tube covered by a metal cap at 30 °C and 200 rpm (Multitron Pro, INFORS HT). Then 500 µL of cell suspension was thoroughly mixed with 500 µL glycerol solution (50% w/v glycerol) and stored at -80 °C.

### 2.3.3 Aerobic Cultivation

A defined M9 medium (DM9) with glucose as the sole carbon substrate was used for the cultivation of *P. putida* KT2440, KT-G, KT-GL, and KT-KG cells. For *P. putida* KT-PCA and KT-control, Delft media with glucose and $Kan^{50}$ was used. The detailed recipe can be found above. For aerobic cultivation 5 g/L of glucose was added to the media respectively. To minimize systematic errors, each batch of experiments was started from cryo-stocks of the respective strains by streaking on an LB agar plate (with Km50 for *P. putida* KT-PCA and KT-control) and incubating for about 24 h at 30 °C (Heratherm™ Microbiological Incubator, Thermo Scientific). Afterward, a single colony was picked from the LB plate and transferred into a baffled shake flask with a metal cap containing DM9 medium or Delft medium with $Km^{50}$ for inoculation. A maximum of 20% of the working volume of the flasks was filled with medium for all growth experiments in this work. The liquid culture was incubated at 30 °C and 200 rpm (Multitron Pro, INFORS HT) until the desired cell density was reached, which was measured using a spectrophotometer (Libra S12, Biochrom Ltd, Cambridge, Great Britain; DM9 medium as blank) at the wavelength of 600 nm (OD600). The cell dry weight (CDW) was then calculated using the following formula: CDW [g/L] = 0.486 * OD600 (Yu*, et al.* 2018). The correlation factor was assumed to be the same for all strains used in this study.

### 2.3.4 Aerobic Growth Kinetics Determination

To determine the lag phase of the growth, the cryo-stocks were activated on the LB agar plate for 24-36 h. Afterward, colonies were picked using an inoculation loop and then inoculated into the DM9 liquid medium with 5 g/L glucose. Samples were then taken in regular intervals to monitor the growth at $OD_{600}$. The exponential growth phase kinetics were determined by preparing the DM9 liquid precultures from LB plates. Fresh DM9 medium were inoculated with cell material from the preculture to reach an initial $OD_{600}$ of ~0.1, and then the growth profiles were monitored over the day time. The exponential growth phase was defined by the linear plot of $Ln(OD_{600})$ against the time, while the maximum growth rates ($\mu$, $h^{-1}$) were determined by the slopes. The biomass yield of the exponential growth phase ($Y_{x/s}$, $[g_{CDW}/g_{glucose}]$) was determined by the slope of linear fitting between the biomass density (in cell dry weight, $[g_{CDW}/L]$) measured by $OD_{600}$ versus the glucose concentrations ([g/L]) measured by HPLC. Finally, the glucose consumption rate ($r_{glucose}$, $[mmol_{glucose}/g_{CDW}/h]$) was calculated by the following equation: $r_{glucose}$ $[mmol_{glucose}/g_{CDW}/h] = \mu$ $[h^{-1}]$ / ($Y_{x/s}$ $[g_{CDW}/g_{glucose}]$ * $MW_{glucose}$ [g/mmol], while $MW_{glucose}$ is the molecular weight of glucose (0.18016 g/mmol).

### 2.3.5 BES

A detailed description of the set-up and operation of the used BES can be found in (Lai*, et al.* 2019).

### 2.3.5.1 BES Set-Up

A bioreactor with an integrated three-electrode system was used for the BES fermentations. Carbon cloth (25 $cm^2$, 1071HCB, FuelCellStore, Texas, USA) was pre-treated by soaking in 2 mM cetrimonium bromide and incubated overnight at 30 °C and 200 rpm to clean the surface and improve its surface hydrophilicity. It was then washed in water, dried in an oven (60 °C), and used as the anode. Stainless steel mesh (FE621018, Advent Research Materials, Oxford, England) was used as the cathode. An Ag/AgCl electrode in saturated KCl (RE-1CP, Als, Tokyo, Japan, Cat. No.: 013691) was deployed as a reference electrode. The bioreactor consists of a double-jacketed glass cylinder with a filling volume of 350 mL, which can be tightly closed using a polyether ether ketone (PEEK) lid, plugs, and a metal clamp. The anode and the cathode chamber are separated by a cation exchange membrane (Membranes International INC., Ringwood, USA, Cat. No.: CMI-7,000). The reference electrode sits in a bridging tube with a porous glass frit (pore size of < 1 µm) at the end, which is also placed into the anode chamber. A cooled glass condenser, sealed with an autoclavable membrane (pore size of 0.22 µm), ensures the release of gas under sterile conditions and minimizes evaporation.

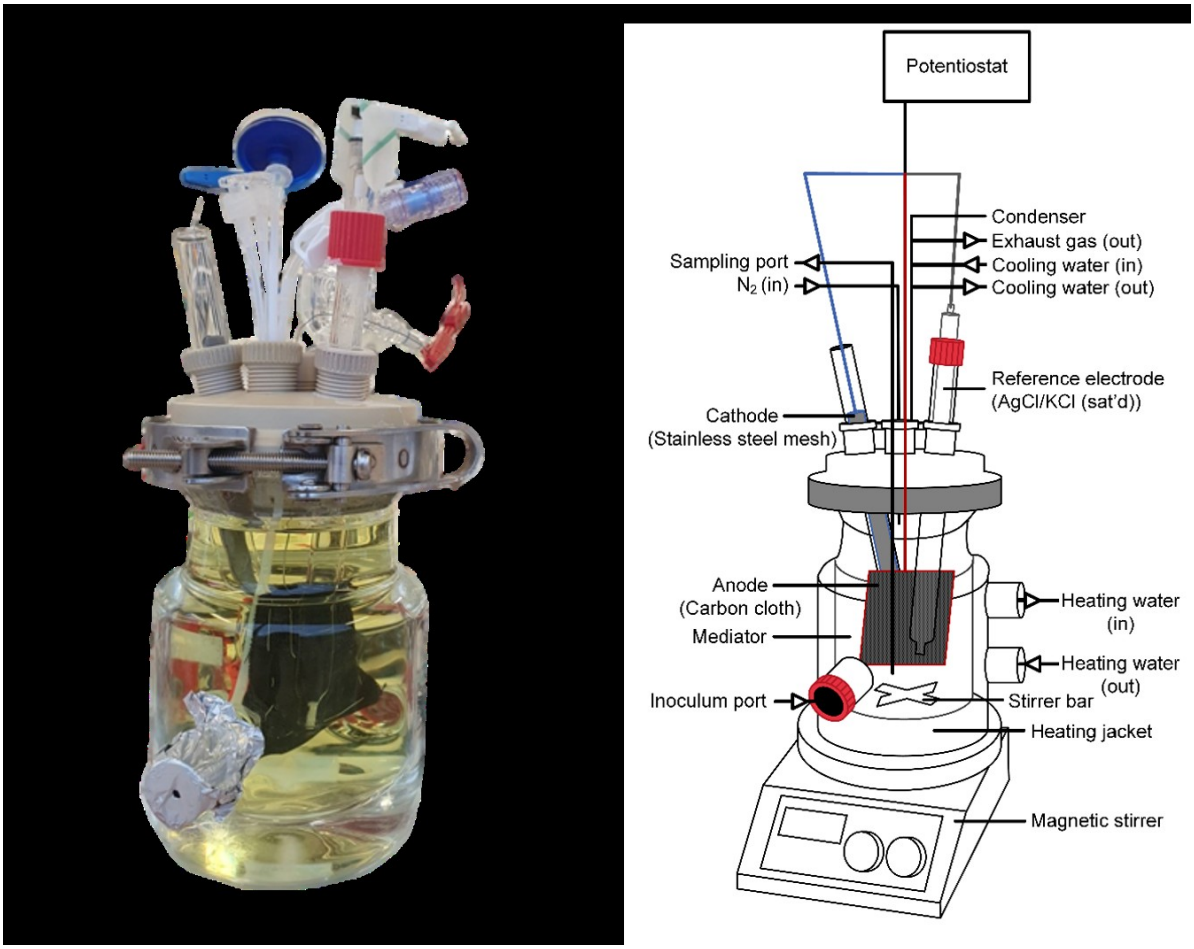


**Figure 5. The BES.** Depicted is a real-life picture **(A)** and a schematic picture **(B)** of the BES used in this study. The reactor consists of a double-jacketed glass vessel with a three-electrode system connected via potentiostat. (Figure modified from Weimer*, et al.* 2024)

*2.3.5.2 BES Operation*

After setting up, the reactors were sterilized by autoclaving. Under sterile conditions, 300 mL DM9 media supplemented with 1.5 g/L glucose was filled into each reactor. The cathode chamber was filled with DM9 salt solution, and the reference electrode chamber was filled with sterile saturated potassium chloride solution. Afterward, the counter and reference electrodes were sterilized with 80% ethanol, placed in the respective chambers, and connected to the anode and the potentiostat (Bio-logic science instrument, Seyssinet-Pariset, France). The headspace of the reactors was gassed with nitrogen (~20 mL/min) through a sterile syringe membrane filter (pore size of 0.22 µm) to ensure anaerobic conditions. The reactors were mixed at 400 rpm via a magnetic stirrer, the working chamber was heated to 30 °C, and the connected condensers cooled at 10 °C to decrease evaporation. Finally, the working electrode potential was set to 0.5 V vs. Ag/AgCl/$KCl_{sat}$ for the majority of BES experiments, and the monitoring of the current output signal was started. After reaching a stable baseline signal, the redox mediator was added through the injection port using a syringe. Unless otherwise indicated, the experiments were conducted using 1 mM FeCN as redox mediator.

For the inoculation of the BES reactors, bacterial cell material was obtained by cultivation under aerobic conditions in DM9 media, as described above. The cells were harvested at the end of the exponential growth phase at an $OD_{600}$ of ~3. All BES reactors were started with an initial $OD_{600}$ of ~1. For this purpose, a respective preculture volume was centrifuged at 7,000 g and 25 °C for 10 min, resuspended in fresh DM9 media without glucose, and injected into the BES reactor using a syringe. After inoculation and after every 24 h, samples were taken from each reactor, and $OD_{600}$, mediator concentration, pH, and exo-metabolite concentrations were measured.

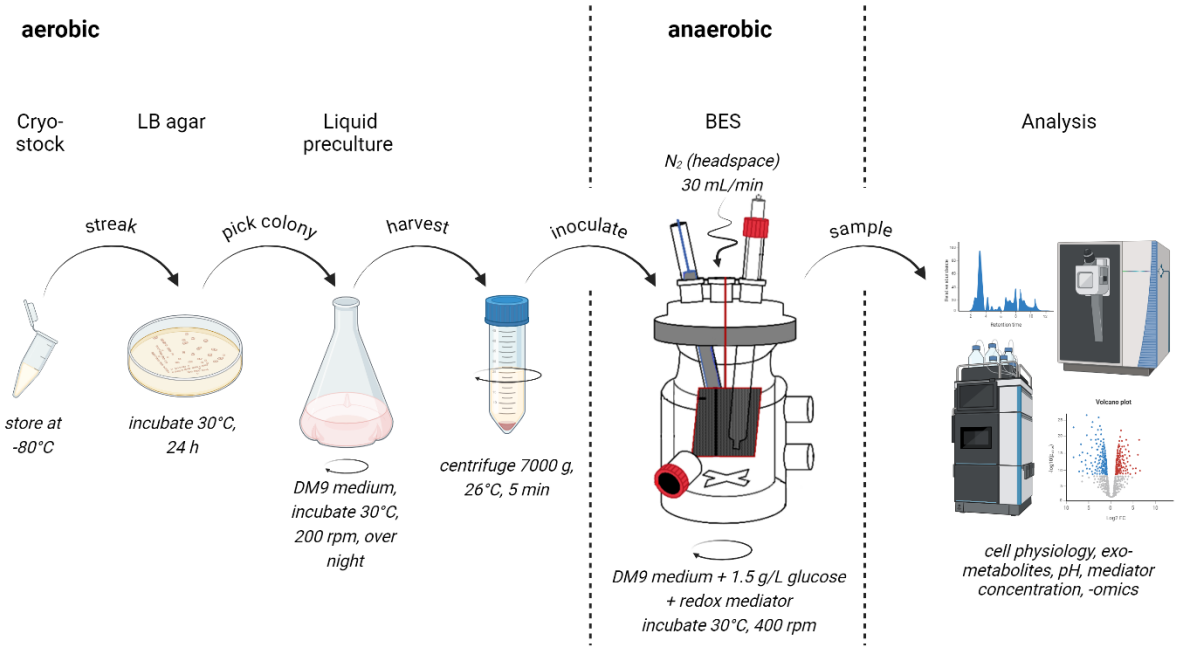


**Figure 6. Standard procedure of a BES-fermentation with *P. putida*.** Cell material for the BES reactor inoculation was obtained under aerobic conditions. LB plates were inoculated from cryo-stocks, and formed single colonies used for the inoculation of liquid precultures. After incubation overnight at 30 °C and 200 rpm, the cell material was harvested by centrifugation at 7,000 g for 5 min. The BES fermentation was run under anaerobic conditions. Samples were taken in a regular manner and analyzed for cell physiology, exo-metabolites, pH, mediator concentration, and -omics.

### *2.3.5.3 BES Operation for the Comparison of Exogenous vs Endogenous Redox Mediators*

An exception to the standard operation protocol for BES fermentation was made for experiments comparing the usage of an endogenous vs. exogenous redox mediator.

The production of the endogenous redox mediator PCA by the strain *P. putida* KT-PCA is only possible under aerobic conditions. Therefore, instead of growing the bacterial cell material in shaking flasks, the cells were grown directly in the BES reactors using Delft media with 3 g/L glucose and $Km^{50}$ instead of DM9 media. After setting up the BES, the media inside of the reactors was bubbled with 50 mL/min compressed air, and no potential was applied. The reactors were then inoculated with cell material of *P. putida* KT-PCA or KT-control, respectively. The strain *P. putida* KT-control only contained the empty vector with the kanamycin resistance and was, therefore, unable to produce PCA. After incubation for 3 h, 1 M of sodium salicylate was added to induce the production of PCA. The reactors were then further incubated for about 24 h until an $OD_{600}$ of ~1 was reached. The concentrations of glucose and PCA were measured via HPLC. Based on the PCA concentration, the concentration of FeCN in the reactors containing the KT-control was adjusted to the same level. Also, glucose was added to reach a concentration of 2 g/L in each reactor. Afterward, the aerobic mode was switched to the anaerobic mode by exchanging the compressed air bubbling with flushing the headspace with nitrogen at a rate

of 20-30 mL/min. Simultaneously, a potential of 0.5 $V_{Ag/AgCl}$ for FeCN-containing reactors and 0.2 $V_{Ag/AgCl}$ for PCA-containing reactors was applied. Finally, the pH was readjusted to a value of 7.0 by the addition of sodium hydroxide (NaOH). The following sampling and analysis were done as described before.

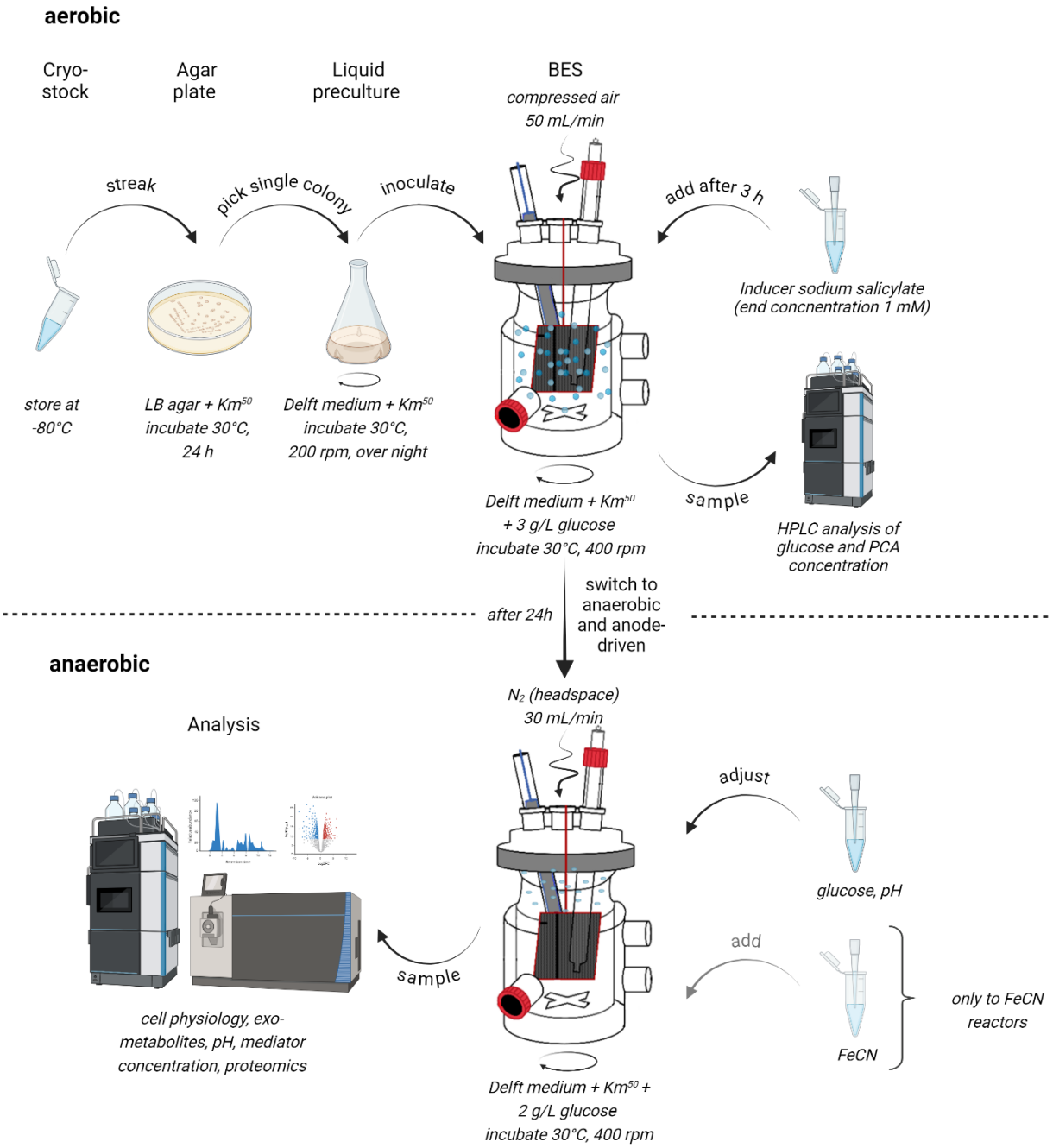


**Figure 7. Procedure for comparison of exogenous vs endogenous redox mediator with *P. putida*.** Cell material was grown in the BES reactors directly under aerobic conditions for PCA secretion. LB plates were inoculated from cryo-stocks, and formed single colonies used for the inoculation of small liquid precultures. After incubation overnight at 30 °C and 200 rpm, the preculture was used for the inoculation of the Delft medium in the BES to an $OD_{600}$ of 0.1. Aerobic conditions were ensured by gassing compressed air into the medium with 50 mL/min. PCA expression was induced 3 h after inoculation by the addition of sodium salicylate to an end concentration of 1 mM. After an OD600 of ~1 was reached, BES conditions were switched to anaerobic by gassing the headspace with 30 mL/min $N_2$ and applying potential. Samples were taken in a regular manner and analyzed for cell physiology, exo-metabolites, pH, mediator concentration, and proteomics.

## 2.4 Analytical Methods

### 2.4.1 Measurement of Extracellular Metabolites

Supernatants from shake flasks and BES reactors were obtained by centrifuging liquid samples at 4 °C and 17,000 g for 10 min. The obtained supernatants were then stored at -20 °C until further analysis. High-performance liquid chromatography (UltiMate 3,000, Thermo Fisher Scientific, Massachusetts, USA) with a Hi-Plex H column (PL1170-6830, 300 x 7.7 mm, Agilent Technologies) was used to detect and quantify glucose and organic acids (including gluconate, 2-KG, acetate, succinate, pyruvate, formate, etc.) (Lai*, et al.* 2016a)For organic acids, 14 mM sulfuric acid (H2SO4) was used as mobile phase with a flow rate of 0.4 mL/min for 38 min. The column oven was heated to 40 °C. The detection was done via a UV/Vis detector at 210 nm. Glucose was analyzed using water as eluent with a constant flow rate of 0.4 mL/min for 22 min. The column compartment was cooled to 15 °C, and a refractive index detector (RefractoMax320, ERC, Czech Republic) was employed for detection.

### 2.4.2 Isotopic Labeling Measurements

For the isotope tracer experiments in BES, precultures were grown in media with naturally labeled glucose as substrate and then inoculated into BES reactors containing $^{13}C_6$-glucose (99%, BIOMOL GmbH).

The presence of acetate, as well as its mass isotopomer distribution, were verified and determined using ion chromatography (Dionex™ ICS-6,000 Capillary HPIC™ System, Thermo Fischer) coupled to a mass spectrometer (Orbitrap Exploris™ 240, Thermo Fischer) (IC-MS). The supernatants were desalted using butanol extraction to prepare the samples for IC-MS. For this purpose, the pH of the samples was decreased to 1-2 by the addition of $H_2SO_4$. At a low pH, salt molecules will be converted into neutral or less charged forms, which in turn enhances their solubilities in the butanol phase and makes the extraction more efficient. Subsequently, 1-butanol was added in a ratio of 1:1 and mixed thoroughly. While the acetic acid is extracted to the organic phase, the salts will remain in the aqueous phase; hence, the butanol phase was used for the IC-MS measurement. Afterwards, 20% of methanol and KOH (final concentration of 1 mM) was added to the desalted samples. For ion chromatography, a Dionex™ IonPac™ AS11-HC IC column was used. The eluent flow was adjusted to 0.38 mL/min, and the injection volume was set to 10 µL. The sodium hydroxide concentration of the eluent was gradually increased from 1 mM to 60 mM over the course of 33 min for elution plus 10 mins for equilibration. The regenerant pump was set to 0.5 mL/min, and via a make-up pump, methanol was spiked into the flow with 0.15 mL/min to improve the ESI efficiency. The MS was operated in targeted data-dependent

MS2 mode in the range of 40-200 m/z with a vaporizer temperature of 300 °C and ion transfer tuber temperature of 325 °C.

The mass isotopomer distribution of secreted acetate was also determined using a gas chromatograph coupled to mass spectrometry (GC-MS) (Agilent 7890A, Quadrupole Mass Selective Detector 5975C, Agilent Technologies, Santa Clara, California, USA). The instrument was equipped with an HP-5MS column as stationary phase (30 m, 250 × 0.25 µm, Agilent Technologies). Helium (5.0) was used as the mobile phase. Before analysis, acetate was derivatized with n-pentanol, followed by extraction with n-hexane (Adler*, et al.* 2013; Adler*, et al.* 2014). For this, 50 µl of culture supernatant was mixed with 100 µl $H_2SO_4$ (10% vol/vol) and 20 µL n-pentanol, incubated at 80 °C for 15 min, subsequently cooled down to 5 °C and extracted with 200 µl n-hexane. The oven program was as follows: 75 °C for 2 min, ramp: 25 °C $min^{-1}$, final temperature: 300 °C). Samples were analyzed in selected ion monitoring (SIM) mode at *m/z* 43 to 45 to obtain the mass isotopomer fractions m+0, m+1 and m+2 of a fragment ion that contained both carbon atoms of acetate. For method validation, 0.5% (w/v) solutions of naturally labeled sodium acetate and [$^{13}C_2$] acetic acid (99% isotopic purity, Cambridge Isotopes) were treated as described above and the respective ion clusters were evaluated.

The obtained $^{13}C$ enrichment data was corrected for the natural abundance of $^{13}C$ to differentiate the labeling obtained by the supplied labeled substrate from the naturally occurring $^{13}C$ (van Winden*, et al.* 2002). This calculation is crucial as approximately 1.1% of all carbon atoms naturally occur as $^{13}C$. The corrected enrichment values were then quantified by summed fractional labeling (SFL) (Wittmann; Heinzle 2005), where the fractional abundance of all isotopologues containing at least one $^{13}C$ atom are summed up.

$$SFL = \frac{\sum abundance\ of\ labeled\ isotopologues}{\sum abundance\ of\ all\ isotopolgues}$$

### 2.4.3 Measurement of Redox Mediators

#### *2.4.3.1 Redox Mediator Concentrations*

The concentration of FeCN and its reduced form, ferrocyanide, can be quantified using a colorimetric method of measuring the optical density of the supernatant at 420 nm and 320 nm, respectively (Lai, et al., 2016).

The concentrations of all other used redox mediators were determined via HPLC (UltiMate 3,000, Thermo Fisher Scientific, USA).

For quantification of PCA, an Acclaim™ 120 C-18 column (Thermo Fisher Scientific, USA) and UV/Vis detection at 363 nm was used. The analysis protocol was adapted from (Askitosari*, et al.* 2020). Eluents

were 0.1% trifluoroacetic acid in water (eluent A) and 0.1% trifluoroacetic acid in acetonitrile (eluent B). The flow rate was constantly 1 mL/min, but the share of the eluents was changed over time. During the first 2 min, 90% eluent A and 10% eluent B were used, and the share of eluent B then constantly increased to 50% after 12 min, then 70% after 20 min, and 100% after 21 min after injection. The column was then washed with 100% eluent B for 5 min, and finally, the share of eluent A again increased to 90% until 27 min and kept steady for the last min. The oven temperature was set to 20 °C.

The concentrations of 1.4-benzoquinone (BQ), duroquinone (DQ), and anthraquinone-2,6-disulfonate (AQDS) were as well determined via HPLC (UltiMate 3,000, Thermo Fisher Scientific, Massachusetts, USA), but with a Primesep 100 (Sielc Technologies, USA) column. 0.1% trifluoroacetic acid in water was again used as eluent A and pure acetonitrile as eluent B. The starting condition was once more set to 90% eluent A and 10% eluent B, followed by a slight increase of eluent B first to 15% in 4 min, and then to 35% until 8 min after injection. During the next 2 min, the share of eluent B was further increased to 100%, and the column flushed for 4 min. Afterward, the share of eluent A was rapidly increased back to 90% in 1 min, and the column was then washed with constant eluent composition for 5 min. The flow rate was 0.6 mL/min over the entire course of the run, and the oven temperature was set to 35 °C. Detection of the analytes was done via UV/Vis at 210 and 280 nm.

#### *2.4.3.2 Stability Measurement of Redox Mediators*

To determine the stability of BQ, DQ, and AQDS in DM9 minimal media at 30 °C, standard solutions of different concentrations of each redox mediator in DM9 media were prepared and placed in the HPLC sample vial compartment, which was heated to 30 °C. Each sample was analyzed every 24 h with the HPLC method developed for BQ, DQ, and AQDS, described above, and the differences in the measured concentrations were calculated.

#### *2.4.3.3 Redox-Potential Determination of Mediators*

Cyclic voltammetry measurements were used to identify the midpoint redox potentials of the different redox mediators under the applied BES conditions. Concentrations of 0.1 and 0.5 mM of the different redox mediators were added into BES reactors filled with DM9 media (pH 7), respectively. The cathode and reference electrode chambers were filled with DM9 salt solution and saturated KCl solution as usual. The reactors were heated to 30 °C before the measurements. During the measurement, the applied working electrode potential was adapted to the respective redox mediator, swept between -1 and 1 V, with a scan rate of 10 mV/s. The midpoint redox potentials were calculated as the average between anodic and cathodic peak potentials.

### 2.4.4 Flux Balance Analysis

Flux balance analysis was conducted based on the product yields on glucose and glucose consumption rates over BES fermentations. The product yields ($Y_{p/s}$, [mmol_product/mmol_glucose]) were calculated by plotting the product (i.e. gluconate, 2-KG, acetate, pyruvate) concentration versus glucose concentration over the BES batches, where the absolute value of the slope of a linear fit represented the yield. Due to the dynamic biomass change over the BES batch, the specific glucose consumption rate ($r_s$, [mmol/$g_{CDW}$/h]) was calculated in two steps: 1) the rate in the unit of [mmol/L/h] was calculated by plotting the glucose concentration versus time over the batch; 2) the rate value was then further divided by an integral averaged biomass density ([$g_{CDW}$/L]) to reach the unit of [mmol/$g_{CDW}$/h]. The flux of the product was then calculated using the formula $r_p = r_s * Y_{p/s}$.

### 2.4.5 Proteomics

#### *2.4.5.1 Proteomics Sample Processing and Measurement*

A shotgun/bottom-up proteomics approach was applied to analyze protein composition changes before and after BES fermentation. Two mL of sample was taken from the precultures and from each bioreactor at 24 h, 100 h, and 380 h after inoculation. The samples were immediately centrifuged at 13,000 g for 1 min at 4 °C, and the obtained cell pellets were frozen in liquid nitrogen and stored at -80 °C until further processing.

The cell pellets were resuspended in 50 µL of 50 mM ammonium bicarbonate buffer for sample processing. Three cycles of freeze-thaw were carried out to disrupt the cells. For this purpose, the pellets were subjected to alternated freezing in liquid nitrogen and heating at 40 °C and 750 rpm for 60 s. After the last round, the samples were placed in an ultrasonic bath for 30 s. Further processing was carried out with only 10 µg of proteins. Quantification of the protein concentration was done by the usage of a 2D-Quant kit (Cytiva, USA). As an internal standard, 0.04 µg of GapDH (from *Staphylococcus aureus* Mrsa252, 336 aa residues) was added. The disulfide bonds of the cysteines in the proteins were reduced by the addition of 1 µL of 1 M Dithiothreitol and incubation at 30 °C for 1 h and 400 rpm. Afterwards, 15 µL of 400 mM 2-iodoacetamide was added to prevent the re-oxidation. The samples were again incubated for 1 h at 400 rpm and room temperature in the dark. The proteins were digested due to the addition of 6.3 µg trypsin (from porcine, sequencing grade, Promega, USA). After incubation overnight at 37 °C and 400 rpm, the reaction was stopped by adding 1 µL of 100% formic acid. ZipTip-µC18 columns (Merck Millipore, Merck KGaA, Germany) were used to desalt the samples to decrease ion suppression in the ionization. Finally, the samples were lyophilized and stored at -80 °C until analysis.

Just before the measurement, the samples were resuspended in 0.1% formic acid in water and subsequently analyzed using a nano-liquid chromatograph (nLC; Dionex Ultimate 3,000RSLC, Thermo Scientific, USA) connected to an Orbitrap Fusion™ Tribrid™ tandem mass spectrometer (MS/MS; Thermo Scientific, USA). The measurement parameters were adjusted according to (Seidel*, et al.* 2018).

#### *2.4.5.2 Proteomics Data Analysis*

The data obtained from the measurement of the proteomics samples were analyzed using the software program Proteome Discoverer (Version 2.4, Thermo Fisher Scientific, USA). SequestHT was used as the search engine with the *P. putida* KT2440 genome database from UniProt. In the applied workflow, trypsin was denoted as the digestion enzyme with a cleavage error allowance of up to 2. A mass tolerance of 0.1 Da and 3 ppm was set to determine fragment and precursor ions. Furthermore, the Target Decoy PSM Evaluator module was used to maintain a false discovery rate (FDR) of below 1%, and to obtain intensity-based label-free quantification of protein abundance, the Minora module implemented in Proteome Discoverer was activated. The proteins identified by the Proteome Discoverer workflow were cleaned from contaminants, normalized by mean subtraction, and $Log_2$ transformed. Samples from BES reactors were compared to the aerobic precultures using the students' T-test. Here, changes were only chosen to be significant when the calculated p-value was smaller than 0.05, and the $Log_2$ fold change ($Log_2$(FC)) was higher than 1 or lower than -1, respectively. For proteins that could not be identified in both compared conditions (preculture and BES), the missing values were replaced by a small imputed value ($10^{-9}$) to enable the following calculations without losing these proteins in the analysis. It has to be stated that the resulting $Log_2$(FC) values for these condition-exclusive proteins do not reflect a quantitative difference in the expression but rather only indicate their presence or absence, respectively.

### 2.4.6 ATP Measurement

#### *2.4.6.1 Sample Processing*

For the quenching and extraction of intracellular metabolites, especially ATP, an approach using hot ethanol was chosen (Wordofa*, et al.* 2017). Samples containing ~2.5 mg of CDW were taken from aerobic precultures and BES reactors and rapidly processed. The bacterial cell material was harvested by vacuum filtration (cellulose membrane filters, pore size of 0.22 µm, Millipore). The filters with the bacterial cells were then transferred into falcon tubes containing 4 mL of boiling ethanol (ethanol/water 75:25, 70 °C), vortexed for 30 s to extract the intracellular metabolites, and transferred into liquid nitrogen. The samples were then stored at -80 °C until further processing. Finally, samples from -80 °C were thawed and centrifuged for 5 min at 17,000 g and 4 °C. The cell pellets were discarded, and the supernatant was lyophilized and stored at -80 °C until analysis.

*2.4.6.2 ATP Measurement via Luminescence Assay Kit*

The ATP, ADP, and AMP amounts in the aerobic precultures and BES reactors samples were analyzed via luminescence ATP assay (ab113849 – Luminescent ATP Detection Assay Kit, Abcam, United States). The freeze-dried metabolites were diluted in 500 µL assay buffer and centrifuged for 5 min at 17,000 g and 4 °C to remove possible remaining cell debris and filter parts. The supernatant was transferred into spin filter columns (10 kDa, Vivaspin 500, GE Healthcare, UK) to remove cellular proteins that would otherwise interfere with the assay. The columns were centrifuged for 30 min at 12,000 g and 4 °C, and the deproteinized extract was divided into 3 aliquots. As the luminescence assay is specialized for the quantification of ATP, the ADP and AMP in the sample have to be transformed into ATP first. For the transformation of ADP to ATP, one share of the extract (100 µL) was incubated with 25 µL of a reaction buffer containing 75 mM potassium phosphate (pH 7.3), 15 mM magnesium chloride, 0.5 mM phosphoenolpyruvate and 20 µg pyruvate kinase. To also transform AMP to ATP, another share of the extract (100 µL) was incubated with 25 µL of a second reaction buffer, which contained 25 µg myokinase. Both reaction mixes were incubated for 15 min at 37 °C, and the enzyme activity was then stopped by heating for 2 min to 100 °C. Afterward, the ATP quantification of the three extracts was determined by following the luminescence assay kit protocol. ADP and AMP concentrations were determined from the differences in the ATP concentrations in the respective samples. The calculation of the adenylate energy charge (AEC) was done according to the following formula:

$$AEC = \frac{[ATP] + \frac{1}{2}[ADP]}{[ATP] + [ADP] + AMP}$$

**2.4.7 Polyphosphate Measurement**

Polyphosphate (polyP) granules in bacterial cells can be visible in scanning electron microscopy (SEM). Energy dispersive X-ray chromatography (EDX) was used to identify the elemental composition of the granules. Subsequently, Raman spectroscopy was applied to verify if the granules consist of polyP.

*2.4.7.1 Sample Preparation for Visualization of PolyP*

For SEM, EDX, and Raman spectroscopy, bacterial cells cannot contain any water. Hence, the water in the cells has to be removed without destroying the cell structure. A cell fixing and dehydration procedure developed by Dr. Hryhoriy Stryhanyuk (ProVIS, UFZ, Germany) was applied to achieve this. A sample (2 mL, $OD_{600}$ of ~1) of bacterial cell material from an aerobic preculture and a BES reactor after 250 h of fermentation was taken and centrifuged at 15,000 g for 5 min and 4 °C. The supernatant was discarded, and the resulting cell pellet was resuspended in 1 mL of 2% paraformaldehyde in sodium cacodylate buffer (CaO buffer; 0.2 M, pH 7.4), vortexed and incubated at 4 °C, overnight, to

end all metabolic activities of the cells. Afterward, the procedure for the SEM and EDX samples had to be slightly changed compared to the preparation of the samples for the Raman spectroscopy. For SEM and EDX, the cells were placed on a filter (iso pore, pore size of 0.22 µm) and fixed using hydrogen peroxide ($H_2O_2$). For EDX, the filter has to be conductive; hence, it was first coated in chrome using a sputter coater (SCD050, Leica, Germany). Then, the cells were placed on the coated filter via a filtration unit; the filter was placed in 1% $H_2O_2$ and incubated for 30 min. Afterward, the water in the cells was replaced by ethanol to enable the subsequent drying procedure. For this purpose, the cells were successively placed in six ethanol solutions with increasing ethanol concentrations (30 %, 50 %, 70 %, 90 %, 95 %, and 100 %). Each step of this ethanol series was incubated for 2 min, and the filter was then transferred to the next solution without allowing the filter to dry. Once the cells on the filter reached the absolute (100 %) ethanol solution, the ethanol was evaporated to obtain dry cells using a critical point dryer (EM CPD300, Leica, Germany). For Raman spectroscopy, it was not possible to place the cells on a filter, as the filter material would cause a disturbing background signal. Therefore, the cells were placed on a metal SEM plate instead, as metal does not induce Raman shifts. For this purpose, the ethanol series was carried out in an Eppendorf tube. The paraformaldehyde-treated sample was centrifuged at 7,000 g and 4 °C for 10 min, and the supernatant was discarded to obtain a cell pellet. The cells were then fixed by adding 1% $H_2O_2$ in CaO buffer into the Eppendorf tube and resuspension of the pellet. Afterward, the cells were subjected to an ethanol series in the same concentrations described for the SEM and EDX samples. The former solution was always exchanged by centrifuging the sample for 10 min at 7,000 g and 4 °C and discarding the supernatant. In this process, it was made sure that the cell pellet never dried out. When the cells were finally dissolved in 100% ethanol, the cell suspension was dropped on the metal SEM plate and air-dried.

#### *2.4.7.2 SEM and EDX*

The dried bacterial cells on the chrome-coated filter were visualized using a high-resolution scanning electron microscope (Zeiss Merlin VP Compact, Carl Zeiss Microscopy, Oberkochen, Germany). The electron acceleration applied was 2 kV, and the imaging of the secondary electrons was done with an Everhard-Thornley-type detector. EDX (Bruker Quantax X-Flash, Bruker Nano GmbH) was additionally coupled to the SEM to identify the elemental composition of the sample, with a special focus on phosphorus.

#### *2.4.7.3 Confocal Raman Micro-Spectroscopy*

For the identification of the compound in which the detected phosphorus was present, a confocal Raman microscope (WITec alpha300Ra, WITec GmbH, Germany) was used. The laser power of the 785 nm infrared laser (WITech GmbH, Germany), which served as the excitation light source, was set to

4.6 mW. The Raman measurement spots were chosen based on previously acquired SEM overview images. An integration time of 0.5 s and 300 spectra accumulations per analysis were chosen. The Raman spectra were acquired by a grating monochromator coupled Peltier-cooled CCD detector (600 g/mm grating, UHTS 300, WITech, Germany).

# 3. Results

The following results outline the key findings of this study about the anodic electro-fermentation with *P. putida* and are presented in four sections. The first section focuses on unraveling the anaerobic glucose uptake of *P. putida*. The second part shows results from a systems biology analysis of the electrogenic phenotype. The third section investigates the role of polyP for energy generation in BES. Finally, in the fourth part, different redox mediators were tested and compared regarding their influence on the BES fermentation.

## 3.1 Benchmark BES Performance of *P. putida* with FeCN

To evaluate the performance of *P. putida* in BES, an example of a classical BES run with *P. putida* KT2440 and FeCN as redox mediator under standard conditions is shown in Figure 8. The duration of the process, the current output profile as well, as the rates of glucose consumption and product formation can vary due to biological variance, and the BES performance of *P. putida* under standard conditions was already established in previous studies (Lai*, et al.* 2019). Nevertheless, this figure serves as a benchmark to enhance the understanding of the subsequent results.

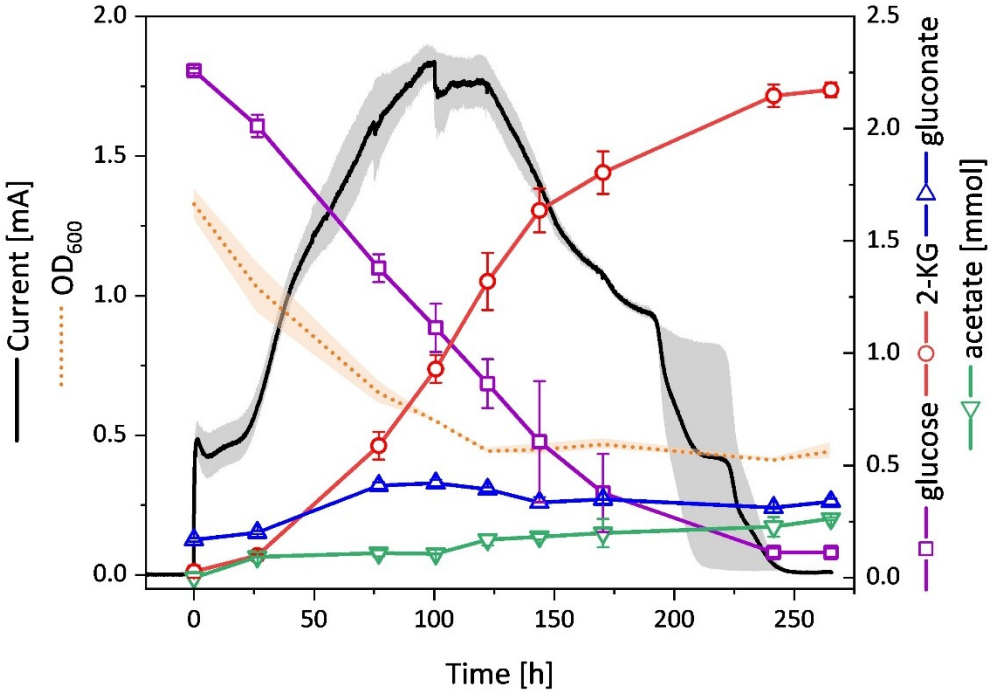


**Figure 8. Benchmark performance of *P. putida* KT2440 in BES.** The left y-axis indicates the current output of the respective BES fermentations, and the right y-axis shows the number of metabolites (mmol) in the reactors. The line or line-symbol presented the averaged values and the shading indicates the standard deviations of biological replicates (n=3).

During anodic electro-fermentation, a current output signal can be measured. This signal resembles the electrons transferred from the cells to the anode via the redox mediator. Therefore, the metabolic activity of the cells can be derived from this signal. When 1 mM of FeCN is used as mediator, the current profile rises initially as the reactors are inoculated with biomass, followed by an adaptation time with a relatively constant current. Subsequently, the signal increases constantly until a peak current of about 1.7 mA is reached. After a plateau with constant current, the signal will decrease until the baseline is reached. The wild-type needs about 250 h on average to consume the 2.4 mmol of glucose initially supplied as the sole carbon source in the system. Most glucose is transformed with very high yields above 90% into the main end product 2-KG. As 2-KG is produced in the periplasm by glucose oxidation, the carbon metabolism is mainly constrained to the periplasmic space. The main byproduct is acetate, but small amounts of pyruvate, succinate, or lactate are also often released. These organic acids originate from the central carbon metabolism in the cytosol. However, the rate of glucose consumption is drastically decreased to only about 5% of the rate under aerobic standard conditions. As there is no cell growth, the biomass density decreases from an initial $OD_{600}$ of 1.3 to 0.6 during the first 76 h after inoculation. For the remaining time of the BES fermentation, the biomass density stays roughly stable at an $OD_{600}$ around 0.45.

## 3.2 Anaerobic Glucose Uptake of *P. putida* KT2440 in BES

This part was published in Microbial Biotechnology, **2023**, DOI: 10.1111/1751-7915.14375

Even though it was shown that *P. putida* can use glucose as the sole substrate for high-yield product generation under anaerobic and anode-driven conditions in a BES (Lai*, et al.* 2016b), the exact uptake pathway remained a significant knowledge gap. Therefore, an extensive study was conducted to unravel the glucose uptake in *P. putida* cells in BES with FeCN as a redox mediator. As described earlier, *P. putida* has three potential pathways to convert glucose into gluconate-6-phosphate (the common entry point into cytosolic central metabolism). After the glucose is taken up into the periplasm, it can either be transported directly into the cytosol via glucose transporter (glcT pathway) or is oxidized in a periplasmic oxidation time one or two times to gluconate or 2-KG respectively, and then taken up via respective transporter (glaT and 2kgaT pathway). Each of these pathways results in a distinct NADPH yield (Figure 9). Under aerobic conditions, *P. putida* mainly takes up glucose via glaT pathway (Nikel, Chavarria et al. 2015, Kohlstedt and Wittmann 2019), which leads to a reduction of pyrroloquinoline quinone, but without affecting the NADPH pool directly. Carbon uptake via the 2kgaT pathway generates four electrons (PQQH2 and FADH2) but oxidizes one NADPH. The uptake via glcT pathway does not lead to periplasmic oxidation but requires one $NADP^+$ (or 2/3 $NAD^+$ and 1/3 $NADP^+$ proposed by (Olavarria, Marone et al. 2015)). The three pathways also pose different demands on ATP

hydrolysis. The glcT pathway was well-studied with outer membrane porin (Saravolac, Taylor et al. 1991) and inner membrane ABC transporter (Pandey, Modak et al. 2016) being involved, and requires two ATPs from glucose to reach the gluconate-6-phosphate. In contrast, the biochemical mechanisms of the gluconate and 2-KG transporters in *P. putida* are not yet understood. Still, it is generally accepted that they do not belong to the ABC transporter family and do not require the hydrolysis of ATP for their biochemical function (del Castillo, Ramos et al. 2007). Therefore, both glaT and 2kgaT pathways only require one ATP to convert glucose to gluconate-6-phosphate.

The following study unraveled the prevalent carbon uptake across the cytoplasmic membrane in *P. putida* KT2440 during anaerobic cultivation in a BES reactor. To find out which of the pathways is the favored one under BES conditions, three strains of *P. putida* KT440 were constructed, which could import glucose exclusively through only one of the three distinct pathways, while the other two were disabled through respective gene deletions. These strains were named KT-G, KT-GL, and KT-KG, corresponding to the glcT, glaT, and 2kgaT pathways, respectively (

Table 1; Figure 9). These knock-out (KO) mutants were cultivated in a BES either with naturally labeled glucose or fully labeled $^{13}C_6$-glucose as the sole substrate. Acetate is the only reliably detectable by-product of this electro-fermentation process and is exclusively produced in the cytosol. Therefore, the labeling information of the excreted acetate was used to quantify the amount of carbon from the substrate, which was ultimately transported into the cytosol and further metabolized there. The activity of glucose oxidation was studied through generated current, the formation of extracellular metabolites, the metabolization of $^{13}C_6$-glucose as an isotopic tracer, metabolic and flux balance analysis.

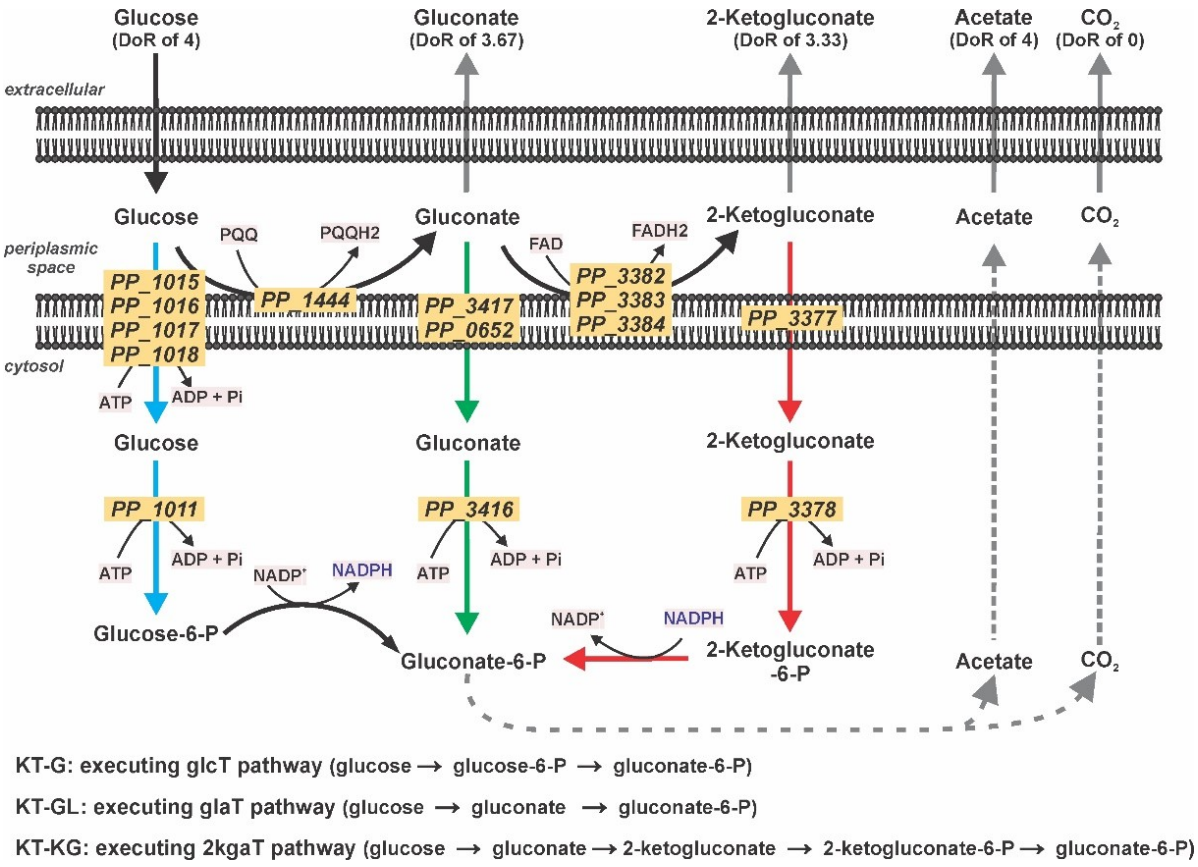


**Figure 9: Glucose oxidation pathways of *P. putida* in BES.** Three pathways exist to convert extracellular glucose to intracellular gluconate-6-P (which is further converted to acetate): Left (blue): via glucose (glcT pathway); Centre (green): via gluconate (glaT pathway); Right (red): via 2-KG (2kgaT pathway). The three deletion mutants KT-G, KT-GL, and KT-KG were engineered to each use only one of the three entry routes. Each pathway affects the $NADP^+$/NADPH ratio differently, as does the ATP demand. DoR: degree of reduction.

### 3.2.1 Effects of Gene Deletion of Sugar Kinases and Membrane Transporters on Aerobic Growth

In addition to molecular confirmation (e.g. by PCR of the cognate loci), the phenotypic nature of the respective gene deletions based on aerobic extracellular metabolite profiles was confirmed (Figure 10). The wild-type consumed glucose and produced gluconate and 2-KG as intermediate products during glucose-dependent growth. The secretion of gluconate/2-KG was eliminated for the KT-G strain, while

2-KG secretion was not detected for the KT-GL mutant. The KT-KG strain produced both intermediates but with higher 2-KG amounts than the wild-type strain.

The deletion of genes can lead to adverse effects on microbial growth and physiology (Takeuchi, Tamura et al. 2014). Therefore, we further determined the aerobic growth kinetics of the recombinant strains compared to the parental strain KT2440 (WT) (Figure 10**;**

Table 1). The mutant KT-GL exhibited a growth profile similar to that of the WT. In contrast, the growth of the strains KT-G and KT-KG was significantly impaired, with maximum growth rates only reaching about 50% of the WT. Additionally, forcing the utilization of the 2kgaT pathway (i.e. KT-KG strain) resulted in a more extended lag phase when cells were initially transferred from solid agar to liquid cultures (see 6. Appendix, Figure S1). Once the cells adapted to glucose conditions, this lag phase was eliminated in subsequent cultivations in a liquid medium.

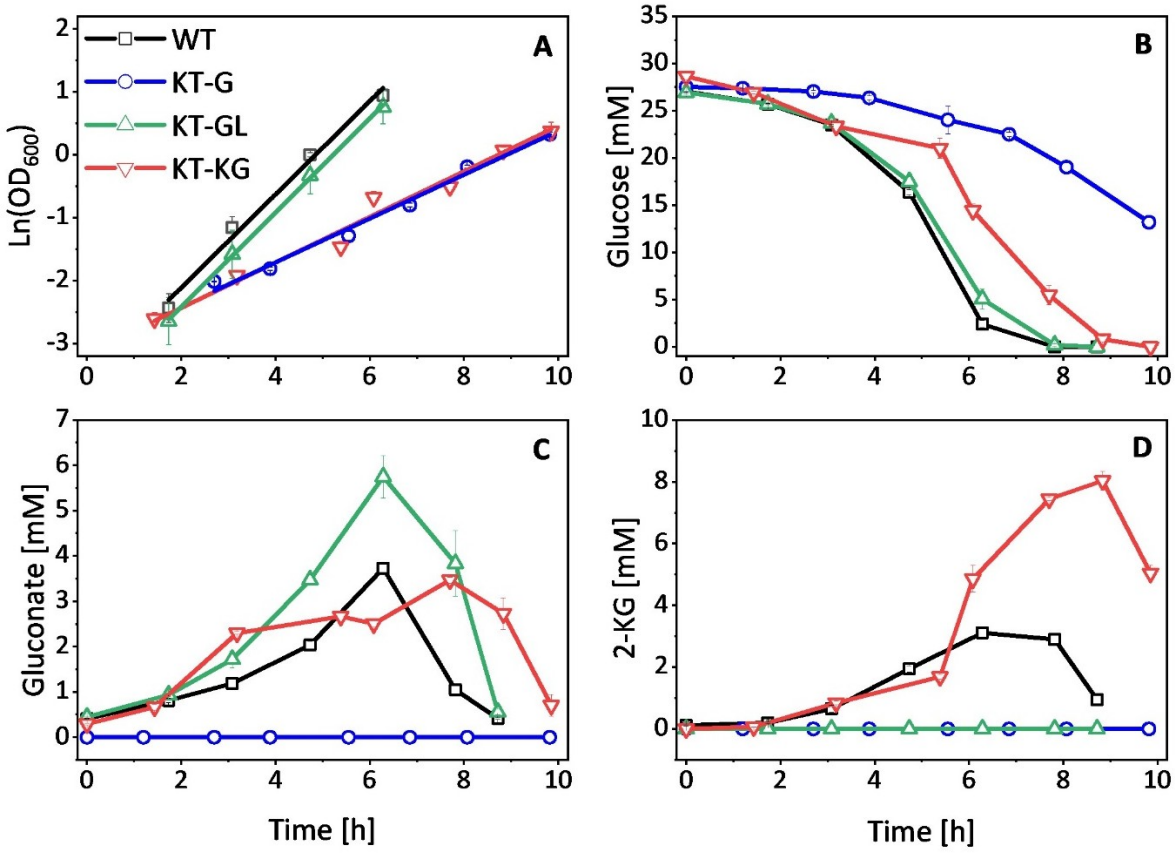


**Figure 10. Cultivation of *P. putida* KT2440 WT and three gene deletion mutants in minimal medium with glucose as substrate under aerobic conditions.** The growth of all four strains measured via $OD_{600}$ **(A)** and the extracellular concentrations of glucose, gluconate, and 2-KG in mmol **(B-D)** are depicted. The presented data are averages and standard deviations of 3 biological replicates. All cultures were inoculated to an $OD_{600}$ of about 0.1.

The gene deletions affected not only the growth rate but also the glucose consumption rate. Like the growth rate, KT-GL differed from the WT in terms of the specific glucose consumption rate and biomass yield (Table 3). However, despite the lower growth rate, KT-KG consumed glucose at a similar rate as the WT, especially when comparing the net glucose consumption after excluding the periplasmic intermediate products (Table 3). Despite the similar glucose uptake rate, the biomass yield for KT-KG was less than half of that for the WT, corresponding to the pattern of maximum growth rate. The opposite phenomenon was observed for the KT-G strain. The glucose consumption rate was decreased

by ~50% after the deletion of the glucose dehydrogenase gene, but the biomass yield remained at a comparable level to the WT.

**Table 3. Growth kinetics of wild-type *P. putida* KT2440 and the respective gene deletion mutants in minimal medium with glucose as substrate under aerobic conditions.** Rates and yields were calculated for the exponential growth phase from 3 biological replicates. The exponential growth phases for the WT, KT-G, KT-GL, and KT-KG were defined as 1.7 - 6.3 h ($R^2$ = 0.991), 3.9 - 9.8 h ($R^2$ = 0.993), 1.7 - 6.3 h ($R^2$ = 0.999) and 1.4 - 9.9 h ($R^2$ = 0.976) respectively (6. Appendix, Figure S2), corresponding to the timeline in Figure 10. The rate and yield values marked by * were calculated by excluding the periplasmic oxidative products (gluconate and 2-KG) from the calculations, thus indicating the net glucose being taken up into the cytosol during the exponential growth phases being examined. The growth curves determined using the Bio-Lector online cultivation were provided in Figure S3 in 6. Appendix. Abbreviations: $r_{glucose}$, specific glucose uptake rate; $Y_{x/s}$, biomass/glucose yield.

| *P. putida* strains | $\mu_{max}$ [$h^{-1}$] | $r_{glucose}$ [$mmol/g_{CDW}/h$] | $Y_{x/s}$ [$g_{CDW}/g_{glucose}$] | $*r_{glucose}$ [$mmol/g_{CDW}/h$] | $*Y_{x/s}$ [$g_{CDW}/g_{glucose}$] |
|---|---|---|---|---|---|
| KT2440 WT | 0.74 ± 0.05 | -14.17 ± 1.48 | 0.29 ± 0.02 | -10.69 ± 0.95 | 0.38 ± 0.02 |
| KT-G | 0.37 ± 0.00 | -7.99 ± 0.58 | 0.26 ± 0.02 | -7.99 ± 0.58 | 0.26 ± 0.02 |
| KT-GL | 0.75 ± 0.10 | -14.91 ± 4.40 | 0.28 ± 0.07 | -11.56 ± 3.08 | 0.36 ± 0.08 |
| KT-KG | 0.35 ± 0.00 | -16.77 ± 1.35 | 0.12 ± 0.01 | -11.92 ± 1.18 | 0.16 ± 0.02 |

### 3.2.2 Electrogenic Activity of *P. putida* Mutants during BES Fermentations

The electrogenic activity and the corresponding glucose metabolism of the WT and the three recombined strains were tested in the BES (Figure 11). The mutant KT-KG showed a similar pattern to the WT regarding current density and metabolic products. The peak current reached 1.56 ± 0.22 mA, slightly higher than that of the WT, but it took KT-KG about 200 h after inoculation, compared to ~120 h for WT (Figure 11 D). Glucose was consumed slower than in the WT at a rate of 0.08 ± 0.01 $mmol/g_{CDW}/h$ (Table 4), but the product spectrum was comparable, resulting mainly in glucose conversion to 2-KG.

In contrast, the strain KT-GL produced a lower current output with a peak of 0.80 ± 0.15 mA at ~150 h after inoculation (Figure 11 C) compared to the WT. Despite the lower current output, KT-GL consumed glucose at a rate (0.18 ± 0.00 $mmol/g_{CDW}/h$) about 55% faster than WT, with gluconate as the main end-product. In all, KT-GL was able to reach an extracellular electron transfer rate of 0.45 ± 0.01 $mmol_{electrons}/g_{CDW}/h$, only about 13% decrease from the value 0.51 ± 0.10 $mmol_{electrons}/g_{CDW}/h$ for the WT (Table 4). Regarding metabolic products from cytosolic metabolism, acetate was secreted as the only by-product of both KT-GL and KT-KG mutants. The molar acetate yield of KT-GL was the same as

that of the WT (both 7.1 ± 1.1%), while it was higher for KT-KG (17.5 ± 0.9%) (see 6. Appendix, Table S1). The carbon and electron balances for the strains that consumed significant amounts of glucose could be closed for each biological replicate and reached 100% and 101.1% for the WT, 101.3% and 102.2% for KT-GL, as well as 103.9% and 104.8% for KT-KG, respectively (see 6. Appendix, Table S1).

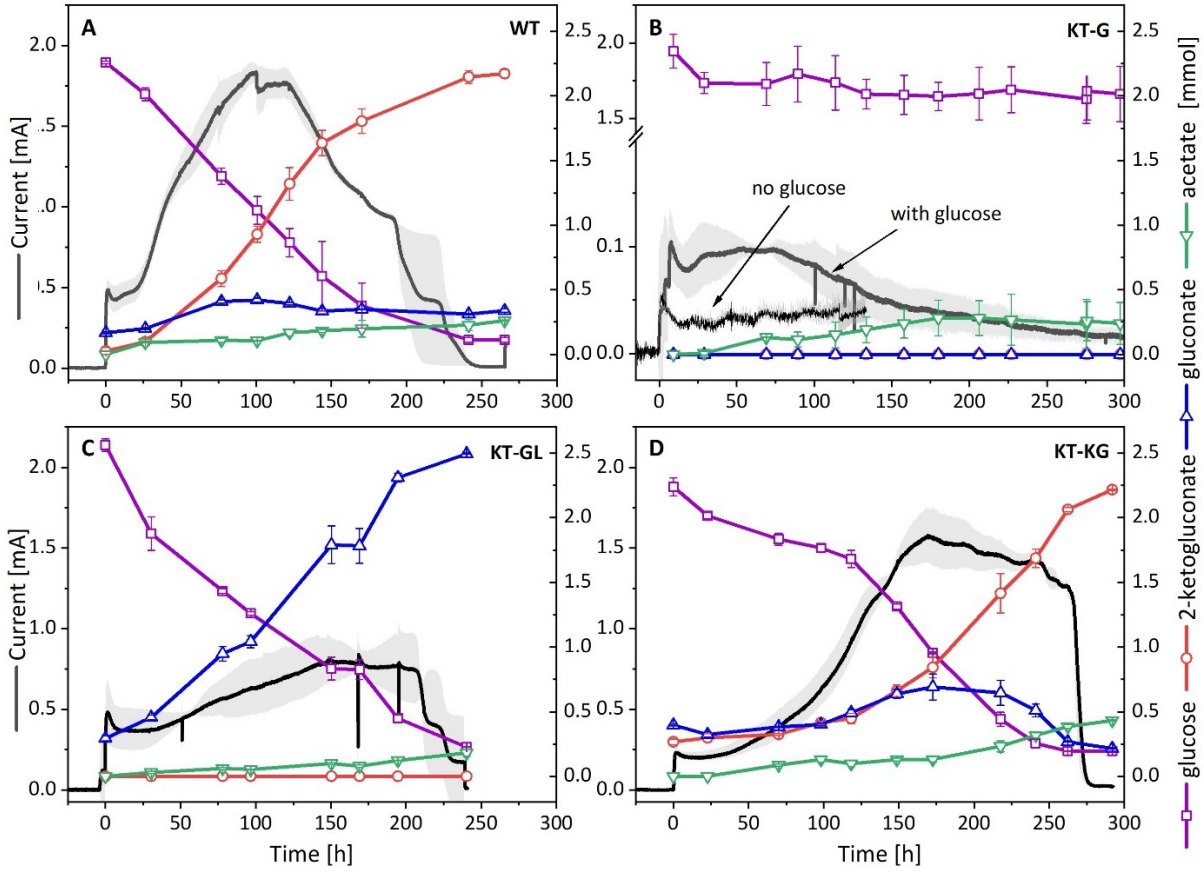


**Figure 11. Representative performance of *P. putida* KT2440 WT and the three gene deletion mutants in BES.** The left y-axis indicates the current output of the respective BES fermentations, and the right y-axis shows the number of metabolites (mmol) in the reactors. Due to the low sugar consumption by the KT-G mutant, a control experiment without glucose was conducted to check the current response from carbon carry-over originating from the preculture. The line or line-symbol presents the averaged values, and the shading indicates the standard deviations of biological replicates (n=3).

The current output measured for the strain KT-G was significantly lower compared to the other two mutants and the WT, with a peak current of only 0.09 ± 0.03 mA (Figure 11 B). The current output also only lasted for a short period. Furthermore, only about 0.3 mmol glucose was consumed by the KT-G mutant over 300 h of cultivation in BES, and the average consumption rate was only ~0.01 mmol/$g_{CDW}$/h (Table 4). No gluconate and 2-KG were detected; however, a similar amount of acetate was measured for KT-G as for the other strains (see 6. Appendix, Figure S8). In a control experiment without added glucose, there was also an observable current response (peak at around 0.05 mA) (Figure 11 B). This indicates that current output could also be generated from intracellular

metabolism when acetate formation is observed. A very low amount of pyruvate was measured in HPLC and further confirmed by GC-MS with isotopic tracer analysis. A similar low current output was also observed for the KT-GL strain, while gluconate was used as the sole substrate in the BES system. Only about 0.35 mmol gluconate was consumed and a similar amount of acetate to the glucose cases in BES was measured (see 6. Appendix, Figure S8 and Figure S10 A). Isotopic enrichment analysis also confirmed about 64% of the carbon in acetate came from the gluconate in the BES (see 6. Appendix, Figure S10 B).

**Table 4. Yields and rates of *P. putida* KT2440 and the respective gene deletion mutants in BES.** The standard deviations were calculated from at least four biological replicates (WT: 6 replicates with 55 data points; KT-G: 6 replicates with 51 data points; KT-GL: 4 replicates with 26 data points; KT-KG: 6 replicates with 56 data points). More information can be found in the supplementary material Table S1.

| *P. putida* strains | $Y_{mmol\_acetate/mmol\_glucose}$ | $Y_{mmol\_electrons/mmol\_glucose}$ | $r_{glucose}$ [mmol/$g_{CDW}$/h] | $r_{electrons}$ [mmol/$g_{CDW}$/h] |
|---|---|---|---|---|
| KT2440 WT | 0.07 ± 0.01 | 4.37 ± 0.08 | -0.19 ± 0.02 | 0.51 ± 0.10 |
| KT-G | 0.48 ± 0.06 | 0.17 ± 0.13 | -0.01 ± 0.01 | 0.002 ± 0.002 |
| KT-GL | 0.07 ± 0.01 | 2.44 ± 0.12 | -0.18 ± 0.01 | 0.45 ± 0.01 |
| KT-KG | 0.18 ± 0.01 | 4.69 ± 0.10 | -0.08 ± 0.01 | 0.39 ± 0.03 |

### 3.2.3 $^{13}C$ Enrichment in Extracellular Acetate during BES Fermentation

Acetate was the only significant by-product in all fermentations unrelated to the periplasmic oxidation pathway. We observed only small amounts of acetate after the BES fermentations. An increase in acetate formation was observed over the batch when glucose was provided. Still, a trace amount of acetate was detected in the BES controls without glucose addition (see 6. Appendix, Figure S8). To identify the origin of the carbon and to determine the ratio between glucose-derived acetate and acetate from other sources, we provided $^{13}C_6$-glucose as a carbon source and analyzed the $^{13}C$ enrichment in extracellular acetate using mass spectrometry (Figure 12).

For all strains, $^{13}C$ labeling was detected in acetate. After correcting for naturally occurring isotopes in the analytes, the summed fractional labeling (SFL) for carbon was calculated. The determined SFL values indicated a $^{13}C$ enrichment in acetate between ~26% for the KT-KG strain and about 50% for the KT-GL strain. This means that half of the carbon in the acetate could be traced back to the substrate $^{13}C_6$-glucose in the BES reactor in one case, while in other cases, the share was well below 50% and

carbon sources originating from the initial biomass inoculum (e.g. products of cell lysis in long BES experiments or usage of intracellular storage compounds, such as PHA, etc.) being the major contributor to acetate formation.

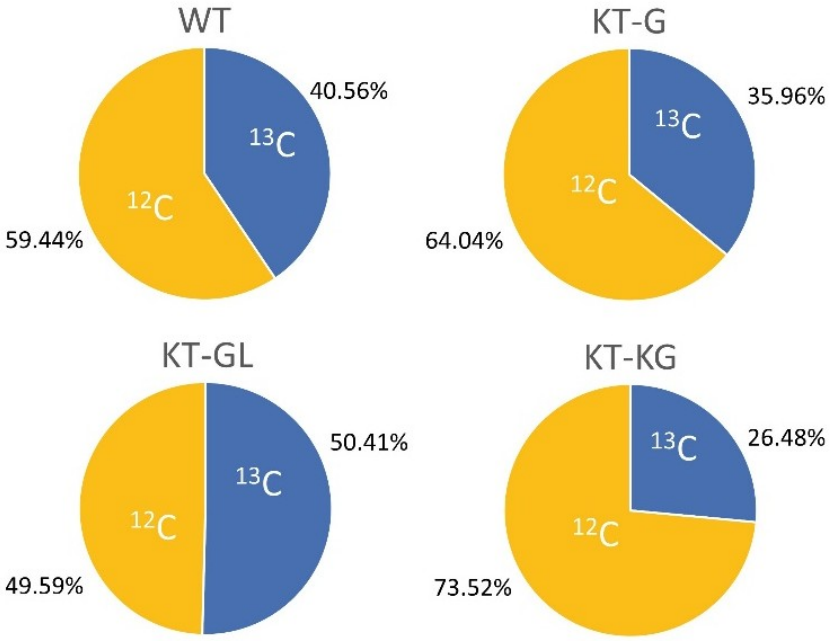


**Figure 12. The summed fractional labeling (SFL) of $^{13}C$ in endogenous acetate for the wild-type and recombinant strains in BES with $^{13}C_6$-glucose as the substrate.** The isotope enrichment was detected using both GC-MS and IC-MS on samples from three independent biological replicates. Color code: red, the $^{13}C$ originated from the de novo synthesis from the fed-in $^{13}C_6$-glucose; dark grey, the $^{12}C$ originated from other sources.

### 3.2.4 Flux Balance Analysis

A flux balance analysis was conducted to further elucidate the carbon and electron fluxes in the different strains in BES, based on measured and calculated rates (see 6. Appendix, Table S1) and the ratio of labeled vs non-labeled carbon in acetate. Due to the extremely low metabolic turnover for the KT-G strain, measurement uncertainties had a considerable impact. The carbon balance remained below 10% when accounting for carbon partitioning in acetate. Therefore, the flux balance analysis was only performed for the WT, KT-GL, and KT-KG strains (Figure 13).

The gene deletions only slightly altered the intracellular net fluxes. Despite the difference in terms of current densities, glucose consumption rates, and acetate production yields stated above, the three strains maintained the intracellular carbon flux through the Entner-Doudoroff pathway to pyruvate at low levels (3.4, 6.5, and 3.9 µmol/$g_{CDW}$/h for WT, KT-GL, and KT-KG, respectively). Relative to the glucose uptake rate, the highest glycolytic flux was observed in the KT-KG strain (Figure 13). Acetate production rates ranged from ~8 to ~14 µmol/$g_{CDW}$/h and were strongly influenced by acetate from

the unlabeled carbon pool (Biomass pool). In the KT-KG strain, the relative contribution of acetate production from biomass reached almost 13 % of the glucose uptake flux.

In a previous study, it was shown that cytochrome C reductase is the likely site of electron withdrawal by the mediator in *P. putida* (Lai*, et al.* 2020; Chukwubuikem*, et al.* 2021). When balancing the redox equivalents ($PQQH_2$, $FADH_2$, $UQH_2$, and NADH), it can be assumed that they enter the ETC at the usual sites and would contribute to the generation of a proton gradient accordingly. A further assumption considered charge balance. Per electron harvested via the anode, a positive charge has to be transferred to the cathode. It was assumed these charges are protons since $H_2$ formation is driven at the cathode. The number of protons translocated across the cytoplasmic membrane exceeds the charge transfer to the cathode. This means protons can drive the ATP synthase. Estimating the ATP synthase flux shows that the WT would have the highest absolute ATP flux available (47% better than the KT-KG strain), but in relative terms, KT-KG had the highest flux through the ATP synthase (Figure 13). For WT, KT-GL, and KT-KG, the substrate-level phosphorylation in lower glycolysis (at the level of phosphoglycerate and pyruvate kinase) will balance with sugar phosphorylation in the upper part of metabolism (at the level of glucokinase and phosphofructokinase), leaving only the ATP synthase as an additional source of ATP. In the KT-G strain, the upper part needs 2 mol ATP per mol of Gluconate-6P, which means that this route provides no net ATP gain. Compared to the lowest reported non-growth associated maintenance in aerobic *P. putida* KT2440 at 920 $\mu mol_{ATP}/g_{CDW}/h$ (Ebert, Kurth et al. 2011) or even in the genome-reduced *P. putida* KT2240 mutant at 710 $\mu mol_{ATP}/g_{CDW}/h$ (Lieder, Nikel et al. 2015), the maximum ATP generation of 147 $\mu mol_{ATP}/g_{CDW}/h$ for the wild-type under anaerobic and anode-driven conditions, might explain why cells are barely surviving in the BES.

When matching the anode-driven flux through the cytochrome C reductase with the fluxes producing redox equivalents, a small deviation could be observed. The anode harvested experimentally more electrons than the flux balance analysis suggests. This might indicate that the catabolism of biomass components towards acetate also released redox equivalents (Figure 13). This is experimentally supported by the observed currents in sugar-free control experiments (Figure 11 B).

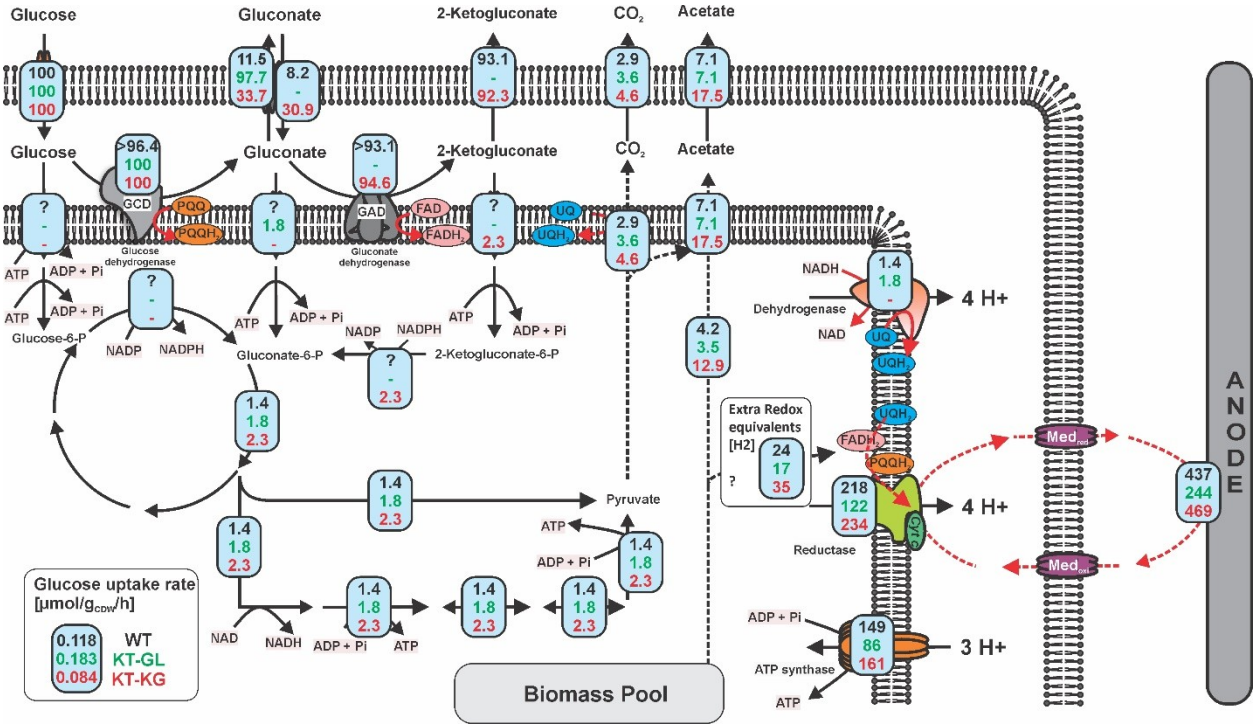


**Figure 13. Flux balance analysis maps for the *P. putida* KT2440 wild-type (black number), KT-GL (green number), and KT-KG (red numbers) strains in BES.** Fluxes are normalized to the glucose uptake rate in [mmol/$g_{CDW}$/h] and calculated based on 6. Appendix, Table S1. The fluxes through acetate and $CO_2$ were estimated based on the $^{13}C$ enrichment and on the assumption that cytoplasmic oxidation of sugar to acetate will release stoichiometric amounts of $CO_2$, while degradation of storage carbon (e.g. poly-hydroxybutyric acid) might not. The ATP rate was calculated based on the stoichiometric balance, considering the proton pumping effect of dehydrogenase and membrane reductase. In addition, the charge balance that one electron transferred to the anode would take one proton from the periplasm to the extracellular space. Three protons are assumed to be needed for the synthesis of one ATP molecule. The "?" in the flux indicates the uncertainties of the flux balance analysis, as it was unable to resolve the exact cross-membrane flux for the WT. Here, we assumed it followed the periplasmic oxidative pathway and then cytosolic glycolysis. The "-" means the respective pathway was metabolically not possible. '>' means a minimum flux is given. Also, a mismatch between anodic electrons and predicted reductase activity (2-electron process) could also point towards some redox equivalents originating from the biomass pool.

In conclusion, the different glucose uptake pathways in *P. putida* under anaerobic and anode-driven BES conditions exhibit distinct impacts on metabolic fluxes, growth rates, and current generation. The experiments with pathway-specific knockout mutants highlighted the glaT pathway as the most efficient for maintaining metabolic activity and extracellular electron transfer, even under energetically constrained conditions. However, the reduced ATP generation and the reliance on intracellular storage compounds for acetate production underscore the physiological limits of *P. putida* in BES. These findings emphasize the need for targeted metabolic engineering to enhance energy efficiency and substrate utilization in future BES applications.

## 3.3 Systems Biology of Electrogenic *P. putida* KT2440

Parts of the results of this section were published in Microbial Cell Factories, **2024**, https://doi.org/10.1186/s12934-024-02509-8.

In a collaborative effort, a systems biology approach was employed to deepen the current understanding of the physiology of *P. putida* KT2440 in the BES with FeCN as redox mediator. In the anode-driven and anaerobic system, *P. putida* has to face conditions characterized by the absence of oxygen and limitations in energy generation. Furthermore, as described before, the uptake of glucose into the cytosol is drastically decreased, with the majority of glucose being oxidized via the periplasmic oxidation chain. Using multi-omics analysis, changes in the proteome, metabolome, and transcriptome of *P. putida* cells during anodic electro-fermentation compared to aerobic conditions were investigated. This study aimed to expand the knowledge about the anaerobic and electrogenic phenotype of *P. putida*. Based on these findings, target genes should be identified and modified to construct genetically engineered mutants, yielding an improved BES performance of *P. putida* regarding 2-KG productivity, yield, and titer.

To obtain the samples for this study, a set of BES fermentations with *P. putida* KT2440 under standard conditions was performed, and samples for the in-depth omics analysis were taken directly after inoculation (T0, start of the process), after 24 h (T1, exponential current increase), 100 h (T2, peak current), and 380 h (T3, end of the fermentation), respectively (Figure 14).

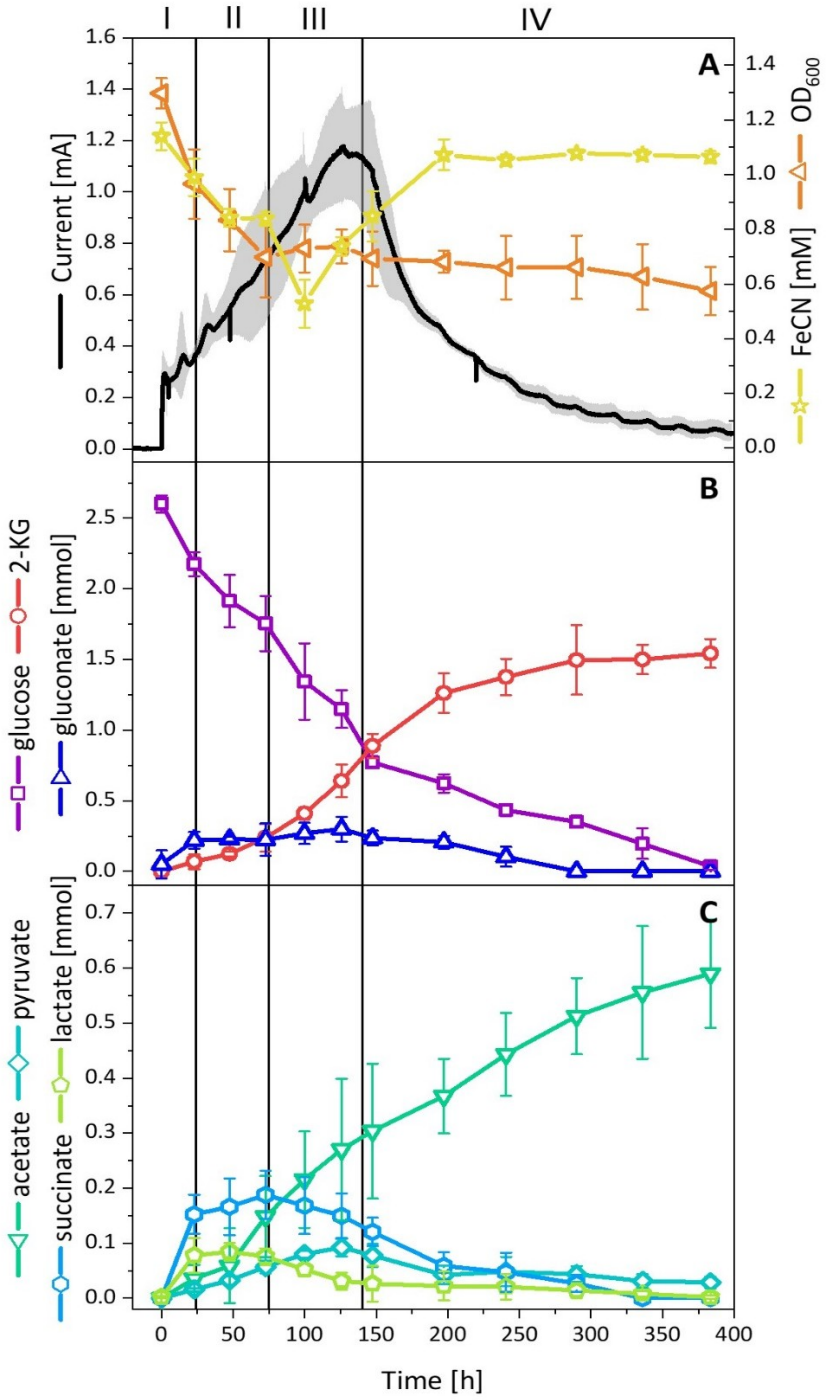


**Figure 14. BES cultivation of *P. putida* KT2440 with FeCN as redox mediator.** Depicted are the current output signal, mediator concentration, and $OD_{600}$ of the cell suspension **(A)**, as well as the concentrations of the substrate glucose and the excreted products gluconate and 2-KG **(B)** and the concentrations of the produced by-products acetate, pyruvate, succinate and lactate **(C)** over time. The BES cultivation was divided into 4 phases labeled I-IV. (Figure adapted from Weimer*, et al.* 2024)

The current profile of the BES fermentations used to obtain samples for the -omics analysis closely mirrored that of the benchmark BES fermentation with *P. putida* KT2440 and FeCN (Figure 8). Similarly, glucose consumption, biomass density, and the product spectrum aligned with expected outcomes.

Therefore, the success of the anodic electro-fermentation process was confirmed, and the samples were used for the systems-wide analysis. Anodic electro-fermentation processes with *P. putida* KT2440 proceed in four phases, which were expected to differ in the cell physiology. Therefore, samples for -omics analysis were taken in each phase. The phase I starts with the inoculation of the cells into the BES and runs for ~24 h. In this adaptation phase, the current output signal rises, the biomass concentration decreases steadily, and product formation starts. 2-KG, gluconate, acetate, succinate, pyruvate, and lactate can be found in small concentrations in the supernatant. In phase II (24 – 75 h), the exponential increase in the current output and the decrease in the cell number continued. While the production of 2-KG, gluconate, acetate, and pyruvate continued, lactate was re-consumed, and the succinate production stopped. The phase III (75 – 140 h) is characterized by the highest electrochemical activity of the cells, which can be seen at the peak formation of the current curve with close to 1.2 mA. In this phase, the cell concentration stabilized, and the formation of 2-KG, gluconate, and acetate accelerates. In phase IV (140 – 380 h), the electrochemical activity decreased again, visible by the decrease of the current output signal, and gluconate, succinate, and pyruvate were taken up again. The concentration of 2-KG and acetate continued to increase. During the whole BES process, the oxidized and the reduced form of the redox mediator were present, with the lowest shares of the oxidized form at peak current.

Furthermore, it has to be mentioned that the calculation of the carbon balance at the end of the process resulted in numbers higher than 100%. The carbon recovery was higher than the amount of carbon available from glucose, suggesting that an additional source of carbon must have been used. Results obtained from further analysis done by Anna Weimer suggested that biomass was most likely broken down and used to ensure survival, which resulted in the additional formation of products. These analyses will be described and discussed in the discussion section.

### 3.3.1 Development of Energy Metabolite Concentrations during BES

In previous studies, limitations in the energy generation of *P. putida* under anaerobic conditions had already been determined. Nevertheless, the concentrations of energy metabolites were analyzed in the samples taken at the beginning of the fermentation and during the BES process. The comparison of these metabolites showed drastically lower ATP levels after 100 h of anodic electro-fermentation (Figure 15**Fehler! Verweisquelle konnte nicht gefunden werden.**). The ATP concentration decreased from 6.9 ± 0.1 µmol/$g_{CDW}$ before the start of the fermentation to 1.2 ± 0.02 mol/$g_{CDW}$ 100 h later. The adenylate energy charge (AEC) during BES, however, was higher than the one measured for oxygen-starved cells (Weimer*, et al.* 2020; Nikel; Lorenzo 2013), with a value of 0.52. In the aerobically grown precultures, an AEC of 0.71 was found.

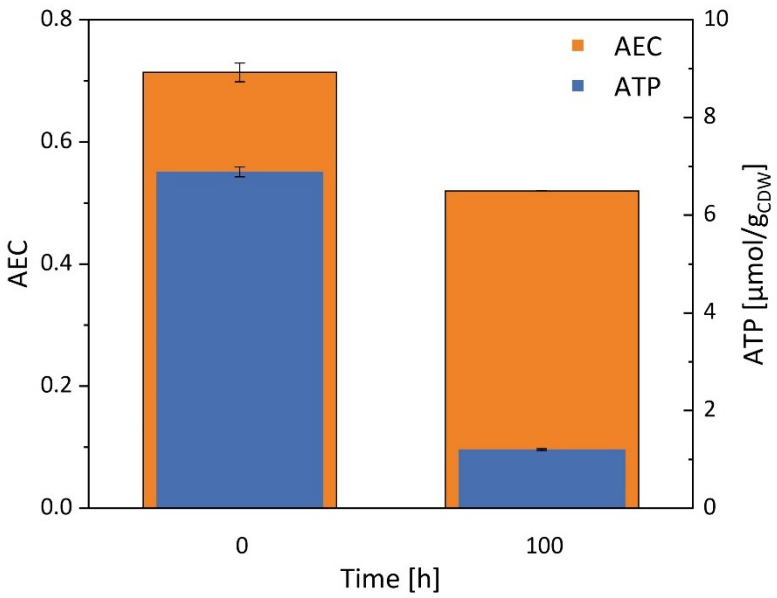


**Figure 15. Adenylate energy charge (AEC) and ATP concentrations in µmol/$g_{CDW}$ were measured at the beginning of the BES fermentation and 100 h after inoculation.**

### 3.3.2 Proteome Changes during BES

To better understand the molecular adaptations of *P. putida* during anodic electro-fermentation, proteomic analysis was conducted to identify significant changes in protein expression under anoxic and anode-driven conditions over time compared to standard aerobic conditions. As described above (see 2.4.5.2 Proteomics Data Analysis), for proteins that were only found in the samples of one of the compared conditions, an imputed low value ($10^{-9}$) was used to replace the missing abundances. While this method ensured that no proteins were lost for the analysis, the resulting $Log_2$(FC) values were noticeably higher or lower than those obtained for proteins present under both conditions. Hence, in the volcano plots (Figure 16 B-D), these proteins appear as subsets with $Log_2$(FC) of below -10 for proteins only present in the preculture and above 10 for BES-exclusive proteins. While the resulting $Log_2$(FC) values cannot be used to make quantitative statements about the expression of these proteins, they still show the presence or absence of potentially biologically relevant condition-specific proteins.

During the first 24 h, 190 proteins showed a $Log_2$(FC) below -10, indicating that these proteins were only present in the aerobic preculture. 25 proteins were significantly downregulated under BES conditions compared to the preculture with $Log_2$(FC) values between -1 and -4. On the other hand, 12 proteins were significantly upregulated, and 4 were only found in samples from the BES reactors. In the samples taken during the later stages of the process, the number of proteins exclusively found in the precultures decreased strongly, while the number of proteins significantly up or downregulated

increased. At all sampling points, more proteins were downregulated than upregulated (Figure 16 B-D). Reasonably, the imposed stress on *P. putida*, created by the anaerobic conditions, leads to a more energy-conserving state. The already-stated shortage in energy metabolites also supports this theory. The bacterium may prioritize essential processes and shut down non-essential ones to survive in such an environment. In general, proteins connected to carbon and nitrogen metabolism, transport processes, and translation were found to be significantly changed during the BES process (Figure 16 A).

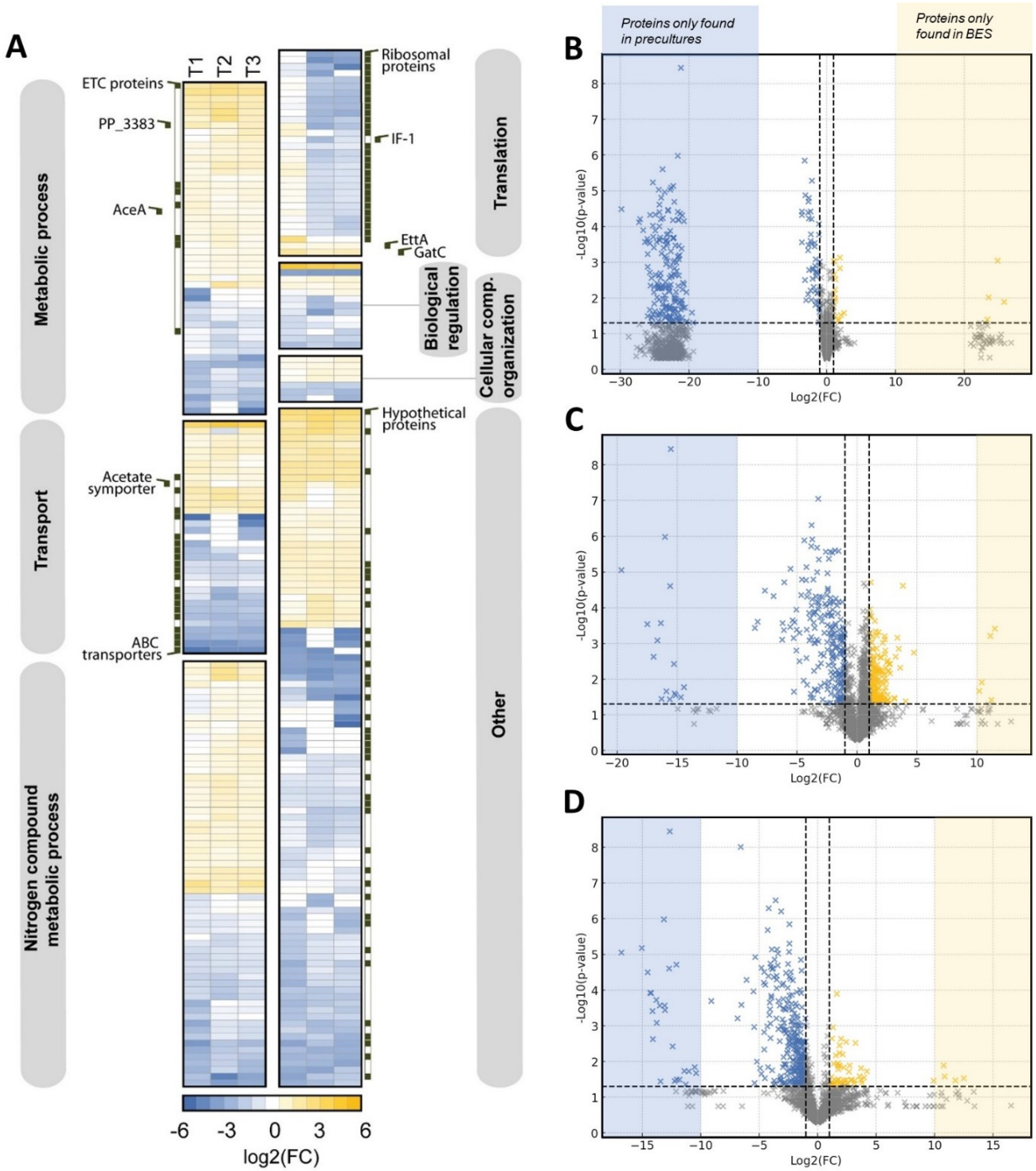


**Figure 16.Heatmap and volcano plots of proteins of *P. putida* KT2440 during BES fermentation with FeCN as redox mediator and glucose as the sole substrate.** In the heatmap **(A)**, changes in the proteome during the BES fermentation can be seen. The volcano plots depict all proteins found in *P. putida* KT2440 at the time points T1 (24h after inoculation – exponential current increase) **(B)**, T2 (100 h after inoculation – peak current) **(C),** and T3 (380 h after inoculation – end of process) **(D)**. Samples were taken 24 h (T1), 100 h (T2), and 380 h (T3) after inoculation of the BES. Highlighted are the proteins that are significantly (p-value < 0.05) up (yellow) or down (blue) regulated by $Log_2$(FC) of at least higher 1 or lower -1 compared to the aerobically grown control culture. Proteins with extreme $Log_2$(FC) of above 10 (transparent yellow) or below -10 (transparent blue) were only found in one condition. (n=3) (Figure modified from Weimer*, et al.* 2024)

Several key enzymes from the ETC exhibited an increase in abundance, such as NADH-quinone oxidoreductase subunit C (NuoC), Succinate dehydrogenase flavoprotein subunit (SdhA), NADH-

quinone oxidoreductase subunit E (NuoE), Cytochrome bo terminal oxidase subunit I (CyoB), NADH dehydrogenase (Ndh), and PP_2867, a protein from the pyridine nucleotide-disulfide oxidoreductase family, which is suspected to be involved in the ETC as well. These proteins are likely upregulated due to their involvement in transferring electrons to the external redox mediator. Furthermore, enzymes associated with alternative metabolic pathways, including the glyoxylate shunt enzyme Isocitrate lyase (AceA), gluconate 2-dehydrogenase (PP_3383), and the acetate symporter acetate permease (ActP-I), showed elevated expression. On the other hand, several energy-intensive ABC transporters displayed reduced abundance, indicating a metabolic shift towards conserving energy.

In samples taken at later stages of the fermentation process (100 and 380 h), the overall proteomic profile remained comparable to that observed at 24 h, except that proteins involved in translation exhibited notable changes in the later stages. Ribosomal proteins showed relatively stable levels during the first 24 h of the process, suggesting that active protein translation was still ongoing during this early phase. However, after 100 h, many translation-associated proteins showed reduced abundance. Therefore, the proteomic analysis highlights translation as a biological process significantly impacted during the BES fermentation, with proteins related to translation generally decreasing in abundance after 100 h. This indicates a substantial reduction in protein synthesis activities, which aligns with a shift towards energy conservation and reduced cellular activity. Notably, the translation initiation factor IF-1 (InfA, PP_4007) was reduced, while the abundance of EttA (PP_0674), a known ADP/ATP ratio sensor and translation inhibitor, increased. In addition, 27 structural ribosomal proteins exhibited decreased abundance.

Another protein to be highlighted here, which is found in decreased abundance after 24 h but upregulated in the later stages of the anodic electro-fermentation, is exopolyphosphatase (ppx). This enzyme is responsible for breaking down polyP chains, releasing inorganic phosphates, which other enzymes can use to generate ATP. Therefore, this enzyme is involved in the stress response of *P. putida* and might support the compensation of lacking energy metabolites during the BES process.

Unfortunately, a significant number of affected proteins remained uncharacterized.

## 3.4 PolyP as Energy Storage Compound in *P. putida*

In BES, *P. putida* is enduring high stress due to the absence of oxygen, and as described previously, the cells also suffer from a severe energy shortage. The maximum ATP generation calculated via flux balance analysis is far below the lowest non-growth associated maintenance demand reported for aerobic cultures. Furthermore, the measurement of the energy metabolite concentrations during the systems analysis confirmed that the concentrations of the energy metabolites are significantly decreased during the BES process. Interestingly, the proteomics analysis revealed that the enzyme

exopolyphosphatase degrades polyP and is upregulated during the later phases of BES. This suggests a potential involvement of polyP in energy generation during this phase, possibly compensating for the energy shortage.

*P. putida*, among many other bacteria, is known to be able to produce inorganic polyP as an energy storage compound (Nikel*, et al.* 2013). Therefore, it was hypothesized that the depletion of polyP could compensate for the lack of energy generation. This storage compound is a linear polymer composed of tens to hundreds of inorganic orthophosphate (Pi) residues linked by high-energy phosphor-anhydride bonds, which are also found in ATP (Rao*, et al.* 2009). It serves as an energy reservoir and phosphate storage molecule and plays a crucial role in stress tolerance. PolyP can be synthesized and accumulated during favorable conditions when nutrients, particularly phosphate, are abundant. When the bacterium faces nutrient limitation or stress, it can utilize the stored polyP as a source of energy and phosphate to sustain cellular activities. The compound helps the bacterium to adapt to adverse conditions such as nutrient starvation, oxidative stress, and changes in pH (Nikel*, et al.* 2013).

To investigate the role of polyP in *P. putida* under anaerobic and anode-driven conditions, the presence of polyP before and after BES fermentation was compared. There are many different methods possible to analyze polyP, like metachromasy (e.g. with methylene blue), enzyme assays (e.g. PKK assay, assay from Christ et al.), 31P nuclear magnet resonance spectroscopy, Fourier transform-infrared spectroscopy and so on. A further method is the visualization of phosphorus via EDX coupled with SEM (Gomes et al. 2013). For EDX, the atoms in the sample are excited by a specific energy from the electron beam. The X-rays released from the sample are characteristic of the elements the sample contains. Therefore, the method can visualize phosphorus in the sample, but the compound in which the phosphorus is bound will not be revealed. Raman spectroscopy is an analytical technique that can be used to provide detailed information about molecular structures by the measurement of the vibrational, rotational, and other low-frequency modes of the molecules. Hence, after EDX, Raman spectroscopy can aid in identifying the molecule to which the detected phosphorus might be bound. The Raman spectrum of polyP shows a dominant peak in the area of 1145-1177 $cm^{-1}$, released by the symmetric stretches of $PO_2^-$ and a smaller peak at 682-700 $cm^{-1}$, occurring from P-O-P stretches (Christ .et al. 2020; Fernando et al. 2019). Therefore, comparing the Raman spectrum in these areas before and after BES fermentation might indicate the presence and fate of polyP in the samples.

### 3.4.1 Scanning Electron Microscopy and Energy-Dispersive X-ray Spectroscopy

In Figure 17, the SEM and EDX visualization of phosphorus in *P. putida* KT2440 before and after the cultivation in the BES system can be seen. The small black dots in the electron scanning pictures (Figure 17 A; C) are the pores of the filter to which the cells are attached. The cloudy particles in these pictures are residues of the paraformaldehyde, which was used to fix the cells. The *P. putida* cells are rod-

shaped. Before the cells were incubated in the BES system, the EDX signal of phosphorus showed very bright signals in the same spots where the *P. putida* cells in the SEM picture are located. This indicated very high phosphorus content (Figure 17 B). Furthermore, the shapes of these signals were round and granule-shaped. In contrast, the phosphorus signals in the sample taken at the end of the BES cultivation were significantly weaker, and the contrast between the background noise and the signal clearly decreased (Figure 17 D). This proves that the cells contained higher amounts of phosphorus during the aerobic cultivation in the preculture. After fermentation in the BES system, this phosphorus is significantly depleted. The decrease of phosphorus in the sample might indicate a consumption of polyP. However, as described earlier, EDX spectroscopy only shows the presence of a certain element but gives no evidence about the molecule in which the element is bound. Raman spectroscopy was applied in the next step to investigate this question further.

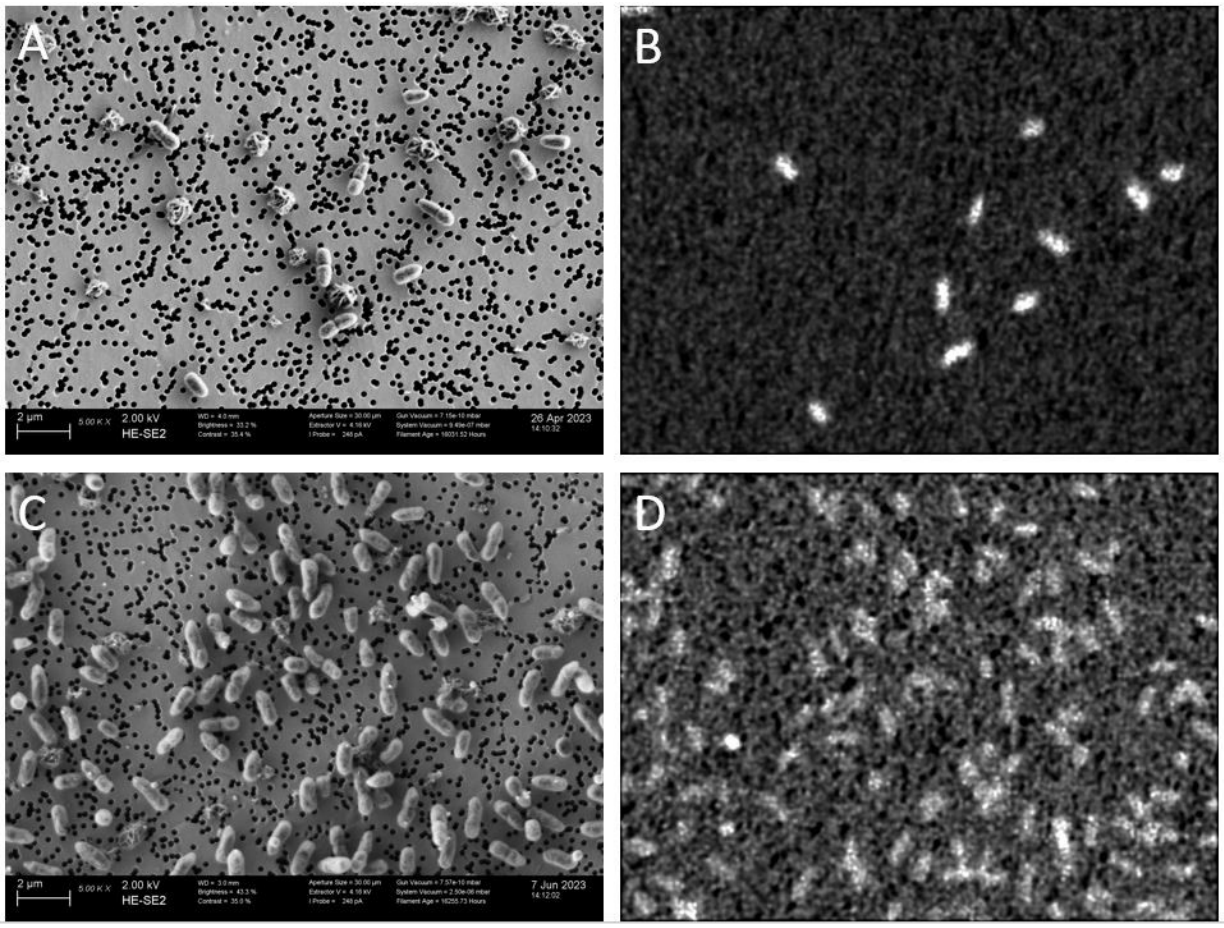


**Figure 17: SEM picture (A, C) and EDX visualization of phosphorus (B, D) of *P. putida* KT2440 before (A, B) and after (C, D) BES fermentation.**

### 3.4.2 Raman Spectroscopy

For the identification of suitable targeting points of the Raman laser, overview pictures of the cell suspensions dried on the SEM metal plates were taken by SEM. To enable the relocation of these spots

in the microscope attached to the Raman device, a cross was engraved into these metal plates (Figure 18). The laser was then aimed at areas where clumps of cells were located (Figure 18, orange circles).

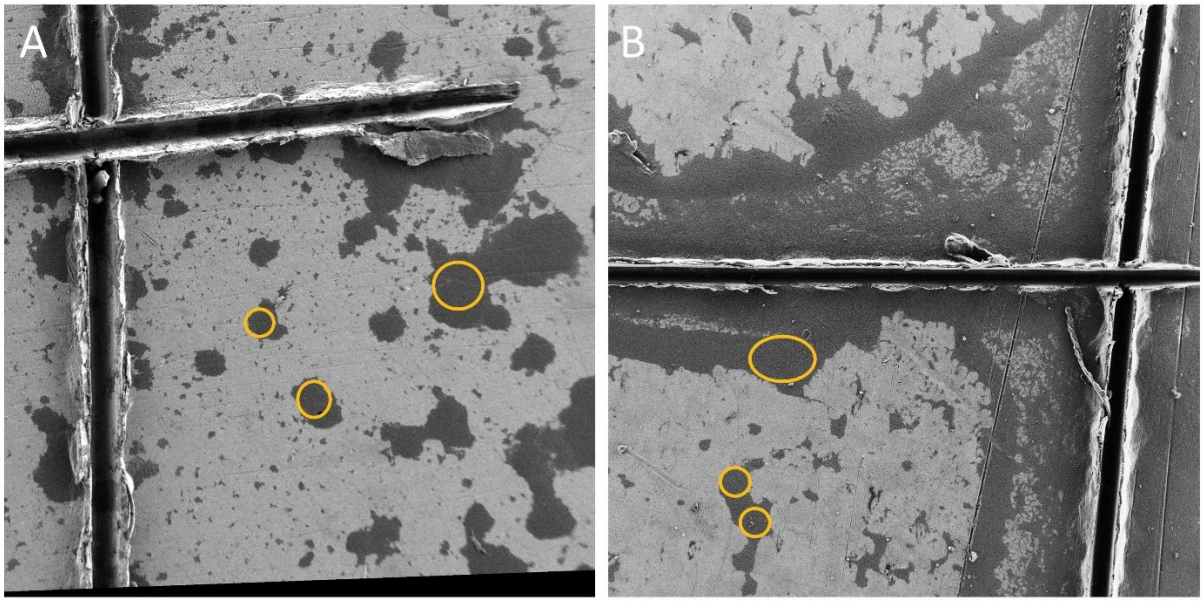


**Figure 18. Overview SEM picture of *P. putida* KT2440 samples before (A) and after (B) BES fermentation.** The cell suspensions were dried on metal SEM plates with engraved cross to enable the identification of suitable laser target points for the Raman measurements. The orange circles mark the points where the Raman laser beam was targeted.

The Raman spectra obtained from the *P. putida* samples were very complex due to the presence of a huge amount of various cellular biomolecules in the cells. Literature references suggest two characteristic peaks for polyP. Due to $PO^{2-}$ stretching vibrations, a strong peak in the area of 1145 - 1177 $cm^{-1}$ can be expected. In the area of 682 – 700 $cm^{-1}$, P-O-P stretches are supposed to cause a comparably weaker signal in the Raman spectrum, with the peak maximum at 690 $cm^{-1}$ (Christ*, et al.* 2020; Fernando*, et al.* 2019). The analyzed spectral range was chosen to be between 465 and 2145 $cm^{-1}$. In this range, cellular components like proteins, nucleic acids, lipids, and carbohydrates also emit different vibration modes, which are visible in Raman spectroscopy. Hence, the obtained Raman spectra showed a wide variety of peaks over the whole analyzed spectral range. However, the average intensities measured for the ranges, which are characteristic of polyP, are depicted in Figure 19.

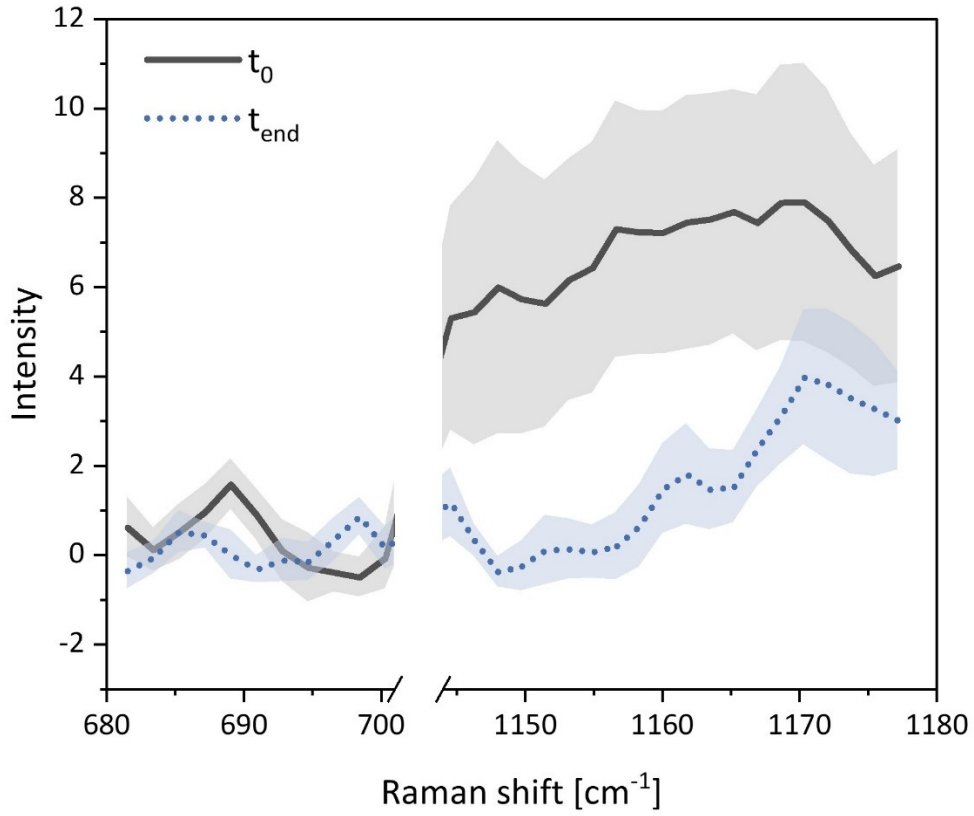


**Figure 19. The average intensity of Raman signals of *P. putida* KT2440 samples taken before (black, continuous line) and after (blue, dotted line) BES fermentation.** Shown is the measured range of 682 - 700 cm$^{-1}$ and 1145 - 1177 cm$^{-1}$. The depicted average was calculated from 10 measured spectra, respectively. The shading marks the standard deviation.

Analyzing the Raman spectrum taken from the aerobically grown sample, there are indeed peaks in the areas of interest. A peak with an average intensity of ~1.8 can be seen at 690 cm$^{-1}$, and also, in the spectral area of 1145-1177 cm-1, a broader and higher peak with a maximum intensity of 7.6 on average was found. Comparing this measurement to the average spectrum obtained for *P. putida* KT2440 cells after the BES fermentation, a decrease of both peaks can be recognized. In the lower end of the spectrum, the peak at 690 cm$^{-1}$ disappeared. Instead, two smaller peaks with an intensity of 0.6 and 0.9 on average appeared at 685 and 698 cm$^{-1}$. Also, in the higher range of the analyzed spectrum, a decrease in the peak area was observed. Between 1145 and 1157 cm$^{-1}$, no Raman signal was registered, but two more narrow peaks were appearing at 1163 and 1171 cm$^{-1}$. However, both of these peaks had a lower intensity in comparison to the spectrum obtained from the aerobically cultured cells.

# 3.5 Redox Mediator Testing

### 3.5.1 Endogenous vs. Exogenous Redox Mediator

The question of whether the usage of endogenous or exogenous redox mediators is more favorable for BES applications has occupied scientists for years. Both methods have clear advantages and disadvantages (see 1.5 Redox Mediators), but a comparison of the two possibilities in the same system with the same microorganism was still lacking. Therefore, a study was conceptualized to at least directly compare one natural and one artificial redox mediator in *P. putida* KT2440 in BES. As an artificial redox mediator, the standard mediator used in all previous experiments, FeCN, was chosen. The endogenous mediator chosen was phenazine-1-carboxylic acid (PCA), as a genetically engineered mutant of *P. putida* KT2440 with the ability to produce PCA was available (named here *P. putida* KT-PCA). A strain containing the empty vector with a kanamycin resistance (named here *P. putida* KT-control) was used for the exogenous mediator FeCN. Both strains were cultivated in the BES, and current output signals, exo-metabolite generation, and proteomics data were compared.

#### *3.5.1.1 Current Output Signals and Mediator Concentrations*

In BES systems, the current output signal shows the electrons released by the microorganisms and, therefore, gives information about the metabolic activity of the respective cells. After inoculation of the BES systems, the reactors were first run in an aerobic mode, without potential, to enable the cells to grow and to enable the KT-PCA strain to produce the redox mediator and secret it into the reactor. In Figure 20, the increase in PCA concentration during the aerobic phase can be seen. Afterward, the mode was switched to anaerobic, and FeCN was added to the reactors without PCA. During the anaerobic mode, the mediator concentrations of all reactors stayed roughly constant, showing that the amount of redox mediator in the systems was not a limiting factor during the runs. When the potential was turned on, an immediate increase in the current output signal was measured in all reactors. While the reactors with PCA as mediator reached a first peak current of about 0.2 mA after the initial time, the reactors with FeCN showed significantly higher signals with about 1 mA. In the following ~ 70 h, the current output signal of the reactors with FeCN as mediator decreased slowly by about 0.3 mA, followed by another substantial increase to ~1.3 mA until 145 h after inoculation. Then, the signal dropped back to near baseline about 155 h after the start of the experiment, indicating the end of the fermentation process. The current output signal of the reactors with PCA as mediator, however, did show a completely different and more stable profile. After the initial rise, the current only increased very slightly further until the peak current of ~0.25 mA was reached ~75 h after inoculation. Then, the signal slightly decreased over the following 300 h until the experiment was manually stopped.

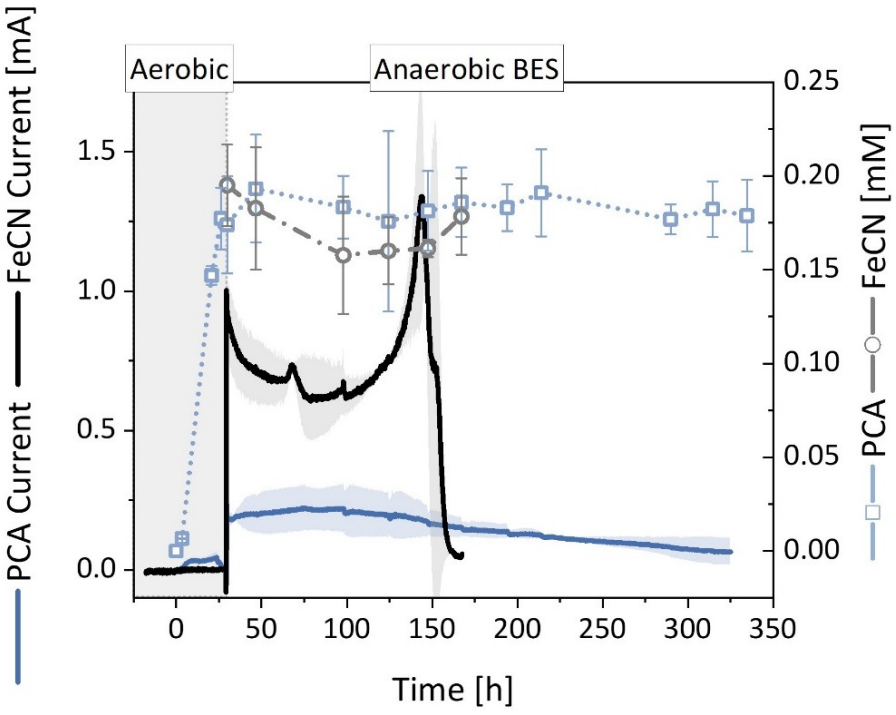


**Figure 20: current output signals and redox mediator concentration of BES fermentations with PCA or FeCN, respectively.** The measured current in mA and the redox mediator concentrations in mM over time are shown.

### *3.5.1.2 Product Spectra Comparison*

In the aerobic phase, the rate of glucose consumption of both strains was, as expected, significantly higher than in the anaerobic mode (Figure 21). The KT-PCA strain took up the substrate slightly faster, with an average rate of 2.60 ± 0.57 mmol/h/$g_{CDW}$, compared to the KT-control strain, with an average rate of 2.35 ± 0.97 mmol/h/$g_{CDW}$. Hence, after ~29 h, the glucose concentration in all reactors was decreased from initially 16 mM to 2 - 3 mM. To ensure comparability and prevent glucose limitation, shortly before the switch to the anaerobic and anode-driven BES mode, glucose was refilled to each reactor to a final concentration of ~6 mM, respectively. The 2-KG production during the aerobic phase, on the other hand side, differed significantly between the two strains. While the 2-KG concentration in the reactors with the KT-PCA strain reached about 6 mM in average, the reactors with KT-control only contained about 1.8 mM 2-KG. The acetate production was similar in all reactors and reached concentrations of about 0.8 mM at the end of the aerobic phase.

After the switch to the anaerobic BES phase, the KT-control strain showed faster glucose consumption and 2-KG production than the KT-PCA strain. FeCN was added to the KT-control BES reactors to the same concentration as the PCA in the KT-PCA BES reactors. The significantly higher current output signals measured for the KT-control strain indicated higher metabolic activity. The glucose consumption rate of the KT-PCA strain was only 0.017 ± 0.003 mmol /$g_{CDW}$/h on average, while the

control strain reached an average rate of 0.089 ± 0.019 mmol /$g_{CDW}$/h driven by the artificial redox mediator. In line with the very low glucose uptake of KT-PCA, the 2-KG production was also very slow, leading only to an increase of 0.205 mM on average in 305 h. The 2-KG concentration in the reactors with FeCN as a mediator increased by 2.43 mM on average in only 137 h. The concentration of the primary by-product acetate reached similar values for both strains at the end of the electro-fermentation processes of about 2.6 mM on average.

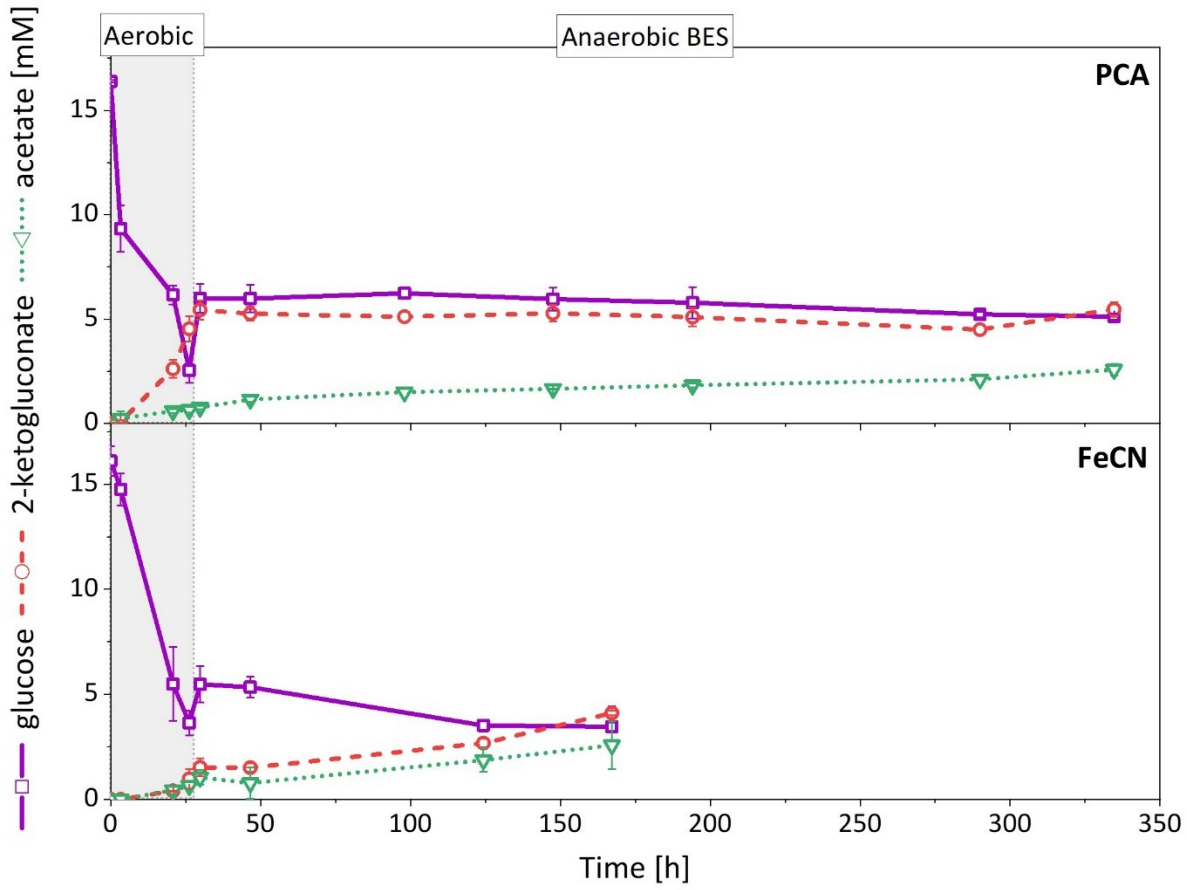


**Figure 21: Extracellular substrate and product concentrations in mM over time during the BES fermentations of *P. putida* KT-PCA and KT-control with PCA and FeCN as redox mediators, respectively.**

### *3.5.1.3 Comparison of Proteome Changes between the Usage of FeCN and PCA*

To gain a more comprehensive understanding, the changes in the proteome for the use of the endogenous mediator PCA versus the artificial mediator FeCN were compared. Aerobically grown *P. putida* cultures of the two respective strains (*P. putida* KT-PCA and *P. putida* KT-control) were used as the control condition. A T-test was carried out to identify only proteins whose abundances were changed significantly (p-value < 0.05). The $Log_2$(FC) values of the proteins under BES conditions versus aerobic control conditions were used to analyze whether these proteins were up or downregulated. In *P. putida* KT-PCA with PCA as a mediator, 349 proteins were found to be upregulated, and 204 proteins

were downregulated. In *P. putida* KT-control with FeCN as mediator, 254 Proteins were up and 158 proteins downregulated. As described before (see 3.3.2 Proteome Changes during BES), proteins with extreme $Log_2$(FC) values of below -10 or above 10 were only found in the precultures or BES samples, respectively. This applied for 27 proteins from the samples of the BES reactors with PCA, and 26 proteins from samples of BES reactors with FeCN. Of these, 25 in each condition were found only in the BES samples.

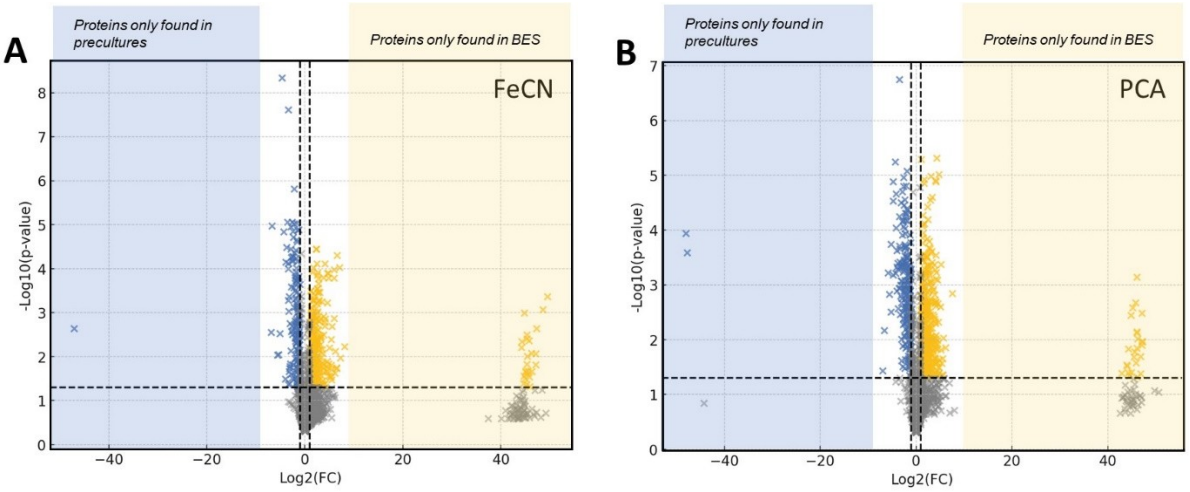


**Figure 22. Volcano plots of proteomes from BES fermentations with FeCN or PCA as redox mediator.** Depicted are all detected proteins found in the strains *P. putida* KT-control cultivated with FeCN **(A)** and KT-PCA cultivated with PCA **(B)** as redox mediators, respectively. Highlighted are the proteins that are significantly (p-value<0.05) up (yellow) or down (blue) regulated by $Log_2$(FC) of at least higher 1 or lower -1 compared to the aerobic control culture. Proteins with extreme $Log_2$(FC) of above 10 (transparent yellow) or below -10 (transparent blue) were exclusively found in one condition. (n=3)

A big share of the significantly upregulated proteins under BES conditions in both strains are connected to stress response and energy metabolism (Figure 22). Heat shock proteins, universal stress protein, alcohol-dehydrogenase, medium-chain aldehyde dehydrogenase, NAD/NADP-dependent betaine aldehyde dehydrogenase, decarboxylating 6-phosphogluconate dehydrogenase, and Poly granule-associated proteins are known to play a role in stress response in bacteria. They are upregulated in both *P. putida* KT-control and KT-PCA.

The Cbb3-type cytochrome c oxidase catalyzes the last step of the ETC under aerobic conditions, which is the transport of electrons from cytochrome c to $O_2$. This enzyme was found in increased abundance in the KT-PCA strain and exclusively in the BES samples for KT-control. Even though $O_2$ is absent under BES conditions, the upregulation of this protein might indicate an overproduction of the protein as an attempt by the cells to balance the lack of $O_2$.

A similar pattern applies to the enzyme acetyltransferase, with the protein found only in samples from the BES in the case of FeCN and an upregulation for PCA. This enzyme transfers an acetyl group from

acetyl-CoA to various substrates. It is known to be involved in various processes like the regulation of metabolic pathways and the response to environmental stresses, contributing to the survival of the cells in changing environments. The MotA/TolQ/ExbB proton channel family protein was exclusively found in the BES samples of both strains. As a proton channel protein, the protein enables transport across the inner membrane and is involved in ATP synthesis, nutrient transport, and maintaining the pH balance.

Further enzymes, which were found to be upregulated in both strains belong to the central carbon metabolism, like enzymes of the citric acid cycle e.g. aconitate hydratase, fumarate hydratase, NADP-dependent Isocitrate dehydrogenase, and dihydrolipoyl dehydrogenase; enzymes of the Entner-Doudoroff pathway like phosphogluconate dehydratase; proteins of the pentose phosphate pathway e.g. glucose-6-phosphate 1-dehydrogenase, decarboxylating 6-phosphogluconate dehydrogenase, and enzymes of the glycolysis and gluconeogenesis like triosephosphate isomerase, glucose-6-phosphate isomerase, and glucokinase. All of these proteins are crucial for the energy generation and maintenance of *P. putida*. Furthermore, gluconate 2-dehydrogenase is up-regulated in both strains, catalyzing the oxidation of gluconate to 2-KG.

For KT-PCA, some proteins responsible for the degradation of aromatic compounds are more abundant than those in KT-control, like Catechol 1,2-dioxygenase and Beta-ketoadipyl-CoA thiolase, of which the latter is even downregulated in KT-control. Two further examples of up-regulation in KT-PCA and down-regulation in KT-control can be found for the enzymes thiamine triphosphatase, which is needed for thiamine (vitamin B1) synthesis, and dihydroorotase-like protein, a protein of the pyrimidine nucleotide synthesis.

However, the biggest share of downregulated proteins was found downregulated in both strains. A big group of downregulated proteins is connected to cell division, protein synthesis, and transcription, like Peptidyl-prolyl cis-trans isomerase C, 30s and 50s ribosomal proteins, ribosome hibernation promoting factor, DNA-directed RNA polymerase, and transposase. Also, proteins influencing the cell structure, like flagellin, NLPA lipoprotein, and outer-membrane lipoprotein carrier protein, were downregulated. Finally, nearly all ABC-transporters, identified as significantly changed compared to the control group, were found in decreased abundancies in both strains. The transport via ABC transporters is fueled via ATP consumption. Due to the lack of energy in the cells, these transporters might not be usable under BES conditions.

Overall, the changes in the proteome between BES and aerobic control conditions are mostly similar for the two compared strains, independent of the usage of PCA or FeCN. Most of the up or downregulated proteins in KT-control with FeCN as mediator were also found up or downregulated for

KT-PCA with PCA as mediator. Therefore, it can be hypothesized that the absence of oxygen and the associated shortage of energy have a significantly more prominent influence on protein abundance than the choice of mediator.


**Figure 23. Heatmap for proteome comparison between the usage of FeCN and PCA as redox-mediator in BES.** In the heatmap, a direct comparison of proteins of certain functions between the two strains can be seen. Like in the volcano plots, the yellow color indicates a significant increase in the abundance of the protein compared to the control with a $Log_2$(FC) of over 1, while the blue color indicates a significant decrease in the abundance by a $Log_2$(FC) below -1.

### 3.5.2 Quinone Redox Mediators

As clearly visible in the comparison of BES fermentations with PCA and FeCN, the chosen redox mediator has a significant impact on the performance of an anodic electro-fermentation process. When choosing a redox mediator for a bio-electrochemical process, many criteria need to be considered, like the toxicity, stability, and redox potential of the compound, as well as the interaction site and the transport of the mediator to this position. Finding a compound that meets all requirements can be very hard or even impossible, and therefore, finding a compromise cannot be prevented sometimes. In the following section, three different quinone redox mediators were tested in the BES system with *P. putida* KT2440. Quinones play a crucial role in the ETC of photosynthesis and respiration by shuttling electrons between protein complexes. This natural involvement in electron transfer processes makes them logical redox mediator candidates. The quinone mediators selected for testing were 1,4-benzoquinone (BQ), duroquinone (DQ), and anthraquinone-2,6-disulfonate (AQDS) for several reasons, which will be explained in the following sections. The testing was done, applying the standard operation protocol for the BES, but instead of the addition of FeCN as redox mediator, the quinone mediators were added, respectively.

#### *3.5.2.1 BQ as Redox Mediator in BES*

BQ is a common member of the quinone family and consists of a benzene ring with two opposite carbon atoms which are oxidized to carbonyl groups, forming a conjugated system. BQ can undergo redox cycling, where it is reversibly reduced to hydroquinone by the transfer of two electrons and two protons.

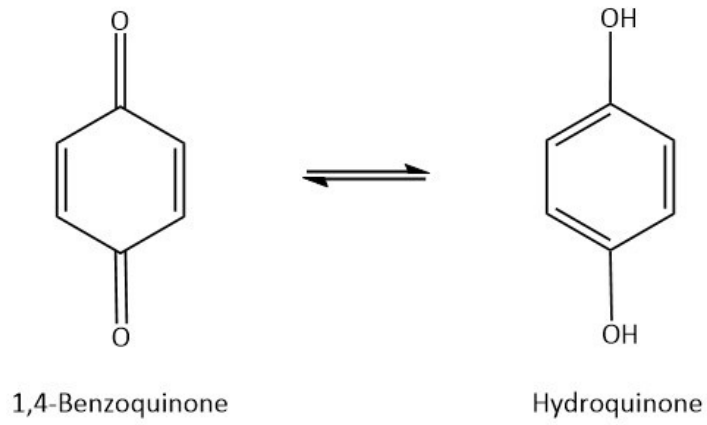


**Figure 24. Chemical structure of BQ and its reduction product hydroquinone.** During the reduction process, two electrons ($e^-$) and two protons ($H^+$) are transferred, converting the two carbonyl groups into hydroxyl groups. The process is reversible by the oxidation of hydroquinone to BQ.

Due to its ability to accept and donate electrons, BQ is not only important in natural but also in industrial processes, e.g. the production of dyes, pharmaceuticals, and polymers, as well as serving as

redox mediator in electrochemical systems (Phani*, et al.* 1993; Zhang*, et al.* 1994; Chang*, et al.* 2019). However, BQ also exhibits notable toxicity, mainly due to its high reactivity, which can lead to the generation of reactive oxygen species (Kondrová*, et al.* 2007). Reactive oxygen species will lead to oxidative stress in cells and can damage proteins, lipids, and DNA. For this reason, a preliminary test was conducted to narrow down the maximum concentration of BQ, which does not negatively influence the growth of *P. putida* KT2440. The preliminary toxicity test was done on DM9 agar plates containing 1 mM, 0.5 mM, 0.3 mM, and 0.1 mM of BQ to delimit the BQ concentration, which should be used for the following BES experiments. For this purpose, a liquid preculture of *P. putida* KT2440 in DM9 medium was made. Then, the cell suspension was diluted and plated out on the agar plates containing BQ. After incubation at 30 °C for 24 h, the number of colonies formed on the plates was counted and compared. While the number of colonies was decreased for a BQ concentration of 1 mM and 0.5 mM BQ, the concentrations 0.1 and 0.3 mM did not lead to reduced colony growth compared to the negative control plate without BQ. Therefore, a BQ concentration of 0.3 mM was set as the maximum for the first trial of BQ as redox mediator for *P. putida* KT2440 in BES. Additionally, lower concentrations of 0.05 mM and 0.1 mM BQ were tested (Figure 25).

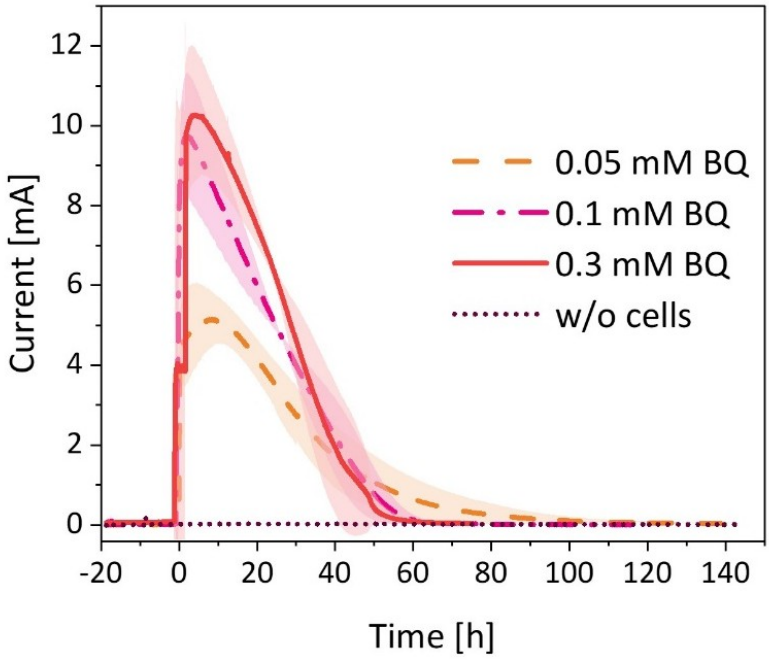


**Figure 25. Current output signals of BES with *P. putida* KT2440 and BQ as redox mediator.** BQ was tested at concentrations of 0.05, 0.1, and 0.3 mM, and the transferred electrons were measured via the current output signal. A BES with 0.1 mM BQ but without inoculation of *P. putida* cells was used as the negative control.

Strikingly, in all three tested concentrations, BQ drastically increased the current output signals measured in all BES reactors with *P. putida* KT2440 while the duration of the fermentation processes decreased significantly (Figure 25). These current profiles immediately suggested a significant

improvement of the anodic electro-fermentation process with *P. putida* by the usage of BQ compared to the BES performance with FeCN. A direct interaction of the mediator with the electrode without the involvement of the *P. putida* cells was ruled out, as the reactors without cells did not show any current production. The peak current measured for a BQ concentration of 0.05 mM was 5.1 mA on average, and the process time until the current dropped back to the baseline was ~100 h. The current profiles for 0.1 mM and 0.3 mM BQ were very similar, with 9.7 mA on average for 0.1 mM and 10.4 mA for 0.3 mM BQ. The fermentation duration was, in both cases, ~60 h. As the difference between 0.1 mM and 0.3 mM was only minor, a BQ concentration of 0.1 mM was chosen as optimum for the following experiments. Minimizing the BQ concentration could decrease possible toxic side effects and process costs. The negative control BES, which contained 0.1 mM BQ but no *P. putida* cells, showed no current output signal, proving that BQ alone cannot interact with the anode.

To confirm that 0.1 mM 0f BQ does not negatively impact the growth of *P. putida* KT2440, a more detailed growth test was conducted in liquid media rather than on agar plates. For this purpose, growth curves were generated in DM9 medium supplemented with 0.1 mM BQ. Pure DM9 medium with 2 g/L glucose was used for the control cultures. Furthermore, a second control condition was set up, using DM9 medium without glucose but with 0.1 mM BQ for the cultivation of *P. putida* cells, to investigate if *P. putida* can use BQ as substrate to enable growth (Figure 26).

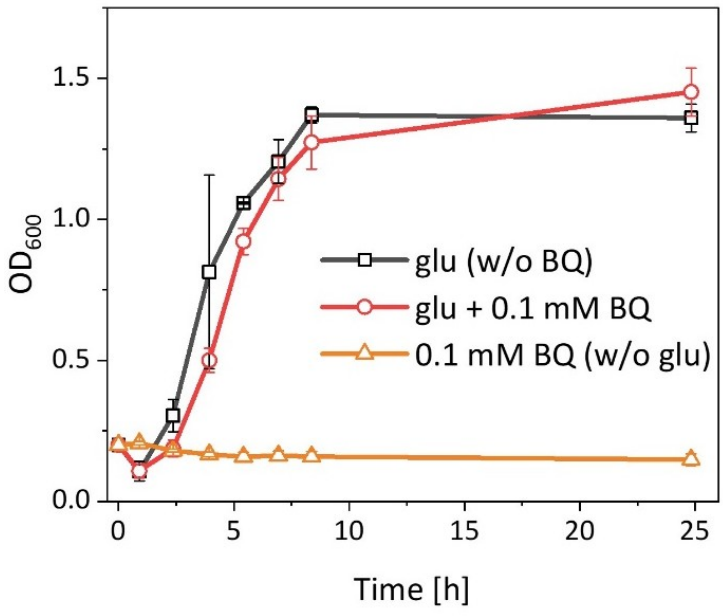


**Figure 26. Toxicity test of 0.1 mM BQ on *P. putida* KT2440.** The growth of *P. putida* under aerobic conditions in DM9 medium with glucose and 0.1 mM BQ was compared to growth in standard DM9 medium with glucose and DM9 medium without glucose but with 0.1 mM BQ. This comparison aimed to elucidate whether BQ has a negative influence on the cells.

The $OD_{600}$ of the cultures containing only BQ and no glucose did not rise over the 24-hour course of the experiment, showing that KT2440 could not grow on BQ as the sole carbon source. The growth curves of the cultures in glucose-containing media with and without BQ were very similar. Also, the growth rates in the exponential phase only differed slightly, with 0.58 ± 0.02 $h^{-1}$ in medium without BQ and 0.53 ± 0.01 $h^{-1}$ in medium containing 0.1 mM BQ. It was, therefore, confirmed that a concentration of 0.1 mM BQ had no negative influence on the *P. putida* cells.

In the next step, supernatant samples taken during the BES fermentations with 0.1 mM BQ as mediator were analyzed for their glucose and extracellular metabolites content to investigate glucose consumption and product formation (Figure 27 A).

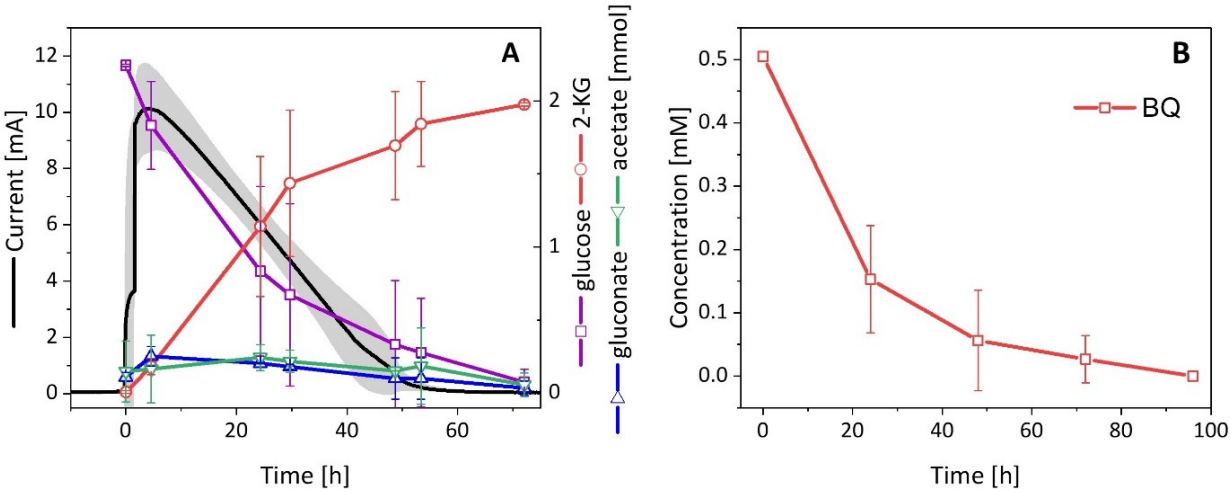


**Figure 27. BES performance of *P. putida* KT2440 with 0.1 mM BQ as redox mediator and concentration change of BQ over time.** The left y-axis indicates the current output of the respective BES fermentations, and the right y-axis shows the amount of metabolites (mmol) in the reactors **(A).** The concentration of BQ in pure DM9 media at 30 °C was measured throughout 96 h **(B).** The line or line-symbol presents the averaged values, and the shading or error bars indicate the standard deviations of (biological) replicates. (n=4)

*P. putida* KT2440 in BES with BQ as mediator consumed glucose, which was used as the sole substrate, steadily over the entire course of the anodic electro-fermentation. After 70 h of incubation, all glucose (2.2 mmol) was consumed with a glucose uptake rate of 0.35 ± 1.03 mmol/h/$g_{CDW}$ during the first 24 h. After 24 h, the glucose consumption slowed to a rate of 0.11 ± 0.02 mmol/h/$g_{CDw}$. The product spectrum was the same as when FeCN was used as mediator, with 2-KG as the main product with a yield of 0.91 ± 0.03 from 2-KG over glucose and acetate as the main by-product with a yield of 0.05 ± 0.01 over glucose.

After these first auspicious results, the glucose amount initially supplied to the BES reactors was increased to prolong the run time of the fermentation process. But even though the initial glucose concentration was doubled, the time until the current output signal dropped back to the baseline was

only increased by roughly 10 h to a processing time of ~70 h. The following HPLC analysis of the supernatant samples taken during the anodic electro-fermentation revealed that the supplied glucose was not fully consumed. Therefore, glucose limitation was not the reason for the end of the process. The question of whether the stability of BQ might be the limiting factor arose. BQ was added to the DM9 medium and incubated at 30 °C inside the HPLC sample chamber to prove this hypothesis. Every 24 h the concentration of BQ was measured (Figure 27 B). Remarkably, the BQ concentration measured after 24 h was decreased by ~70% on average. After 48 h, only ~10 % of the initial concentration remained, and after 96 h, no BQ was detectable anymore.

### *3.5.2.2 DQ as Redox Mediator in BES*

After discovering the insufficient stability of BQ in DM9 medium, a more stable quinone was searched. By the addition of substituents, the stability of a molecule can be increased. Therefore, DQ was tested next as a redox mediator in the BES system with *P. putida* KT2440. DQ is the tetramethyl derivative of BQ and, like BQ, acts as a redox agent.

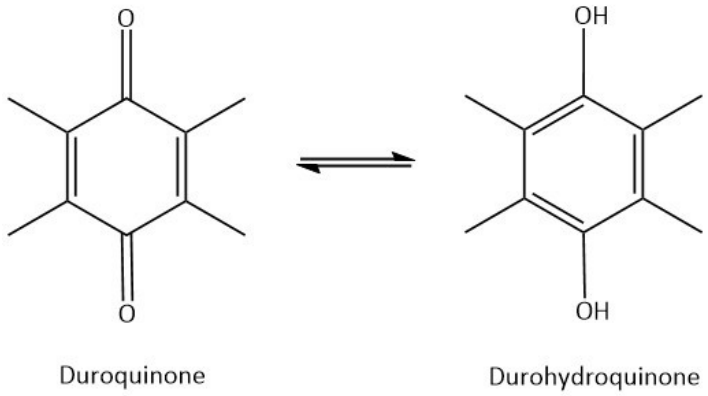


**Figure 28. Chemical structure of DQ and its reduction product durohydroquinone.** The chemical structure of DQ and durohydroquinone differs from BQ and hydroquinone by the presence of four methyl groups attached to the benzene ring. The reduction and oxidation process of DQ and durohydroquinone also involves the transfer of 2 $e^-$ and 2 $H^+$, converting the carbonyl groups into hydroxyl groups and vice versa.

Like with BQ before, different concentrations of DQ were tested in the BES (Figure 29 A). In parallel, the stability of DQ was analyzed in the same way as that of BQ (Figure 29 B).

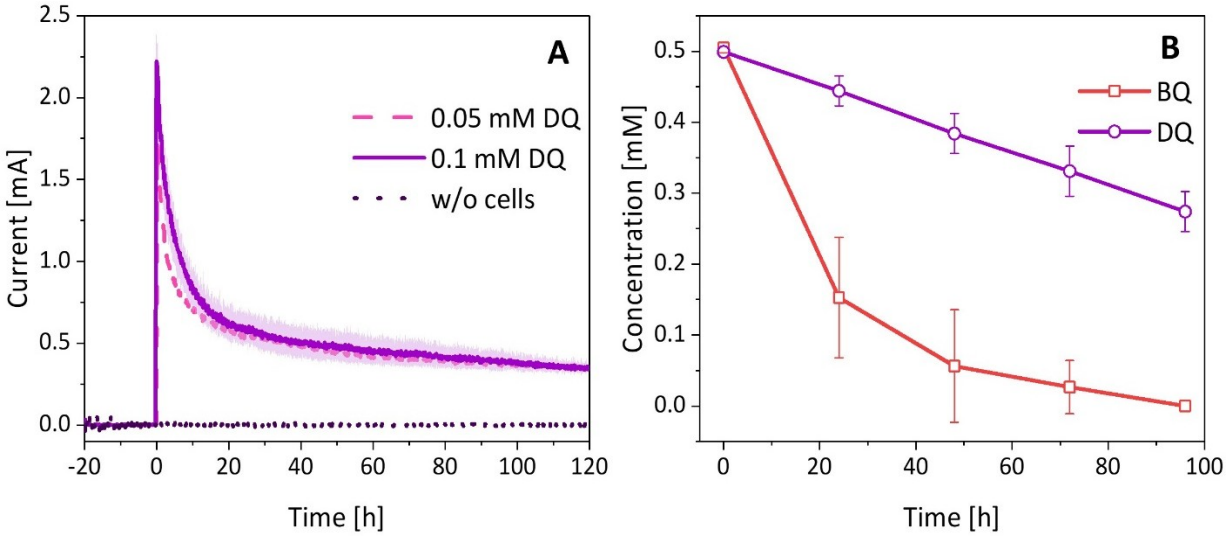


**Figure 29. Current output signals and concentration change of DQ over time.** Different redox mediator concentrations were tested in the BES with *P. putida* KT2440, and the transferred electrons were measured via the current output signal. A BES, which was not inoculated with cells was used as a negative control **(A)**. The concentration of DQ in pure DM9 media at 30 °C was measured for 96 h and is depicted in comparison to BQ (**B)**. (n=3)

Based on the concentration optimum determined for BQ, concentrations of DQ of 0.05 mM and 0.1 mM were tested. The measured current production for both concentrations was nearly congruent. After an initial rise of the current output signal to ~2.25 mA, directly after the inoculation, the signal rapidly dropped back to ~0.65 mA during the first 20 h. Afterward, the currents steadily decreased slowly until the process stopped at 120 h. The ever-decreasing current output signal already suggests a very low metabolic activity of *P. putida* in the BES with DQ as redox mediator. Again, HPLC analysis of supernatant samples was used to prove this assumption (Figure 30).

The stability of DQ was better than that of BQ, with a decrease of the initial concentration of about 40% during 96 h. However, a stable redox mediator with a constant concentration during BES operation would be more favorable.

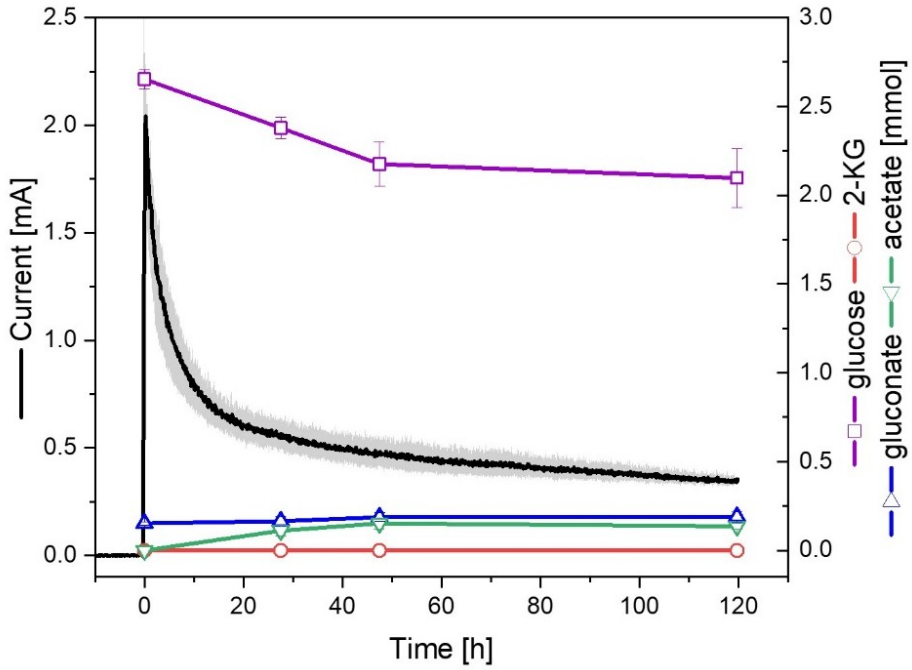


**Figure 30. BES performance of *P. putida* KT2440 with 0.1 mM DQ as redox mediator.** The left y-axis indicates the current output of the respective BES fermentations, and the right y-axis shows the amounts of metabolites (mmol) in the reactors. The line or line-symbol presents the averaged values, and the shading or error bars indicate the standard deviations of (biological) replicates. (n=3)

The HPLC analysis results proved the low metabolic activity already indicated by the current output signals. During the first 48 days after inoculation, a slight glucose consumption of 0.4 mmol was observed. However, in the following 72 h, no further decrease in the glucose concentration was measured. During the time of glucose consumption, acetate was produced as the only product with a yield of 0.45 over glucose. No increase in 2-KG concentration or any other organic acid was detected. The inability of the cells to consume glucose and produce 2-KG in BES with DQ showed that *P. putida* KT2440 couldn't efficiently use DQ as a redox mediator. The most likely explanation for this is that the addition of substituents to a molecule changes not only its stability but also its redox potential. Due to the methyl groups, the redox potential of DQ is more negative than that of BQ. To effectively draw electrons from the ETC of *P. putida* while still allowing the build-up of a proton gradient necessary for ATP synthesis, the redox potential of the mediator must be in a sufficient range. Therefore, a more stable quinone compound with a redox potential similar to BQ might be a more promising candidate.

### *3.5.2.3 AQDS as Redox Mediator in BES*

AQDS is an organic compound with a three-ring aromatic structure, with two ketone and two sulfonate groups. Due to the sulfonate groups the solubility of the compound in water is increased compared to other anthraquinones.

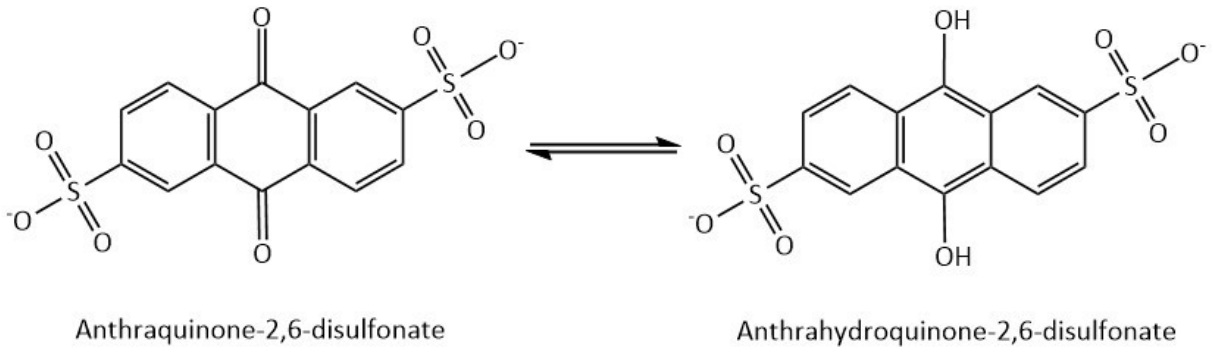


**Figure 31. Chemical structure of AQDS and anthrahydroquinone-2,6-disulfonate.** The redox process is similar to the one of BQ and DQ, as AQDS is reduced to anthrahydroquinone-2,6-disulfonate $AH_2QDS$ by the transformation of the two carbonyl-groups to hydroxyl groups via the transfer of two $e^-$ and two $H^+$.

AQDS is known for its ability to shuttle electrons between molecules or electrodes and is a commonly used quinone redox mediator in (microbial) electrochemical systems e.g. microbial fuel cells (Feng*, et al.* 2010; Martinez*, et al.* 2017; Sun*, et al.* 2017). It has high stability and reversibility, as it can undergo repeated redox cycling to anthrahydroquinone-2,6-disulfonate and back without significant degradation. As the redox potential of redox-active compounds depends on the environment's characteristics, like the pH, temperature, and ionic strength of the solvent, the redox potential has to be determined for each system specifically. The redox potential of a mediator determines whether it can withdraw electrons from the ETC or not and can explain whether *P. putida* can use a mediator. To investigate if the redox potential of AQDS is more suitable for the interaction with the ETC of *P. putida* than DQ, cyclic voltammetry was used to determine the exact redox potentials of all tested quinone redox mediators in the BES (Figure 32). Cyclic voltammetry is a standard electrochemical method in which the applied potential is cyclically varied, and the current response is measured. Due to this method, the electrochemical behavior of molecules can be analyzed. The formal redox potential can be determined as the average of the anodic and cathodic peak potentials resulting from the cyclic voltammogram.

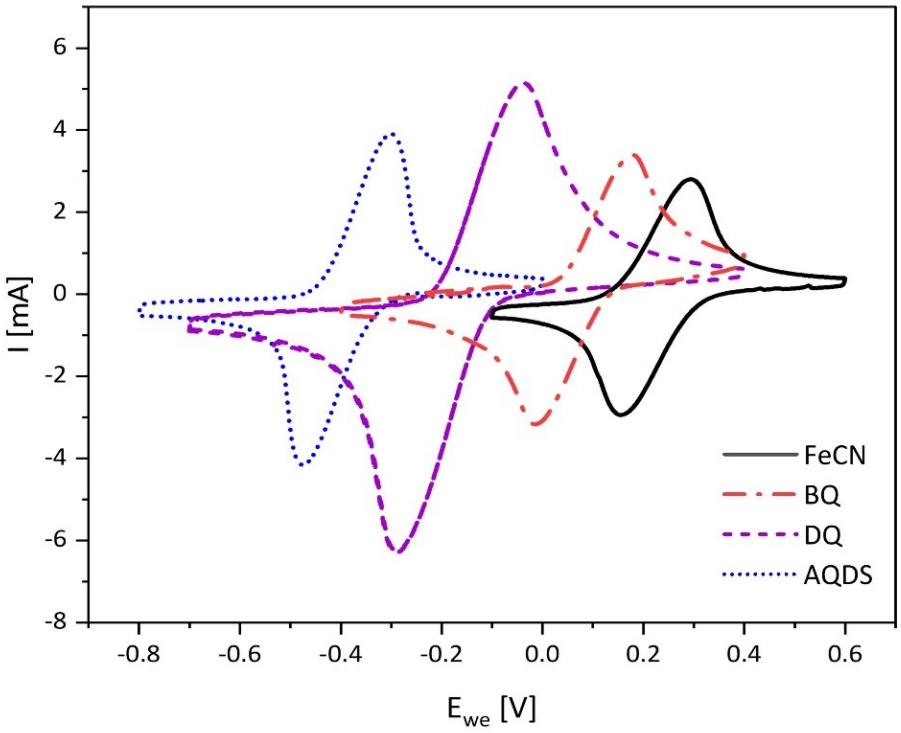


**Figure 32. Cyclic voltammetry of all tested quinone redox mediators.** Depicted is the change of the current output signal in mA depending on the applied potential in V. FeCN, BQ, DQ, and AQDS were added to the BES reactors in a concentration of 0.1 mM, respectively.

The cyclic voltammetry measurements of the respective redox mediators in the present BES system and at the conditions used for this study resulted in redox potentials of -0.39 V vs. SHE for AQDS, -0.17 V vs. SHE for DQ, 0.09 V vs. SHE for BQ and 0.22 V vs. SHE for FeCN. The cyclic voltammetry measurement proves the four times methylation of BQ decreased the redox potential by nearly 0.3 V. However, the redox potential of AQDS is even more negative than that of DQ. BQ and FeCN have significantly higher redox potentials, with FeCN having the highest redox potential of all tested quinone variants. This result implies that *P. putida* will most likely be unable to use AQDS as an efficient electron shuttle in the BES system. Nevertheless, an anodic electro-fermentation process of *P. putida* with AQDS was carried out to prove this hypothesis and eventually rule out AQDS as a possible mediator (Figure 33 A).

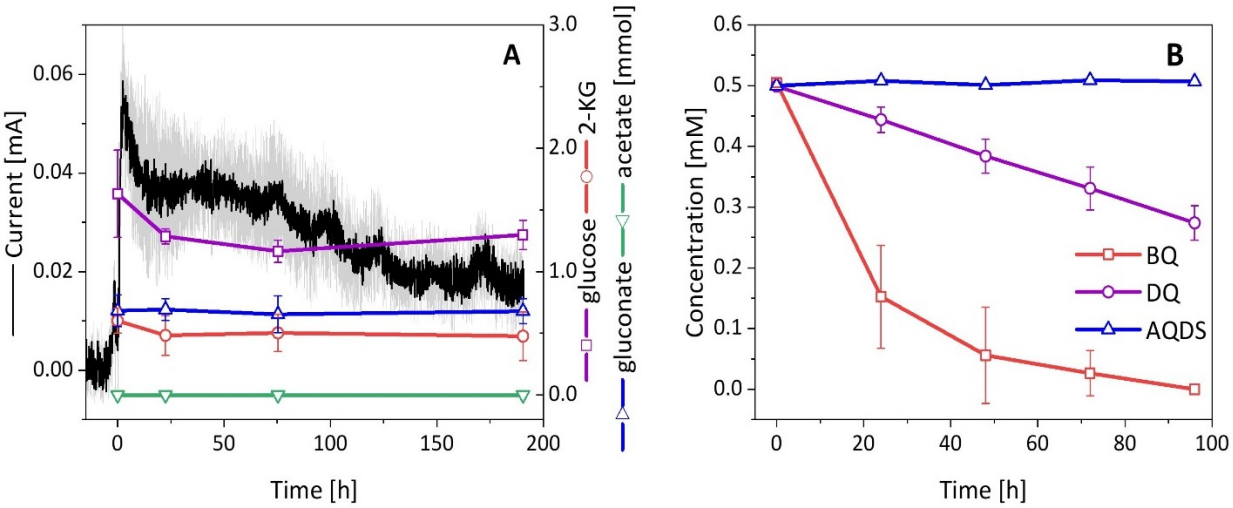


**Figure 33. BES performance of *P. putida* KT2440 with 1 mM AQDS as redox mediator.** The left y-axis indicates the current output of the respective BES fermentations, and the right y-axis shows the number of metabolites (mmol) in the reactors. The line or line-symbol presents the averaged values, and the shading or error bars indicate the standard deviations of (biological) replicates **(A)**. (n=3) The concentration of AQDS in pure DM9 media at 30 °C was measured for 96 h and is depicted in comparison to BQ and DQ **(B)**.

AQDS is known to be non-toxic for many microorganisms, including *P. putida*, when used at typical concentrations in BES. For testing the BES performance with *P. putida* using AQDS, a moderate concentration of 0.5 mM and a higher concentration of 1 mM were chosen. In parallel, the stability of AQDS was again tested via HPLC, as already done for the previous mediator candidates. The concentration of AQDS did not change during 96 h, confirming the high stability of the compound in the respective medium and conditions. However, the current output signal measured during the anodic electro-fermentation with *P. putida* KT2440 was significantly lower than for all other tested mediators during the 200-h course of the experiment. The concentration of the mediator did not influence the current generation, indicating that the cells were not able to use AQDS as an electron shuttle to transfer their terminal electrons to the anode. The subsequent HPLC analysis of glucose and exo-metabolite concentrations proved the inability of *P. putida* to metabolize glucose under this condition, as the concentration only slightly decreased during the first 24 h and stagnated after that. Congruent to this, no increase in the concentration of 2-KG, gluconate, or acetate was observed. Hence, AQDS is not a suitable redox mediator for the anodic electro-fermentation with *P. putida* KT2440 in the present system.

### *3.5.2.4 Comparison of the Tested Quinone Mediators and FeCN*

FeCN is considered the benchmark redox mediator for *P. putida* in BES. In a previous study by Lai et al. in 2016, FeCN enabled the best BES performance of all tested mediators at that time (Lai*, et al.* 2016b). In a classical BES run with 1 mM FeCN, *P. putida* needs about 250 h to metabolize ~2.5 mmol glucose, reaching peak current output signals of about 2 mA (Figure 34 A) and yielding 2-KG over glucose above

90%. The process time was drastically decreased by replacing FeCN with BQ as redox mediator. When BQ was used, the current output signal dropped back to the baseline already ~50 h after inoculation, shortening the duration of the anodic electro-fermentation to one-fifth of the time. Furthermore, the peak current and, therefore, the number of electrons transferred from the cells to the electrode was greatly increased by using BQ to about 10 mA. For DQ, an initial peak current of 2 mA was recorded immediately following the inoculation of biomass into the BES. However, after this initial increase, the current rapidly declined to 0.5 mA and continued to decrease slightly throughout the experiment. AQDS delivered the worst BES performance of all tested redox mediators with current output signals below 0.06 mA and, therefore, just marginally higher than the baseline.

The stability comparison of the tested redox mediators showed that only FeCN and AQDS maintained constant concentrations in DM9 medium at 30 °C over time (Figure 34 B). The concentrations of BQ and DQ decreased throughout the experiment, with BQ having a lower stability than DQ.

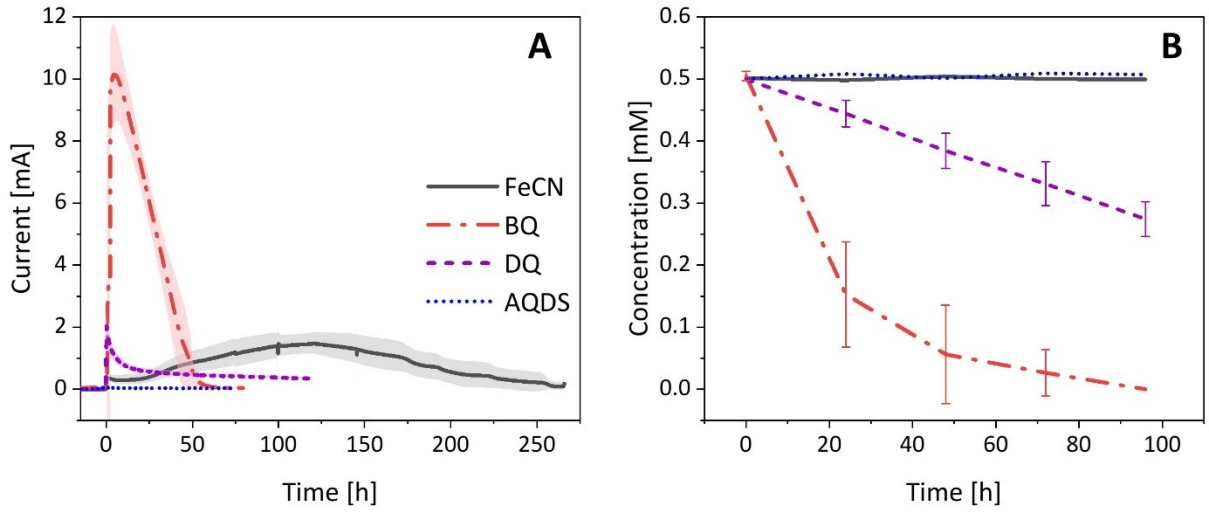


**Figure 34. Comparison of current output signal and stability of FeCN, BQ, DQ, and AQDS.** The current output signals were measured in BES with *P. putida* KT2440 WT under the usage of the different redox mediators, respectively. BQ and DQ were used in concentrations of 0.1 mM, and FeCN and AQDS in concentrations of 1 mM **(A).** Concentrations of the mediators in DM9 were measured over time to analyze the stability of the compounds in the DM9 medium **(B)**.

# 4. Discussion

This study aimed to gain an in-depth understanding of the anoxic, anode-driven phenotype of *P. putida* during electro-fermentation, with the ultimate goal of improving the performance of the system. This research focused primarily on elucidating the precise pathway of glucose uptake and metabolism in the BES. During an in-depth system analysis, the proteomic changes within the electrogenic *P. putida* were examined, and the role of polyP as an energy storage compound during the prolonged oxygen starvation within the BES was explored. Additionally, the influence of the redox mediator was investigated, on the one hand, by directly comparing an exogenous and an endogenous redox mediator in terms of electron transfer, product formation, and proteomic changes. On the other hand, different quinone redox mediator candidates were tested and compared to determine whether replacing the benchmark mediator, FeCN, with alternative compounds could enhance the anodic electro-fermentation performance of *P. putida*, especially in terms of metabolic rates.

## 4.1 Anaerobic Glucose Uptake of *P. putida* KT2440 in a BES

This part was published in Microbial Biotechnology, **2023**, DOI: 10.1111/1751-7915.14375

A previous study found that *P. putida* cells showed more oxidized redox carriers and a reduced ATP concentration despite an increased adenylate energy charge when a current was produced. In addition, compared to aerobic conditions, the cells consumed glucose at a rate of 1%- 3% and did not exhibit any growth. (Yu*, et al.* 2018). This active but extremely restricted phenotype sparked an interest in revealing metabolic constraints. It was hypothesized that the route of glucose uptake might be a key determining factor in the anodic electro-fermentation process. To test this, three gene deletion mutants were used, i.e. KT-G, KT-GL, and KT-KG, capable of exclusively using one of the three described glucose uptake routes (Figure 9). Since all three routes co-exist in the wild-type, an increase in the overall BES performance due to the gene deletion was not expected, but rather, that inferior performance might indicate a limiting factor.

The KT-GL mutant, only capable of taking up glucose via gluconate transporter, showed an almost identical aerobic growth profile as the WT. No significant difference was observed in terms of growth rate, glucose consumption, and biomass yield (Table 3). This was well-supported by literature showing that *P. putida* naturally had about 55-78% of its total carbon flux via the gaT pathway (Nikel*, et al.* 2015; Kohlstedt; Wittmann 2019), while cultivated aerobically. Both KT-G and KT-KG, which can take up glucose via glucose or 2-KG transporter, respectively, exhibited a halved maximum growth rate compared to the other two strains. The NADPH availability in KT-KG should be lower than in the WT due to the involvement of 2-ketogluconate 6-phosphate reductase (KguD) and is assumed to be higher

in KT-G because of the enforced flux through glucose 6-phosphate dehydrogenases (Zwf1-3). The decreased growth rate for KT-G was accompanied by a dramatically reduced glucose consumption rate and a slightly decreased biomass yield. However, the KT-KG mutant consumed glucose at a somewhat higher rate than the WT but at a marginally lower biomass yield.

*P. putida* KT2440, as well as the three mutants, showed a distinctive phenotype in the BES compared to aerobic conditions. For instance, compared to the wild-type, the glucose consumption rate was doubled in the mutant KT-GL, while it was decreased in the KT-KG mutant (Table 4). These results differed from those measured for aerobic cultivation (Table 3), as similar glucose consumption rates were measured for these three strains cultivated aerobically. In the BES, the secretion of gluconate as the end product increased the glucose turnover compared to the WT, while the secretion of 2-KG as the end product showed the opposite effect.

The extremely low electrogenic activity of KT-G in BES was unexpected. Former studies using *P. putida* F1 or fructose as the substrate revealed that the intracellular redox equivalents were largely shifted to the oxidized pools (Lai*, et al.* 2016b; Nguyen*, et al.* 2021). Thus, it was hypothesized that the increased NADPH supply via the glcT pathway might play an essential role in providing redox equivalents under BES conditions. Unfortunately, obtaining reproducible data for the intracellular redox pools in the experimental setup was impossible, preventing direct verification of this hypothesis. However, in the case of strain KT-G, sugar consumption was nearly eliminated, with a specific consumption rate of approximately 0.01 mmol/$g_{CDW}$/h—less than 0.15% of the rate observed under aerobic cultivation. To confirm that carbon reaches the cytoplasm, we conducted extra measurements of $^{13}C$ labeling in the pyruvate molecule for the KT-G strain (see 6. Appendix, Figure S9) in addition to acetate labeling (Figure 12). This confirmed that glucose-derived carbon reached the pyruvate node. It was hypothesized that the increased ATP demand of the glcT pathway compared to the other two pathways could lead to energy starvation. The lower glycolytic reactions would provide the needed amount of ATP to generate gluconate-6P. Without current, no ATP synthase activity could be expected in KT-G, unlike the other strains (Figure 13).

An additional BES experiment using the KT-GL strain with gluconate as the sole carbon source was conducted to analyze this phenotype further. Under this condition, gluconate could only be taken up into the cytosol. Still, no periplasmic oxidation was possible, comparable to the KT-G strain on glucose, but with a difference in the NADPH balance and ATP demand of the upper pathway (Figure 13). The observed substrate consumption, current output, and acetate enrichment were similar to the KT-G strain on glucose. This confirmed the hypothesis that periplasmic oxidation was needed for efficient current generation and carbon turnover.

However, pinpointing a cytosolic limitation purely on energy or redox requirements remained elusive since both experiments (KT-G with glucose and KT-GL with gluconate as sole carbon sources, respectively) gave comparable results at very different pathway stoichiometry. Despite different contributions from biomass carbon, the similar accumulation of acetate in the three strains of *P. putida* KT2440 under BES conditions further made it difficult to attribute a limitation of the metabolism to redox balancing or energy demand. Therefore, an involvement of regulatory mechanisms was hypothesized, which might contribute to the observed phenotype. Under aerobic conditions, a couple of transcriptional repressors (e.g. HexR, GnuR, and PtxS) were reported in *P. putida* KT2440 to regulate the glucose metabolism (del Castillo, Duque et al. 2008), but if they play a role under anaerobic conditions in *P. putida* remains to be shown. Besides, a two-component GtrS-GltR system was reported in *Pseudomonas aeruginosa* that regulated glucose metabolism based on the presence of 2-KG (Daddaoua*, et al.* 2014). A similar mechanism (but acting on different key metabolites) might also exist in *P. putida* KT2440, regulating anaerobic cytosolic metabolism in BES. However, investigating the influence of regulatory mechanisms of *P. putida* on BES performance might be an interesting starting point for further studies.

In summary, it was possible to utilize the genetically engineered *P. putida* strains to study and compare the three glucose uptake routes under anode-steered conditions. It was successfully shown that periplasmic glucose oxidation to gluconate and 2-KG are essential pathways for the current generation in BES. In contrast, direct uptake of glucose or gluconate did not support current formation. This indicated that cytosolic oxidation via the anode was constrained. It was also shown that the extent of the inoculated biomass contributed to the formation of acetate and, most likely, also to the anodic current. The new data in this study show that the cytosolic fluxes of glucose degradation were previously overestimated. Whether metabolism was constrained by a metabolic, a regulatory, or a combined mechanism remains to be studied.

## 4.2 Anaerobic Phenotype of the *P. putida* KT2440 in BES

Parts of this section were published in Microbial Cell Factories, **2024**, https://doi.org/10.1186/s12934-024-02509-8.

### 4.2.1 Energy Starvation and Adapted Protein Synthesis

Under anaerobic and anode-driven conditions, *P. putida* endures high stress, leading to extensive changes in the metabolism and physiology of the cells. During the electro-fermentation, *P. putida* is unable to grow. Instead, a share of the inoculated cells dies, leading to a decrease in the cell

concentration, especially during the first two phases of the process. However, the cells are metabolically active during the full process of over 16 days, transforming the substrate glucose into the main product 2-KG and the main by-product acetate, accompanied by small amounts of gluconate, succinate, pyruvate, and lactate. The measurement of the adenylate energy charge metabolites AMP, ADP, and ATP showed reduced AEC and ATP levels compared to aerobically grown cells. Nevertheless, the energy balance achieved by the involvement of the anode as terminal electron acceptor was higher than the one observed for oxygen-starved cells (Nikel; Lorenzo 2013).

To cope with the drastically decreased energy availability, *P. putida* made significant adjustments in the transcriptome and proteome and adaptations of the used metabolic pathways. The proteomics data proved pronounced down regulations of energy-intensive processes, particularly translation, after the initial phase of the process. Under aerobic conditions, up to 80% of the ATP used for anabolism is used for protein and rRNA synthesis (Stouthamer; Bettenhaussen 1973; Tempest; Neijssel 1984). The cell can save most of the available energy by shutting down these processes. A sucrose gradient sedimentation analysis further supported these observations, as polysomes and monosomes, which are essential for translation, could not be found anymore after 100 h. These findings indicate a strong decrease in ribosomal activity and active protein synthesis and mark a transition toward cell homeostasis for the prolonged fermentation process, where a decreased transcriptional response persists. Still, the translation of these responses into the production of new proteins was diminished. It has to be mentioned that the decrease in rRNA amounts resulted in a relative increase in mRNA levels and subsequently might lead to overestimations of the transcriptomics data. Therefore, relevant transcriptomics conclusions could only be drawn from the samples taken during the initial 24 h.

After 24 h, a significant number of genes (2,011 of 5,564 coding genes) were found to be upregulated, and only 176 genes were downregulated compared to the start of the process, reflecting a broad adaptation to the BES conditions. Among the upregulated genes were mainly membrane-related processes like transport, secretion, and cell wall organization, while the downregulation was associated with cell mobility.

Proteomics and transcriptomics data highlighted increased levels of several key ETC proteins and genes. The abundance of proteins like NADH-quinone oxidoreductase, cytochrome $b_0$ terminal oxidase, and succinate dehydrogenase was increased as these proteins likely are involved in the electron transfer from the ETC to the redox mediator FeCN, supporting ATP generation under anaerobic conditions. The upregulation of genes associated with membrane transport and structural reorganization probably enabled *P. putida* to redirect the electron flux toward the anode and ensure efficient redox cycling despite the absence of oxygen.

Furthermore, the transcriptomics data show the switch of the central carbon metabolism. Upregulated genes involved in the gluconate-2-dehydrogenase complex, the pyruvate node, and the glyoxylate shunt indicated a redirection towards 2-KG and acetyl-CoA accumulation. Additionally, the downregulation of isocitrate dehydrogenase probably redirected metabolic fluxes via the glyoxylate shunt. At the same time, there was a switch from NADH-forming to quinol-forming malate dehydrogenase, likely affecting electron transport.

In parallel to the conducted -omics analysis, an isotopic $^{13}C$ tracer study was conducted to provide insights into the metabolic origin of intra and extracellular amino acids and highlight distinct carbon utilization pathways during the BES process. For this purpose, fully labeled $^{13}C$ glucose was used as the sole carbon source for a BES run, and the labeling information in the respective precursors and amino acids was measured. The incorporation of the $^{13}C$ label proves the de novo synthesis from the supplied substrate, while the absence of $^{13}C$ enrichment indicates carbon originating from the breakdown of biomass components.

After 100 h, gluconate, and 2-KG, the metabolites originating from the periplasmic oxidation chain, were found to be fully $^{13}C$ labeled and, therefore, de novo synthesized from the fed fully labeled $^{13}C$ glucose. In contrast, the organic acids acetate, pyruvate, and succinate showed only partial $^{13}C$ labeling, suggesting these metabolites incorporated carbon from biomass breakdown rather than solely from glucose. This result aligns with the decrease of biomass concentration during the first phases of the anodic electro-fermentation. Pyruvate displayed 75.4% $^{13}C$ carbon, pointing to glucose metabolism through the Entner-Doudoroff and the lower Embden-Meyerhof-Parnas pathways. The significantly lower $^{13}C$ enrichment with acetate and succinate, with 39.4% and 30.7%, respectively, appeared to derive from biomass degradation primarily.

In addition, the intracellular amino acid pool after 100 h showed $^{13}C$ incorporation in L-alanine, L-aspartate, L-leucine, L-threonine, L-valine, and L-serine, indicating ongoing de novo synthesis from glucose under BES conditions. Protein-incorporated amino acids obtained via cell hydrolysis also exhibited $^{13}C$ labeling, confirming new protein synthesis during the BES process. However, the relatively low degree of labeling in these amino acids suggests that protein synthesis was limited and likely restricted to a specific subset of essential proteins, reflecting the adaptive response of *P. putida* to the constrained anaerobic and anode-driven environment.

### 4.2.2 Acetate Biosynthesis under BES Conditions

The acetate production in *P. putida* under BES conditions is of special interest. The $^{13}C$ tracer study revealed that acetate primarily originates from acetyl-CoA derived from biomass degradation, marking a notable shift from aerobic conditions where acetate typically results from pyruvate metabolism. This shift is closely linked to significant changes in lipid metabolism. LC-MS/MS analysis of intracellular CoA

thioesters revealed that, under BES conditions, succinyl-CoA levels were substantially lower than in aerobic cells due to the disrupted citric acid cycle. Malonyl-CoA abundance was also markedly reduced, indicating almost no de novo fatty acid synthesis. Instead, acetyl-CoA levels increased by 20%, driven by the β-oxidation of fatty acids, which became a significant carbon source. This adaptation is similar to other microorganisms that rely on lipid degradation for energy and reducing power during stationary growth phases (Beganovic*, et al.* 2023; Jovanovic Gasovic*, et al.* 2023; Stegmüller*, et al.* 2024). Thus, fatty acid degradation provided an alternative energy and redox source, as supported by transcriptomics and proteomics data showing the upregulation of genes involved in β-oxidation and downregulation of those involved in de novo fatty acid synthesis.

In addition to changes in lipid catabolism, *P. putida* also adapted its membrane composition under BES conditions, incorporating more trans-oriented fatty acids. This alteration results in tighter membrane packing, which increases rigidity and reduces fluidity. Such changes are likely advantageous under BES stress, as they enhance cellular resilience and support the long-term maintenance of ETC complexes and transporters. Similar membrane adaptations have been observed in *P. putida* strains under non-growth conditions, where reduced fluidity aids in stability (Okuyama*, et al.* 1990; Härtig*, et al.* 2005).

Acetate formation from acetyl-CoA in BES can proceed through four possible metabolic pathways (Figure 35. Possible acetate production pathways of *P. putida* under BES conditions.Figure 35).

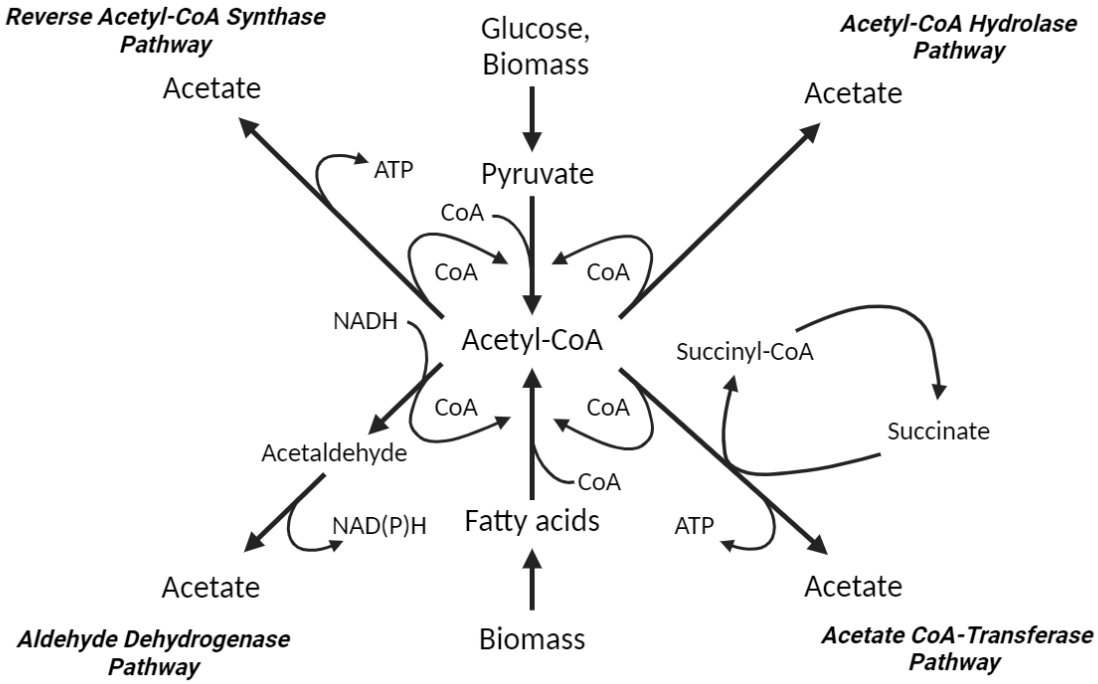


**Figure 35. Possible acetate production pathways of *P. putida* under BES conditions.**

The first possibility is the reverse-acting acetyl-CoA synthase pathway (Lindahl; Chang 2001), which enables ATP generation from acetyl-CoA under anaerobic BES conditions. In this pathway, acetyl-CoA

is converted to acetate, releasing energy used to phosphorylate ADP to ATP. This process bypasses the need for the citric acid cycle and oxidative phosphorylation, allowing *P. putida* to maintain ATP production and sustain metabolic activity despite limited energy resources in the BES environment. This pathway exemplifies the metabolic adaptability of *P. putida*, optimizing energy conservation for survival under stress.

The second option is the ATP-independent acetyl-CoA hydrolase pathway (Lee*, et al.* 1996). It provides a means to convert acetyl-CoA into acetate without consuming or generating ATP. In this pathway, acetyl-CoA is hydrolyzed directly to acetate, releasing free CoA in the process. This reaction does not involve ATP, which makes it beneficial for cells under energy-limited conditions like those in BES. By operating independently of ATP, the acetyl-CoA hydrolase pathway supports cellular function by recycling CoA without further taxing the energy reserves of the cells, allowing *P. putida* to conserve ATP for other essential processes.

The third possible pathway for acetate generation is the NAD(P)H-generating aldehyde dehydrogenase pathway (Riveros-Rosas*, et al.* 2019), which enables the conversion of acetyl-CoA to acetate while producing NAD(P)H. In this pathway, acetyl-CoA is first converted to an aldehyde intermediate, which is then oxidized to acetate by aldehyde dehydrogenase. This oxidation reaction generates NAD(P)H, a crucial reducing power source that supports various metabolic processes under BES conditions, where electron availability is limited. The aldehyde dehydrogenase pathway thus not only facilitates acetate production but also boosts cellular reducing capacity, aiding in redox balance and enhancing metabolic resilience under anaerobic conditions.

The fourth acetate-generating pathway in *P. putida* is the acetate CoA-transferase pathway (Taylor; Anthony 1976), which converts acetyl-CoA to acetate while simultaneously regenerating succinyl-CoA from succinate, which enables ATP production. In this pathway, acetyl-CoA donates its CoA group to succinate, producing acetate and succinyl-CoA. Succinyl-CoA then enters the succinyl-CoA synthetase reaction, which converts it back to succinate, generating ATP in the process. This pathway is especially advantageous under BES conditions, as it couples acetate production with ATP formation, providing *P. putida* a way to sustain energy levels in anaerobic environments where traditional ATP-generating pathways are less active.

Each of these pathways has advantages for the energy-deprived *P. putida* in BES. Knockout mutants were constructed to elucidate the preferred pathway under anaerobic and anode-driven conditions, each lacking one of the four possible pathways for acetate production. In all of these mutants, a reduced acetate production was observed, corresponding with increased glucose oxidation to 2-KG, proving the involvement of all four routes in the acetate production under BES conditions. However, the double mutant *P. putida* KT2440 Δ*ald*BI Δ*ald*BII, lacking the aldehyde dehydrogenase pathway,

showed the highest reduction in acetate production of 80% compared to the wild-type, highlighting the aldehyde dehydrogenase pathway as the primary route for acetate formation. This mutant also displayed twice the glucose uptake rate and a substantial increase in 2-KG yield, selectivity, and productivity (96%).

Moreover, the acetate CoA-transferase and reverse acetyl-CoA synthase pathways contributed directly to ATP generation, whereas the aldehyde dehydrogenase pathway supplied NAD(P)H. These distinct roles of acetate formation pathways reflect a finely tuned metabolic balance, supporting both energy generation and reducing power under BES conditions.

In summary, the multi-omics phenotyping results highlight the impressive ability of *P. putida* to reorganize its metabolism and energy management under the restrictive conditions of anodic electro-fermentation. By adjusting carbon fluxes, enhancing β-oxidation, and utilizing alternative pathways for ATP and NAD(P)H generation, *P. putida* effectively navigates limited energy availability while maintaining essential cellular processes. Identifying the aldehyde dehydrogenase pathway as a major acetate production pathway underscores a finely tuned balance between energy generation and reducing power in this unique electrochemical environment. These insights into the metabolic flexibility of *P. putida* set the stage for further discussion on the role of polyP in supporting its energy demands under BES stress

## 4.3 The Role of PolyP in BES

As indicated by flux balance analysis and supported by the systems biology analysis, *P. putida* is facing significant energy limitations under anaerobic, anode-driven conditions in the BES. The findings of this study provide insight into the potential role of polyP in *P. putida* under these conditions. Consistent with the function of polyP as an energy reservoir, the observed depletion of polyP during prolonged electro-fermentation suggests that *P. putida* may rely on polyP to compensate for reduced ATP generation in the absence of oxygen. However, it is important to interpret these findings cautiously, as further experimental evidence is needed to confirm this hypothesis. These results are nonetheless consistent with studies that highlight the role of polyP in maintaining cellular processes during energy shortages (Nikel*, et al.* 2013).

The observed changes in polyP levels throughout the fermentation process suggest that polyP may also play a broader role in modulating stress responses. Accumulation of polyP under aerobic conditions, followed by its depletion in the BES, reflects a dynamic balance between energy storage and consumption. This mechanism could be crucial for the survival of *P. putida* in such energy-limited environments. These findings further support the idea that polyP serves not only as a buffer for phosphate and energy but also contributes to stress tolerance during anodic electro-fermentation.

The results obtained from SEM and EDX imaging provided evidence of high phosphorus content in cells grown aerobically. Phosphorus signals were concentrated in round structures, which are highly suggestive of polyP granules, as polyP is known to form granules (Renninger*, et al.* 2004). After the BES process, the phosphorus signal intensity within the cells decreased significantly, indicating the potential degradation of polyP granules to release phosphate. Metabolic processes could utilize this phosphate for ATP production, helping cells survive under conditions where energy and ATP production pathways are limited.

The enzymes polyphosphate kinase (ppk) and exopolyphosphatase (ppx) are central to polyP metabolism. Polyphosphate kinase facilitates the reversible transfer of phosphate between polyP and ADP, producing ATP. Thus, it plays a dual role in both polyP synthesis and depletion. Exopolyphosphatase, on the other hand, is involved exclusively in polyP degradation, releasing inorganic phosphate, which can then be used by different metabolic pathways to generate ATP. Interestingly, the comprehensive proteomic analysis performed during BES fermentation showed no significant change in the abundance of polyphosphate kinase when comparing anaerobic electro-fermentation with aerobic conditions, likely reflecting its role in maintaining polyP homeostasis. However, the abundance of exopolyphosphatase decreased after 24 h but increased in the later stages of fermentation, suggesting its involvement in polyP degradation during energy-limited phases.

Raman spectroscopy results further support the hypothesis that polyP is being depleted during BES fermentation. The reduction in characteristic polyP signals at 690 $cm^{-1}$ and 1145-1177 $cm^{-1}$ suggests that polyP reserves are consumed as *P. putida* responds to anoxic, energy-limited conditions. However, this interpretation should be cautiously approached, as Raman signals in these regions could also originate from other biomolecules. Proteins, nucleic acids, and carbohydrates can emit signals in the same spectral ranges, complicating the identification of polyP. For instance, C-S bond stretches in amino acids, such as cysteine and methionine, and ring vibrations from nucleobases in DNA/RNA can contribute to signals in the 682-700 $cm^{-1}$ range (Gelder*, et al.* 2007; Larkin 2018). Similarly, in the 1145-1177 $cm^{-1}$ range, Raman shifts can be attributed to C-H bending in aliphatic side chains, C-N stretching in nucleobases, and O-P-O stretching in the phosphate backbone of DNA (Gelder*, et al.* 2007; Larkin 2018).

The decrease in Raman signal intensity during BES fermentation could be explained not only by a reduction in polyP levels but also by other factors, such as decreased protein, DNA, and sugar content, as *P. putida* does not exhibit significant growth under BES conditions.

It is also important to consider the broader biological role of polyP in different contexts. For instance, in *P. aeruginosa*, polyP synthesis increases during nitrogen starvation as part of a stress response, where polyP is associated with cell cycle exit rather than being used as an energy source (Racki*, et al.*

2017). This suggests that polyP may serve more of a stress adaptation role during prolonged starvation rather than as an immediate energy source. Conversely, Renninger et al. demonstrated in 2004 that *P. aeruginosa* can degrade polyP under phosphate starvation, indicating that polyP can also function as a phosphate reservoir rather than an energy source, depending on the environmental context (Renninger*, et al.* 2004) .

In the case of *P. putida* in BES, the environmental conditions differ significantly from those described in the nitrogen starvation study of *P. aeruginosa*. While *P. aeruginosa* might not consume polyP for energy under nitrogen-limited conditions, the versatile metabolism of *P. putida* allows for a different response under BES conditions. Several studies have demonstrated that under energy-limited conditions, such as anoxic or nutrient deprivation, bacteria can degrade polyP to release phosphate, which is then used in ATP synthesis or other metabolic processes (Nikel*, et al.* 2013; Sharfstein; Keasling 1994; Vargas*, et al.* 2013). Thus, it is likely that *P. putida* is degrading polyP in response to the energy-limited, anode-driven conditions in the BES.

One open question is the fate of the phosphate released from polyP degradation. If polyP were only converted to ATP, one would expect similar phosphorus signal intensities, albeit more distributed, as in aerobically grown cells. However, the decreased phosphorus signals observed in BES could be explained by phosphate efflux from the cells. Under anoxic conditions, especially in BES, bacteria may alter their phosphate metabolism and release phosphate into the extracellular environment. This has been observed in other bacterial species, where phosphate release is associated with energy stress or shifts in environmental conditions (Hou*, et al.* 1966).

Overall, while the decrease in the Raman signals cannot be attributed with certainty to the degradation of polyP, in combination with the signals for phosphorus in the EDX measurements, it gives a strong indication that polyP is used for the compensation for the lack of energy during anodic electro-fermentation. Nevertheless, additional analyses, such as the polyP-specific assay described by Nikel et al. in 2013 (Nikel*, et al.* 2013), could be done to prove the degradation of polyP during BES beyond any doubt.

## 4.4 Redox Mediator Testing

### 4.4.1 Endogenous vs. Exogenous Redox Mediator

The direct comparison of the artificial redox mediator FeCN and the natural mediator PCA in the same BES system with *P. putida* provided valuable insights into their advantages and limitations, respectively. FeCN demonstrated significantly higher current output and faster glucose-to-product conversion, with an immediate increase in the current output signal to 1 mA upon switching to BES conditions, compared to the lower but more stable current when PCA is used. Therefore, it can be stated that the

electron transfer capacity of FeCN is more efficient, resulting in higher metabolic activity and faster glucose uptake and product formation in *P. putida*. These properties are advantageous for industrial applications requiring rapid substrate-to-product turnover. However, the need for external addition of FeCN increases costs and process complexity. Developing recycling methods for artificial mediators would be crucial for enhancing the sustainability of such a system (Gemünde*, et al.* 2022).

Additionally, the FeCN-mediated process in this experiment showed reduced current output compared to the benchmark fermentation. A possible explanation might be the addition of antibiotics, which are needed to ensure the presence of the plasmid in *P. putida* KT-control and KT-PCA. The reduced current output might indicate increased stress on the cells and could, therefore, impact the performance of the BES fermentation. In the case of the artificial redox mediator, introducing a plasmid is unnecessary, as *P. putida* can naturally transfer electrons to FeCN. However, genetic modification is crucial to enable PCA production in *P. putida*. This aspect is another advantage of using FeCN over PCA, at least when a plasmid-based genetic engineering technique is used.

PCA, in contrast, offers a self-sufficient and potentially more cost-effective option, as *P. putida* KT-PCA can produce PCA endogenously. Hence, it is not necessary to externally add a mediator. This reduces the process steps and costs and makes PCA an attractive mediator candidate for large-scale processes with higher sustainability. However, the PCA-mediated system exhibited slower glucose consumption and 2-KG production rates and would, therefore, be unsuitable for rapid product formation. As mentioned above, a major disadvantage of using a genetically engineered PCA-producing strain in large-scale production processes is the reliance on antibiotics to maintain plasmid stability. This reliance not only adds to the cost but also reduces sustainability and creates regulatory challenges. Alternative genetic engineering strategies could be used to address this issue. One option is the implementation of a toxin-antitoxin system for plasmid stabilization. These systems involve a toxin gene and a corresponding antitoxin gene encoded on the plasmid. Cells that lose the plasmid fail to produce the antitoxin, leading to toxin activity and cell death or growth inhibition. This provides selective pressure for plasmid maintenance without the need for antibiotics. Examples of toxin/antitoxin systems include the *hok/sok* and *parDE* systems, which can be engineered into plasmids for industrial use (Hayes 2003). Another promising approach is genome integration of the PCA production pathway into the *P. putida* chromosome. This involves inserting the desired gene directly into a specific locus in the genome using homologous recombination or CRISPR-Cas9 systems (Aparicio*, et al.* 2019). Genomic integration ensures stable inheritance across generations.

Furthermore, it eliminates the need for the insertion of plasmids and, therefore, for the use of antibiotics. This would, in turn, simplify the process and improve the sustainability. Furthermore,

integrating the PCA pathway into a neutral or actively expressed genomic region could enhance its expression and make the system more efficient.

Proteomic analysis revealed similar cellular responses in both strains, with upregulation of stress-response proteins, such as heat shock proteins and alcohol dehydrogenases, driven by the anaerobic and energy-limited BES conditions. However, distinct differences were observed, including a higher abundance of Cbb3-type cytochrome c oxidase in FeCN systems, correlating with faster glucose metabolism. Both strains downregulated energy-intensive pathways, prioritizing survival and energy conservation under BES conditions.

In summary, FeCN enables faster electron transfer from *P. putida* to the anode and higher productivity than PCA, thus making it more suitable for processes demanding fast and effective product formation. However, the need for external mediator addition, associated costs, and recycling requirements limit its scalability. While less efficient in electron transfer and product formation, the natural mediator PCA offers a more sustainable alternative as it is endogenously produced. The reliance on antibiotics remains a significant obstacle for large-scale production. Implementing toxin/antitoxin systems for antibiotic-free plasmid stabilization or integrating the PCA production pathway directly into the genome would be a solution to overcome this limitation. These strategies could make PCA-based systems more practical and competitive for sustainable industrial applications. However, further studies comparing a broader range of natural and artificial mediators are required in order to draw clear conclusions about the superiority of one of the systems.

### 4.4.2 Quinone Mediators

The selection of an optimal redox mediator is essential for the success of the anodic electro-fermentation with *P. putida*. The mediator is crucial in facilitating the extracellular electron transfer between the microorganism and the anode. For this purpose, a mediator must meet several essential criteria: it has to be non-toxic to the organism, the redox potential has to be compatible with the molecular interaction site in the microbial ETC, it has to be stable under the applied conditions, and be transported rapidly to the site of interaction (Gemünde*, et al.* 2022)Each of these parameters is of great importance, as they directly influence the efficiency of metabolic activity and current generation in the system and will, therefore, determine the performance of the overall process.

In previous work by Lai et al. in 2016 (Lai*, et al.* 2016b), various redox mediators were tested and compared in terms of their influence on the performance of the BES process with *P. putida* F1. The mediators evaluated were FeCN, riboflavin, $[Co(Sep)]Cl_3$, Na[Fe(EDTA)], Thionine chloride, and $[Co(bpy)_3](ClO_4)_2$. FeCN, with a formal redox potential of 0.416 V vs. SHE, proved to be the best candidate of all tested mediators, supporting efficient electron transfer to the anode and robust metabolic activity in *P. putida*. Mediators with more negative redox potentials, such as neutral red (-

0.365 V) and riboflavin (-0.2 V), failed to produce significant current, indicating they could not effectively interact with the microbial ETC. FeCN was, therefore, adopted as the mediator of choice and benchmark mediator for this study.

The fundamental role of the redox mediator is to withdraw electrons from the ETC of the microorganism and transfer them to the anode, enabling *P. putida* to get rid of their terminal electrons when oxygen is unavailable. The redox potential of the mediator is a critical determinant of this ability. To fulfill this purpose, the redox potential of the mediator must be more positive than that of the molecular interaction side in the ETC to extract electrons efficiently. Lai et al. (2016) found that the minimum redox potential for effective extracellular electron transfer in *P. putida* ranges from 0.078 to 0.208 V vs SHE. Mediators with redox potentials below this range, such as riboflavin, cannot efficiently withdraw electrons from the microbial ETC, resulting in poor current generation.

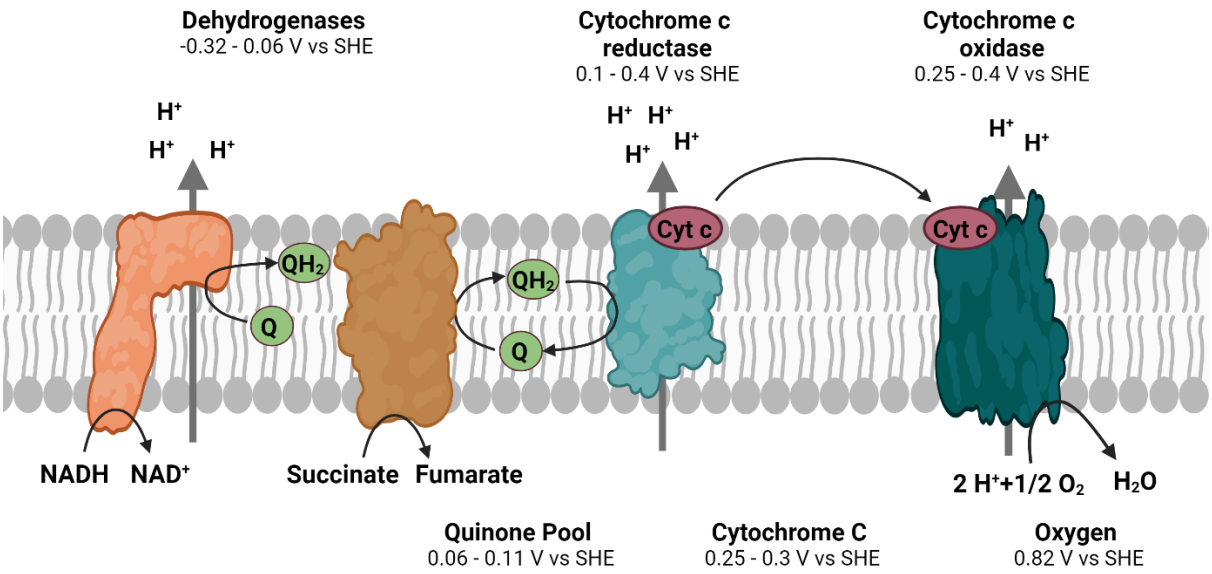


**Figure 36. Electron transfer chain of *P. putida* with redox potentials of the possible molecular interaction sites.** (Created in BioRender.com)

The redox potentials of the components of the ETC are progressively increasing in positivity to drive the flow of electrons along the chain toward the terminal electron acceptor. Hence, mediators with more positive redox potentials withdraw electrons further downstream in the ETC. This enables the microorganism to generate a stronger proton motive force and, therefore, a higher ATP generation via ATP synthase. As the standard redox potential of the oxygen reduction to water is 0.82 V vs. SHE, it could be hypothesized that a redox potential in the same range would be optimal for a mediator.

The redox potential of 0.42 V vs. SHE suggests that FeCN can withdraw electrons at a molecular interaction site between cytochrome c reductase, which has a redox potential between 0.1 and 0.4 V

vs. SHE, and cytochrome c oxidase, with a redox potential in the range of 0.25 and 0.4 V vs. SHE. This hypothesis was confirmed by a combination of proteomics analysis and inhibitor study by Lai et al. in 2020, which identified cytochrome c reductase as a key complex involved in the extracellular electron transfer with FeCN in *P. putida* under anaerobic and anode-driven conditions (Lai*, et al.* 2020).

The present study resumed the search for an optimal redox mediator for *P. putida*. Three quinone redox mediators—BQ, DQ, and AQDS—were tested alongside FeCN, which served as the benchmark. All mediators were tested in terms of their resulting influence on the BES performance, their redox potential under the applied BES conditions, their stability, and biocompatibility with *P. putida*.

The redox potential of each mediator was measured via cyclic voltammetry in the BES system under the applied standard conditions. FeCN exhibited a potential of 0.22 V vs. SHE, BQ 0.09 V, DQ -0.17 V, and AQDS -0.39 V vs. SHE. Based on these values, BQ and DQ likely interact with components of the ETC, such as succinate dehydrogenase or the quinone pool. However, the very negative redox potential of AQDS may not allow interaction with any ETC component.

BQ emerged as the most promising candidate among the quinone-based mediators tested, showing the best performance observed for anodic electro-fermentation with *P. putida* KT2440. BQ dramatically increased the current output, with peak currents reaching up to 10 mA, five times higher than those generated with FeCN. Additionally, BQ reduced the processing time needed for the anaerobic bio-conversion of ~8 mM glucose to just ~60 h, marking a significant improvement compared to the 250 h required when using FeCN. These results suggest that BQ facilitated a much faster electron transfer rate, translating into a more rapid glucose metabolism and product formation.

The enhanced performance of BQ might be connected to a faster transport mechanism. FeCN is an iron-containing complex. Therefore, it was hypnotized that the transport of the compound relies on TonB-dependent transporters. TonB-dependent transporters can be found in the outer membrane of Gram-negative bacteria and are involved in the uptake of iron via siderophore complexes (Wang; Newton 1971). An unpublished study by Weimer et al. confirmed the transport of FeCN via TonB-dependent transporters.

The drawback of this transport mechanism is that the TonB-dependent transport requires energy transduction from the proton motive force through the TonB-ExbB-ExbD complex, localized in the cytoplasmic membrane (Jeong*, et al.* 1997). The energy generation of *P. putida*, especially under BES conditions, dramatically relies on the proton motive force, which is generated via the electrochemical gradient resulting from periplasmic oxidation and ETC. The proton motive force drives ATP generation via ATP synthase. Consequently, the depletion of the proton motive force caused by FeCN uptake leads to decreased energy availability for the metabolism of the cell. It will, therefore, reduce the efficiency of the BES performance.

BQ, in contrast, is a small, uncharged, and relatively hydrophobic molecule. Due to these characteristics, BQ is most likely transported via passive diffusion into the periplasm (Brandl*, et al.* 2007). Passive diffusion is not only independent of energy consumption but also generally faster than transporter-mediated uptake, as it relies solely on the concentration gradient and membrane permeability (Schultz 1968). This potentially explains the higher current output and decreased process time observed when BQ is used as redox mediator for *P. putida*.

However, despite the promising performance, BQ suffers from significant instability under the conditions applied in the BES. BQ is known to degrade rapidly in the presence of heat, acids, bases, and light. This instability was confirmed by concentration measurements of a BQ solution in DM9 medium over time via HPLC analysis. During the experiment, the concentration of BQ dropped by more than 70% within 24 h, and after 48 h, only trace amounts of the compound remained. This rapid degradation limits the possible duration of the BES process. Although the instability of BQ prevents its use as a feasible long-term mediator, its exceptional performance highlights the potential of anodic electro-fermentation with *P. putida* when fast mediator transport and compatible redox potential are achieved. This suggests that the uptake mechanism of the respective mediator is a key limiting factor for the efficiency of the BES process.

Following the instability observed with BQ, DQ was tested as a more stable alternative. DQ is a tetramethyl derivative of BQ, and adding methyl groups increases its molecular stability. Indeed, DQ showed better stability in the BES system, with a slower degradation rate than BQ. However, this structural modification also shifted the redox potential to a more negative value (-0.17 V vs. SHE), most likely changing the molecular interaction site within the ETC of *P. putida* and leading to decreased efficiency of the process.

As a result, DQ could not support efficient electron transfer or metabolic activity. Although the peak current initially reached 2 mA immediately after inoculation, comparable to that observed with FeCN, the signal steadily declined after that, and only minimal glucose consumption was observed. This outcome reinforces the importance of redox potential in the selection of mediators. While increased stability is desirable, it cannot come at the expense of a compatible redox potential. The lower redox potential of DQ prevented it from effectively drawing electrons from the ETC, rendering it an unsuitable mediator for *P. putida* in BES.

The last mediator tested in the course of this study was AQDS. The molecule is commonly used in microbial fuel cells due to its high stability and ability to shuttle electrons between molecules or electrodes. Additionally, AQDS has previously been used as a humic substance analog for anaerobic Fe(III)-reducing soil bacteria capable of utilizing it as an electron acceptor (Lovley et al., 2,000; Xia et

al., 2023). Given that *P. putida* is a soil bacterium frequently exposed to humic substances, it was anticipated that the microorganism might also be able to interact with AQDS similarly.

In this study, the AQDS concentration was maintained consistently throughout the BES process, proving its stability under the applied conditions. However, the measured redox potential in the BES system (-0.39 V vs. SHE) was far too negative to interact effectively with the microbial ETC of *P. putida*, resulting in very low current output and negligible glucose consumption.

The results of this study underline the complexity of optimizing redox mediators for BES systems. Finding the right balance between stability, redox potential, and transport efficiency is crucial to maximize performance. The success of BQ, despite its instability, demonstrates the importance of fast and, in the best energy, neutral transport and compatible redox potential. The optimal redox mediator for the anodic electro-fermentation with *P. putida* would have a redox potential close to the one of BQ or higher, high stability, and a passive transportation mechanism. If such a mediator could be identified, the efficiency of the BES process could be significantly improved.

The redox potential of a mediator is influenced by its chemical structure and the environmental conditions in which it is applied. Structural changes or variations in the medium can alter the redox potential. For instance, lowering the pH of the medium can increase the redox potential by promoting protonation, shifting it to a more positive value. Similarly, using a solvent with a higher dielectric constant may raise the potential. Nevertheless, altering the medium can have a significant impact on the viability of the microorganism, limiting the extent of environmental changes that can be applied without adverse effects. To achieve compatibility with the ETC of *P. putida*, the redox potentials of DQ and AQDS would need to be significantly shifted. It is unlikely that environmental adjustments alone would be sufficient to achieve this. Structural modifications, such as substitutions with electron-withdrawing groups like halogens or nitro groups or complexation with metal ions like Fe(III), could help stabilize the oxidized form and increase the redox potential. However, such changes may also affect the transport mechanism of the compound or increase its toxicity.

Given the limitations of the mediators tested, future studies should explore other quinone derivatives and novel redox mediator compounds with higher stability and more positive redox potentials.

In conclusion, while BQ demonstrated exceptional BES performance, its instability prevents it from being a practical solution. The search for a mediator that combines high redox potential, rapid transport, and stability under BES conditions remains ongoing. A breakthrough in this area would significantly improve the efficiency and scalability of anodic electro-fermentation with *P. putida*.

Other quinone derivatives, which have been used in microbial electrochemistry before, include anthraquinone-2-sulfonate (AQS) (Tang*, et al.* 2014), 2-hydroxy-1,4-naphtoquinone (Lawsone) (Rau*, et al.* 2002; Rhoads*, et al.* 2005), Menadione (Vitamin K3) (Heiskanen 2004), 2,3-Dimethoxy-5-methyl-

1,4-benzoquinone (Coenzyme Q0 (Q0)) (Ito*, et al.* 2002), and 2,6-Dimethoxy-1,4-benzoquinone (DMBQ) (Vasiliadou*, et al.* 2019). The redox potentials of AQS, Lawsone, and Vitamin K3 are in the negative range between -0.23 and -0.08 V vs SHE. Therefore, there are no suitable candidates for efficient electron transfer from the ETC of *P. putida* (Franza; Gaudu 2022). More promising might be Q0 and DMBQ with redox potentials of +0.06 V to +0.10 V vs. SHE and +0.45 V to +0.50 V vs. SHE under standard conditions, respectively, and therefore in the same range as the ones of BQ and FeCN. Due to the substitution with methoxy groups and, in the case of Q0, a methyl group, the stability of these BQ derivatives should be higher than that of BQ, as the electron delocalization decreases the reactivity. Additionally, both compounds have a similar small size, like BQ, and might be taken up passively.

Furthermore, there are also quinones, which have never been tested in microbial but only in abiotic electrochemical systems so far, including 2,5-ditert-butyl-1,4-benzoquinone (DB-p-BQ), tetrachloro-1,4-benzoquinone (Chloranil), and 2,3-dichloro-5,6-dicyano-1,4-benzoquinone (DDQ).

## 4.5 Summary and Outlook

This study provides significant insights into the physiology of *P. putida* under anoxic, anode-driven conditions in BES, marking a crucial step toward advancing electro-fermentation technologies. While BES with *P. putida* is still far from large-scale commercial feasibility, our findings identify critical metabolic constraints that limit system performance, primarily a severe energy shortage and restricted mediator uptake efficiency. These limitations influence glucose metabolism and overall productivity and underscore the need for targeted interventions. Through analyses of glucose uptake pathways, polyP utilization, and redox mediator performance, this work establishes a foundation for future efforts to enhance BES efficiency with *P. putida*.

To address these challenges, future studies should focus on several promising strategies to unlock the potential of *P. putida* in BES. First, further investigation into the periplasmic glucose uptake mechanism and redox cofactor dynamics is essential. Currently, an ion chromatography-mass spectrometry method is under development, which will enable precise monitoring of redox cofactor levels in *P. putida* under BES conditions, helping to clarify the redox status of these strains. Furthermore, gene expression analyses could be performed to screen for regulatory circuit shifts that may result from the anoxic and anode-driven conditions. This approach could help to identify potential adaptive pathways or point towards limiting factors.

In addition, to confirm the role of polyP in balancing the lack of energy under BES conditions, further polyP-specific assays, as described by Nikel et al. in 2013 (Nikel*, et al.* 2013), could be performed. This would provide direct evidence of the role of polyP as an emergency energy reserve under oxygen-

limited, anode-driven conditions and help clarify its contribution to the survival and activity of *P. putida* in BES.

Regarding redox mediators, while no new candidates proved ideal, BQ exhibited promising characteristics, especially with its rapid transport and compatibility with the ETC of *P. putida*. Further mediator screening will expand to quinone derivatives such as Q0 (coenzyme Q0) and DMBQ, both of which have redox potentials compatible with the ETC of *P. putida* and offer potential stability improvements over BQ due to their structural modifications. Additional candidates, including DB-p-BQ and chloranil, previously used only in abiotic electrochemical systems, also warrant exploration as novel mediators that may enable more efficient electron transfer.

Moreover, genetic engineering presents another promising approach to addressing the ATP deficit in *P. putida*. Engineering metabolic pathways to improve ATP yield under BES conditions could significantly enhance cell function and energy balance. Simultaneously, expanding research to alternative bacterial candidates, such as *Bacillus subtilis* (Vassilev*, et al.* 2021), which may exhibit higher compatibility with BES, could provide additional avenues for advancing anodic electro-fermentation.

In conclusion, this study marks an essential step in understanding the physiological response of *P. putida* to BES. It identified key limiting factors and highlighted targeted strategies to improve system performance. While challenges remain, the insights gained here set the stage for future research to integrate novel analytical methods, genetic engineering, and redox chemistry, all of which could bring BES technology closer to practical application.

# 5. BibliographyBibliography

**Adler, P.**; **Bolten, C. J.**; **Dohnt, K.**; **Hansen, C. E.**; **Wittmann, C.** (2013). Core fluxome and metafluxome of lactic acid bacteria under simulated cocoa pulp fermentation conditions. *Applied and Environmental Microbiology*. 79. 5670–5681. 10.1128/AEM.01483-13.

**Adler, P.**; **Frey, L. J.**; **Berger, A.**; **Bolten, C. J.**; **Hansen, C. E.**; **Wittmann, C.** (2014). The key to acetate: metabolic fluxes of acetic acid bacteria under cocoa pulp fermentation-simulating conditions. *Applied and Environmental Microbiology*. 80. 4702–4716. 10.1128/AEM.01048-14.

**Aiyer, K.**; **Doyle, L. E.** (2022). Capturing the signal of weak electricigens: a worthy endeavour. *Trends in Biotechnology*. 40. 564–575. 10.1016/j.tibtech.2021.10.002.

**Allen, R. M.**; **Bennetto, H. P.** (1993). Microbial fuel-cells. *Applied Biochemistry and Biotechnology*. 39-40. 27–40. 10.1007/BF02918975.

**Anraku, Y.** (1988). Bacterial electron transport chains. *Annual Review of Biochemistry*. 57. 101–132. 10.1146/annurev.bi.57.070188.000533.

**Aparicio, T.**; **Lorenzo, V.** de; **Martínez-García, E.** (2019). CRISPR/Cas9-enhanced ssDNA recombineering for *Pseudomonas putida*. *Microbial Biotechnology*. 12. 1076–1089. 10.1111/1751-7915.13453.

AQUACYCL. Changing the world of industrial wastewater treatment. https://aquacycl.com/company/. November 21, 2024.

**Askitosari, T. D.**; **Berger, C.**; **Tiso, T.**; **Harnisch, F.**; **Blank, L. M.**; **Rosenbaum, M. A.** (2020). Coupling an electroactive *Pseudomonas putida* KT2440 with bioelectrochemical rhamnolipid production. *Microorganisms*. 8. 10.3390/microorganisms8121959.

**Askitosari, T. D.**; **Boto, S. T.**; **Blank, L. M.**; **Rosenbaum, M. A.** (2019). Boosting heterologous phenazine production in *Pseudomonas putida* KT2440 through the exploration of the natural sequence space. *Frontiers in Microbiology*. 10. 1990. 10.3389/fmicb.2019.01990.

**Badalamenti, J. P.**; **Krajmalnik-Brown, R.**; **Torres, C. I.** (2013). Generation of high current densities by pure cultures of anode-respiring *Geoalkalibacter* spp. under alkaline and saline conditions in microbial electrochemical cells. *mBio*. 4. e00144-13. 10.1128/mBio.00144-13.

**Bagdasarian, M.**; **Lurz, R.**; **Rückert, B.**; **Franklin, F. C.**; **Bagdasarian, M. M.**; **Frey, J.**; **Timmis, K. N.** (1981). Specific-purpose plasmid cloning vectors. II. Broad host range, high copy number, RSF1010-derived vectors, and a host-vector system for gene cloning in *Pseudomonas*. *Gene*. 16. 237–247. 10.1016/0378-1119(81)90080-9.

**Bedendi, G.**; **Moura Torquato, L. D.** de; **Webb, S.**; **Cadoux, C.**; **Kulkarni, A.**; **Sahin, S.**; **Maroni, P.**; **Milton, R. D.**; **Grattieri, M.** (2022). Enzymatic and microbial electrochemistry: Approaches and methods. *ACS Measurement Science Au*. 2. 517–541. 10.1021/acsmeasuresciau.2c00042.

**Beganovic, S.**; **Rückert-Reed, C.**; **Sucipto, H.**; **Shu, W.**; **Gläser, L.**; **Patschkowski, T.**; **Struck, B.**; **Kalinowski, J.**; **Luzhetskyy, A.**; **Wittmann, C.** (2023). Systems biology of industrial oxytetracycline production in *Streptomyces rimosus*: the secrets of a mutagenized hyperproducer. *Microbial Cell Factories*. 22. 222. 10.1186/s12934-023-02215-x.

**Belda, E.**; **van Heck, R. G. A.**; **José Lopez-Sanchez, M.**; **Cruveiller, S.**; **Barbe, V.**; **Fraser, C.**; **Klenk, H.-P.**; **Petersen, J.**; **Morgat, A.**; **Nikel, P. I.**; **Vallenet, D.**; **Rouy, Z.**; **Sekowska, A.**; **Martins Dos Santos, V. A. P.**; **Lorenzo, V.** de; **Danchin, A.**; **Médigue, C.** (2016). The revisited genome of *Pseudomonas putida*

KT2440 enlightens its value as a robust metabolic chassis. *Environmental Microbiology*. 18. 3403–3424. 10.1111/1462-2920.13230.

**Bennetto, H. P.** (1990). Electricity generation by microorganisms. *Biotechnology Education*. 1. 163–168.

**Bennetto, H. P.**; **Stirling, J. L.**; **Tanaka, K.**; **Vega, C. A.** (1983). Anodic reactions in microbial fuel cells. *Biotechnology and Bioengineering*. 25. 559–568. 10.1002/bit.260250219.

**Bergel, A.**; **Féron, D.**; **Mollica, A.** (2005). Catalysis of oxygen reduction in PEM fuel cell by seawater biofilm. *Electrochemistry Communications*. 7. 900–904. 10.1016/j.elecom.2005.06.006.

**Bosire, E. M.**; **Rosenbaum, M. A.** (2017). Electrochemical potential influences phenazine production, electron transfer and consequently electric current generation by *Pseudomonas aeruginosa*. *Frontiers in Microbiology*. 8. 892. 10.3389/fmicb.2017.00892.

**Brandl, M.**; **Eide Flaten, G.**; **Bauer‐Brandl, A.** (2007). Passive diffusion across membranes. 10.1002/9780470048672.wecb432.

**Brouwers, G. J.**; **Vrind, J. P.** de; **Corstjens, P. L.**; **Cornelis, P.**; **Baysse, C.**; **Vrind-de Jong, E. W.** de (1999). cumA, a gene encoding a multicopper oxidase, is involved in $Mn^{2+}$ oxidation in *Pseudomonas putida* GB-1. *Applied and Environmental Microbiology*. 65. 1762–1768. 10.1128/AEM.65.4.1762-1768.1999.

**Bruins, M. R.**; **Kapil, S.**; **Oehme, F. W.** (2000). Microbial resistance to metals in the environment. *Ecotoxicology and Environmental Safety*. 45. 198–207. 10.1006/eesa.1999.1860.

**Carter, J. P.**; **Richardson, D. J.**; **Spiro, S.** (1995). Isolation and characterisation of a strain of *Pseudomonas putida* that can express a periplasmic nitrate reductase. *Archives of Microbiology*. 163. 159–166. 10.1007/BF00305348.

**Castro, F. A. V.**; **Mariani, D.**; **Panek, A. D.**; **Eleutherio, E. C. A.**; **Pereira, M. D.** (2008). Cytotoxicity mechanism of two naphthoquinones (menadione and plumbagin) in *Saccharomyces cerevisiae*. *PLOS One*. 3. e3999. 10.1371/journal.pone.0003999.

**Chang, S.**; **An, H.**; **Chen, Y.**; **Hou, Y.**; **Zhang, J.**; **Zhu, Q.** (2019). Multiunit catalysts with synergistic reactivity: Three-dimensional polyoxometalate-based coordination polymers for highly efficient synthesis of functionalized p-benzoquinones. *ACS Applied Materials & Interfaces*. 11. 37908–37919. 10.1021/acsami.9b14928.

**Chaudhary, S.**; **Yadav, S.**; **Singh, R.**; **Sadhotra, C.**; **Patil, S. A.** (2022). Extremophilic electroactive microorganisms: Promising biocatalysts for bioprocessing applications. *Bioresource Technology*. 347. 126663. 10.1016/j.biortech.2021.126663.

**Chen, H.**; **Yu, Y.**; **Yu, Y.**; **Ye, J.**; **Zhang, S.**; **Chen, J.** (2021). Exogenous electron transfer mediator enhancing gaseous toluene degradation in a microbial fuel cell: Performance and electron transfer mechanism. *Chemosphere*. 282. 131028. 10.1016/j.chemosphere.2021.131028.

**Choi, O.**; **Sang, B.-I.** (2016). Extracellular electron transfer from cathode to microbes: Application for biofuel production. *Biotechnology for Biofuels*. 9. 11. 10.1186/s13068-016-0426-0.

**Christ, J. J.**; **Willbold, S.**; **Blank, L. M.** (2020). Methods for the analysis of polyphosphate in the life sciences. *Analytical Chemistry*. 92. 4167–4176. 10.1021/acs.analchem.9b05144.

**Chukwubuikem, A.**; **Berger, C.**; **Mady, A.**; **Rosenbaum, M. A.** (2021). Role of phenazine-enzyme physiology for current generation in a bioelectrochemical system. *Microbial Biotechnology*. 14. 1613–1626. 10.1111/1751-7915.13827.

**Cohen, B.** (1931). The bacterial culture as an electrical half-cell.

**Cook, T. B.**; **Rand, J. M.**; **Nurani, W.**; **Courtney, D. K.**; **Liu, S. A.**; **Pfleger, B. F.** (2018). Genetic tools for reliable gene expression and recombineering in *Pseudomonas putida*. *Journal of Industrial Microbiology & Biotechnology*. 45. 517–527. 10.1007/s10295-017-2001-5.

**Çoruh, S.**; **Gürkan, E. H.** (2014). Adsorption of neutral red from aqueous solutions using waste foundry sand: Full factorial design analysis. *Environmental Progress & Sustainable Energy*. 33. 1086–1095. 10.1002/ep.11879.

**Costa, K. C.**; **Moskatel, L. S.**; **Meirelles, L. A.**; **Newman, D. K.** (2018a). PhdA catalyzes the first step of phenazine-1-carboxylic acid degradation in *Mycobacterium fortuitum*. *Journal of Bacteriology*. 200. 10.1128/jb.00763-17.

**Costa, N. L.**; **Clarke, T. A.**; **Philipp, L.-A.**; **Gescher, J.**; **Louro, R. O.**; **Paquete, C. M.** (2018b). Electron transfer process in microbial electrochemical technologies: The role of cell-surface exposed conductive proteins. *Bioresource Technology*. 255. 308–317. 10.1016/j.biortech.2018.01.133.

**Daddaoua, A.**; **Molina-Santiago, C.**; **La Torre, J.** de; **Krell, T.**; **Ramos, J.-L.** (2014). GtrS and GltR form a two-component system: the central role of 2-ketogluconate in the expression of exotoxin A and glucose catabolic enzymes in *Pseudomonas aeruginosa*. *Nucleic Acids Research*. 42. 7654–7663. 10.1093/nar/gku496.

**Debuy, S.**; **Pecastaings, S.**; **Bergel, A.**; **Erable, B.** (2015). Oxygen-reducing biocathodes designed with pure cultures of microbial strains isolated from seawater biofilms. *International Biodeterioration & Biodegradation*. 103. 16–22. 10.1016/j.ibiod.2015.03.028.

**del Castillo, T.**; **Ramos, J. L.**; **Rodríguez-Herva, J. J.**; **Fuhrer, T.**; **Sauer, U.**; **Duque, E.** (2007). Convergent peripheral pathways catalyze initial glucose catabolism in *Pseudomonas putida*: Genomic and flux analysis. *Journal of Bacteriology*. 189. 5142–5152. 10.1128/JB.00203-07.

**Delaney, G. M.**; **Bennetto, H. P.**; **Mason, J. R.**; **Roller, S. D.**; **Stirling, J. L.**; **Thurston, C. F.** (1984). Electron ‐ transfer coupling in microbial fuel cells. 2. performance of fuel cells containing selected microorganism—mediator—substrate combinations. *Journal of Chemical Technology and Biotechnology*. 34. 13–27. 10.1002/jctb.280340104.

**Delvigne, F.**; **Lecomte, J.** (1981). Foam formation and control in bioreactors. 10.1002/9780470054581.eib326.

**Dennis, P. G.**; **Virdis, B.**; **Vanwonterghem, I.**; **Hassan, A.**; **Hugenholtz, P.**; **Tyson, G. W.**; **Rabaey, K.** (2016). Anode potential influences the structure and function of anodic electrode and electrolyte-associated microbiomes. *Scientific Reports*. 6. 39114. 10.1038/srep39114.

**Dohnalkova, A. C.**; **Marshall, M. J.**; **Arey, B. W.**; **Williams, K. H.**; **Buck, E. C.**; **Fredrickson, J. K.** (2011). Imaging hydrated microbial extracellular polymers: Comparative analysis by electron microscopy. *Applied and Environmental Microbiology*. 77. 1254–1262. 10.1128/AEM.02001-10.

**Doyle, L. E.**; **Marsili, E.** (2018). Weak electricigens: A new avenue for bioelectrochemical research. *Bioresource Technology*. 258. 354–364. 10.1016/j.biortech.2018.02.073.

**Ebert, B. E.**; **Kurth, F.**; **Grund, M.**; **Blank, L. M.**; **Schmid, A.** (2011). Response of *Pseudomonas putida* KT2440 to increased NADH and ATP demand. *Applied and Environmental Microbiology*. 77. 6597–6605. 10.1128/aem.05588-11.

**Erable, B.**; **Vandecandelaere, I.**; **Faimali, M.**; **Delia, M.-L.**; **Etcheverry, L.**; **Vandamme, P.**; **Bergel, A.** (2010). Marine aerobic biofilm as biocathode catalyst. *Bioelectrochemistry*. 78. 51–56. 10.1016/j.bioelechem.2009.06.006.

**Esteve-Núñez, A.** 2014. METfilter. in collaboration with IMDEA Water, CENTA Foundation. https://metfilter.com/. November 21, 2024.

**Esteve-Núñez, A.** 2015. iMETland. A new generation of Microbial Electrochemical Wetland for effective decentralized wastewater treatment. FUNDACION IMDEA AGUA. https://cordis.europa.eu/project/id/642190. November 21, 2024. 10.3030/642190.

**Feng, C.**; Le Ma; **Li, F.**; **Mai, H.**; **Lang, X.**; **Fan, S.** (2010). A polypyrrole/anthraquinone-2,6-disulphonic disodium salt (PPy/AQDS)-modified anode to improve performance of microbial fuel cells. *Biosensors & Bioelectronics*. 25. 1516–1520. 10.1016/j.bios.2009.10.009.

**Feng, J.**; **Qian, Y.**; **Wang, Z.**; **Wang, X.**; **Xu, S.**; **Chen, K.**; **Ouyang, P.** (2018). Enhancing the performance of *Escherichia coli*-inoculated microbial fuel cells by introduction of the phenazine-1-carboxylic acid pathway. *Journal of Biotechnology*. 275. 1–6. 10.1016/j.jbiotec.2018.03.017.

**Fernando, E. Y.**; **McIlroy, S. J.**; **Nierychlo, M.**; **Herbst, F.-A.**; **Petriglieri, F.**; **Schmid, M. C.**; **Wagner, M.**; **Nielsen, J. L.**; **Nielsen, P. H.** (2019). Resolving the individual contribution of key microbial populations to enhanced biological phosphorus removal with Raman-FISH. *The ISME Journal*. 13. 1933–1946. 10.1038/s41396-019-0399-7.

**Förster, A. H.**; **Gescher, J.** (2014). Metabolic engineering of *Escherichia coli* for production of mixed-acid fermentation end products. *Frontiers in Bioengineering and Biotechnology*. 2. 16. 10.3389/fbioe.2014.00016.

**Franza, T.**; **Gaudu, P.** (2022). Quinones: More than electron shuttles. *Research in Microbiology*. 173. 103953. 10.1016/j.resmic.2022.103953.

**Fredrickson, J. K.**; **Romine, M. F.**; **Beliaev, A. S.**; **Auchtung, J. M.**; **Driscoll, M. E.**; **Gardner, T. S.**; **Nealson, K. H.**; **Osterman, A. L.**; **Pinchuk, G.**; **Reed, J. L.**; **Rodionov, D. A.**; **Rodrigues, J. L. M.**; **Saffarini, D. A.**; **Serres, M. H.**; **Spormann, A. M.**; **Zhulin, I. B.**; **Tiedje, J. M.** (2008). Towards environmental systems biology of *Shewanella*. *Nature Reviews. Microbiology*. 6. 592–603. 10.1038/nrmicro1947.

**Fruehauf, H. M.**; **Enzmann, F.**; **Harnisch, F.**; **Ulber, R.**; **Holtmann, D.** (2020). Microbial electrosynthesis - An inventory on technology readiness level and performance of different process variants. *Biotechnology Journal*. 15. e2000066. 10.1002/biot.202000066.

**Fu, Q.**; **Kobayashi, H.**; **Kawaguchi, H.**; **Wakayama, T.**; **Maeda, H.**; **Sato, K.** (2013). A thermophilic gram-negative nitrate-reducing bacterium, *Calditerrivibrio nitroreducens*, exhibiting electricity generation capability. *Environmental Science & Technology*. 47. 12583–12590. 10.1021/es402749f.

**Ge, Z.**; **He, Z.** (2016). Long-term performance of a 200 liter modularized microbial fuel cell system treating municipal wastewater: Treatment, energy, and cost. *Environmental Science: Water Research & Technology*. 2. 274–281. 10.1039/C6EW00020G.

**Geelhoed, J. S.**; **Stams, A. J. M.** (2011). Electricity-assisted biological hydrogen production from acetate by *Geobacter sulfurreducens*. *Environmental Science & Technology*. 45. 815–820. 10.1021/es102842p.

**Gelder, J.** de; **Gussem, K.** de; **Vandenabeele, P.**; **Moens, L.** (2007). Reference database of Raman spectra of biological molecules. *Journal of Raman Spectroscopy*. 38. 1133–1147. 10.1002/jrs.1734.

**Gemünde, A.**; **Lai, B.**; **Pause, L.**; **Krömer, J.**; **Holtmann, D.** (2022). Redox mediators in microbial electrochemical systems. *ChemElectroChem*. 9. 10.1002/celc.202200216.

**Gralnick, J. A.**; **Newman, D. K.** (2007). Extracellular respiration. *Molecular Microbiology*. 65. 1–11. 10.1111/j.1365-2958.2007.05778.x.

**Hannon, J. R.** (2007). Comparing the scale-up of anaerobic and aerobic processes.

**Harnisch, F.**; **Deutzmann, J. S.**; **Boto, S. T.**; **Rosenbaum, M. A.** (2024). Microbial electrosynthesis: Opportunities for microbial pure cultures. *Trends in Biotechnology*. 10.1016/j.tibtech.2024.02.004.

**Härtig, C.**; **Loffhagen, N.**; **Harms, H.** (2005). Formation of trans fatty acids is not involved in growth-linked membrane adaptation of *Pseudomonas putida*. *Applied and Environmental Microbiology*. 71. 1915–1922. 10.1128/AEM.71.4.1915-1922.2005.

**Hartmans, S.**; **Smits, J. P.**; **van der Werf, M. J.**; **Volkering, F.**; **Bont, J. A.** de (1989). Metabolism of styrene oxide and 2-phenylethanol in the styrene-degrading *Xanthobacter* strain 124X. *Applied and Environmental Microbiology*. 55. 2850–2855. 10.1128/aem.55.11.2850-2855.1989.

**Hassett, D. J.**; **Charniga, L.**; **Bean, K.**; **Ohman, D. E.**; **Cohen, M. S.** (1992). Response of *Pseudomonas aeruginosa* to pyocyanin: Mechanisms of resistance, antioxidant defenses, and demonstration of a manganese-cofactored superoxide dismutase. *Infection and Immunity*. 60. 328–336. 10.1128/iai.60.2.328-336.1992.

**Hayes, F.** (2003). Toxins-antitoxins: Plasmid maintenance, programmed cell death, and cell cycle arrest. *Science*. 301. 1496–1499. 10.1126/SCIENCE.1088157.

**Heiskanen, A.** (2004). Amperometric monitoring of redox activity in living yeast cells: Comparison of menadione and menadione sodium bisulfite as electron transfer mediators. *Electrochemistry Communications*. 6. 219–224. 10.1016/j.elecom.2003.12.003.

**Hernandez, M. E.**; **Kappler, A.**; **Newman, D. K.** (2004). Phenazines and other redox-active antibiotics promote microbial mineral reduction. *Applied and Environmental Microbiology*. 70. 921–928. 10.1128/AEM.70.2.921-928.2004.

**Hiegemann, H.**; **Herzer, D.**; **Nettmann, E.**; **Lübken, M.**; **Schulte, P.**; **Schmelz, K.-G.**; **Gredigk-Hoffmann, S.**; **Wichern, M.** (2016). An integrated 45 L pilot microbial fuel cell system at a full-scale wastewater treatment plant. *Bioresource Technology*. 218. 115–122. 10.1016/j.biortech.2016.06.052.

**Hintermayer, S.**; **Yu, S.**; **Krömer, J. O.**; **Weuster-Botz, D.** (2016). Anodic respiration of *Pseudomonas putida* KT2440 in a stirred-tank bioreactor. *Biochemical Engineering Journal*. 115. 1–13. 10.1016/j.bej.2016.07.020.

**Hou, C. I.**; **Gronlund, A. F.**; **Campbell, J. J.** (1966). Influence of phosphate starvation on cultures of *Pseudomonas aeruginosa*. *Journal of Bacteriology*. 92. 851–855. 10.1128/jb.92.4.851-855.1966.

**Huang, W.**; **Chen, J.**; **Hu, Y.**; **Chen, J.**; **Sun, J.**; **Zhang, L.** (2017). Enhanced simultaneous decolorization of azo dye and electricity generation in microbial fuel cell (MFC) with redox mediator modified anode. *International Journal of Hydrogen Energy*. 42. 2349–2359. 10.1016/j.ijhydene.2016.09.216.

**Hwang, L.-L.**; **Chen, J.-C.**; **Wey, M.-Y.** (2013). The properties and filtration efficiency of activated carbon polymer composite membranes for the removal of humic acid. *Desalination*. 313. 166–175. 10.1016/j.desal.2012.12.019.

**Ito, Y.**; **Yamazaki, S.**; **Kano, K.**; **Ikeda, T.** (2002). *Escherichia coli* and its application in a mediated amperometric glucose sensor. *Biosensors & Bioelectronics*. 17. 993–998. 10.1016/S0956-5663(02)00091-X.

**Jeong, B. C.**; **Hawes, C.**; **Bonthrone, K. M.**; **Macaskie, L. E.** (1997). Iron acquisition from transferrin and lactoferrin by *Pseudomonas aeruginosa* pyoverdin. *Microbiology*. 143 (Pt 7). 2497–2507. 10.1099/00221287-143-7-2509.

**Jones, R. W.**; **Gray, T. A.**; **Garland, P. B.** (1976). A study of the permeability of the cytoplasmic membrane of *Escherichia coli* to reduced and oxidized benzyl viologen and methyl viologen cations: Complications in the use of viologens as redox mediators for membrane-bound enzymes. *Biochemical Society transactions*. 4. 671–673. 10.1042/bst0040671.

**Jovanovic Gasovic, S.**; **Dietrich, D.**; **Gläser, L.**; **Cao, P.**; **Kohlstedt, M.**; **Wittmann, C.** (2023). Multi-omics view of recombinant *Yarrowia lipolytica*: Enhanced ketogenic amino acid catabolism increases polyketide-synthase-driven docosahexaenoic production to high selectivity at the gram scale. *Metabolic Engineering*. 80. 45–65. 10.1016/j.ymben.2023.09.003.

**Junker, B. H.**; **Stanik, M.**; **Barna, C.**; **Salmon, P.**; **Buckland, B. C.** (1998). Influence of impeller type on mass transfer in fermentation vessels. *Bioprocess Engineering*. 19. 403. 10.1007/s004490050540.

**Kampers, L. F. C.**; **Koehorst, J. J.**; **van Heck, R. J. A.**; **Suarez-Diez, M.**; **Stams, A. J. M.**; **Schaap, P. J.** (2021). A metabolic and physiological design study of *Pseudomonas putida* KT2440 capable of anaerobic respiration. *BMC Microbiology*. 21. 9. 10.1186/s12866-020-02058-1.

**Kampers, L. F. C.**; **van Heck, R. G. A.**; **Donati, S.**; **Saccenti, E.**; **Volkers, R. J. M.**; **Schaap, P. J.**; **Suarez-Diez, M.**; **Nikel, P. I.**; **Martins Dos Santos, V. A. P.** (2019). In silico-guided engineering of *Pseudomonas putida* towards growth under micro-oxic conditions. *Microbial Cell Factories*. 18. 179. 10.1186/s12934-019-1227-5.

**Kashefi, K.**; **Tor, J. M.**; **Holmes, D. E.**; **van Gaw Praagh, C. V.**; **Reysenbach, A.-L.**; **Lovley, D. R.** (2002). *Geoglobus ahangari* gen. nov., sp. nov., a novel hyperthermophilic archaeon capable of oxidizing organic acids and growing autotrophically on hydrogen with Fe(III) serving as the sole electron acceptor. *International Journal of Systematic and Evolutionary Microbiology*. 52. 719–728. 10.1099/00207713-52-3-719.

**Kiely, P. D.**; **Regan, J. M.**; **Logan, B. E.** (2011). The electric picnic: Synergistic requirements for exoelectrogenic microbial communities. *Current Opinion in Biotechnology*. 22. 378–385. 10.1016/j.copbio.2011.03.003.

**Koch, C.**; **Harnisch, F.** (2016). Is there a specific ecological niche for electroactive microorganisms? *ChemElectroChem*. 3. 1282–1295. 10.1002/celc.201600079.

**Kochius, S.**; **Magnusson, A. O.**; **Hollmann, F.**; **Schrader, J.**; **Holtmann, D.** (2012). Immobilized redox mediators for electrochemical NAD(P)$^+$ regeneration. *Applied Microbiology and Biotechnology*. 93. 2251–2264. 10.1007/s00253-012-3900-z.

**Kohlstedt, M.**; **Wittmann, C.** (2019). GC-MS-based $^{13}$C metabolic flux analysis resolves the parallel and cyclic glucose metabolism of *Pseudomonas putida* KT2440 and *Pseudomonas aeruginosa* PAO1. *Metabolic Engineering*. 54. 35–53. 10.1016/j.ymben.2019.01.008.

**Kondrová, E.**; **Stopka, P.**; **Soucek, P.** (2007). Cytochrome P450 destruction by benzene metabolites 1,4-benzoquinone and 1,4-hydroquinone and the formation of hydroxyl radicals in minipig liver microsomes. *Toxicology in Vitro*. 21. 566–575. 10.1016/j.tiv.2006.11.002.

**Kracke, F.**; **Vassilev, I.**; **Krömer, J. O.** (2015). Microbial electron transport and energy conservation - the foundation for optimizing bioelectrochemical systems. *Frontiers in Microbiology*. 6. 575. 10.3389/fmicb.2015.00575.

**Kumar, A.**; **Hsu, L. H.-H.**; **Kavanagh, P.**; **Barrière, F.**; **Lens, P. N. L.**; **Lapinsonnière, L.**; **Lienhard V, J. H.**; **Schröder, U.**; **Jiang, X.**; **Leech, D.** (2017). The ins and outs of microorganism – electrode electron transfer reactions. *Nature Reviews Chemistry*. 1. 10.1038/s41570-017-0024.

**Lai, B.**; **Bernhardt, P. V.**; **Krömer, J. O.** (2020). Cytochrome c reductase is a key enzyme involved in the extracellular electron transfer pathway towards transition metal complexes in *Pseudomonas putida*. *ChemSusChem*. 13. 5308–5317. 10.1002/cssc.202001645.

**Lai, B.**; **Nguyen, A. V.**; **Krömer, J. O.** (2019). Characterizing the anoxic phenotype of *Pseudomonas putida* using a bioelectrochemical system. *Methods and Protocols*. 2. 10.3390/mps2020026.

**Lai, B.**; **Plan, M.**; **Hodson, M.**; **Krömer, J.** (2016a). Simultaneous determination of sugars, carboxylates, alcohols and aldehydes from fermentations by high performance liquid chromatography. *Fermentation*. 2. 6. 10.3390/fermentation2010006.

**Lai, B.**; **Yu, S.**; **Bernhardt, P. V.**; **Rabaey, K.**; **Virdis, B.**; **Krömer, J. O.** (2016b). Anoxic metabolism and biochemical production in *Pseudomonas putida* F1 driven by a bioelectrochemical system. *Biotechnology for Biofuels*. 9. 39. 10.1186/s13068-016-0452-y.

**Larkin, P. J.** (2018). IR and Raman spectra–structure correlations. 10.1016/B978-0-12-804162-8.00006-9.

**Lee, F. J.**; **Lin, L. W.**; **Smith, J. A.** (1996). Acetyl-CoA hydrolase involved in acetate utilization in *Saccharomyces cerevisiae*. *Biochimica et Biophysica Acta*. 1297. 105–109. 10.1016/0167-4838(96)00109-4.

**Li, H.**; **Opgenorth, P. H.**; **Wernick, D. G.**; **Rogers, S.**; **Wu, T.-Y.**; **Higashide, W.**; **Malati, P.**; **Huo, Y.-X.**; **Cho, K. M.**; **Liao, J. C.** (2012). Integrated electromicrobial conversion of $CO_2$ to higher alcohols. *Science*. 335. 1596. 10.1126/science.1217643.

**Liang, P.**; **Duan, R.**; **Jiang, Y.**; **Zhang, X.**; **Qiu, Y.**; **Huang, X.** (2018). One-year operation of 1000-L modularized microbial fuel cell for municipal wastewater treatment. *Water Research*. 141. 1–8. 10.1016/j.watres.2018.04.066.

**Lindahl, P. A.**; **Chang, B.** (2001). The evolution of acetyl-CoA synthase. *Origins of Life and Evolution of the Biosphere*. 31. 403–434. 10.1023/a:1011809430237.

**Liu, M.**; **Yuan, Y.**; **Zhang, L.**; **Zhuang, L.**; **Zhou, S.**; **Ni, J.** (2010). Bioelectricity generation by a Gram-positive *Corynebacterium* sp. strain MFC03 under alkaline condition in microbial fuel cells. *Bioresource Technology*. 101. 1807–1811. 10.1016/j.biortech.2009.10.003.

**Logan, B. E.**; **Rabaey, K.** (2012). Conversion of wastes into bioelectricity and chemicals by using microbial electrochemical technologies. *Science*. 337. 686–690. 10.1126/science.1217412.

**Logan, B. E.**; **Rossi, R.**; **Ragab, A.**; **Saikaly, P. E.** (2019). Electroactive microorganisms in bioelectrochemical systems. *Nature Reviews. Microbiology*. 17. 307–319. 10.1038/s41579-019-0173-x.

**Lovley, D. R.**; **Holmes, D. E.** (2022). Electromicrobiology: The ecophysiology of phylogenetically diverse electroactive microorganisms. *Nature Reviews. Microbiology*. 20. 5–19. 10.1038/s41579-021-00597-6.

**Lu, M.**; **Chen, S.**; **Babanova, S.**; **Phadke, S.**; **Salvacion, M.**; **Mirhosseini, A.**; **Chan, S.**; **Carpenter, K.**; **Cortese, R.**; **Bretschger, O.** (2017). Long-term performance of a 20-L continuous flow microbial fuel cell for treatment of brewery wastewater. *Journal of Power Sources*. 356. 274–287. 10.1016/j.jpowsour.2017.03.132.

**Luo, J.**; **Sam, A.**; **Hu, B.**; **DeBruler, C.**; **Wei, X.**; **Wang, W.**; **Liu, T. L.** (2017). Unraveling pH dependent cycling stability of ferricyanide/ferrocyanide in redox flow batteries. *Nano Energy*. 42. 215–221. 10.1016/j.nanoen.2017.10.057.

**Malki, M.**; **Lacey, A. L.** de; **Rodríguez, N.**; **Amils, R.**; **Fernandez, V. M.** (2008). Preferential use of an anode as an electron acceptor by an acidophilic bacterium in the presence of oxygen. *Applied and Environmental Microbiology*. 74. 4472–4476. 10.1128/AEM.00209-08.

**Malvankar, N. S.**; **Lovley, D. R.** (2012). Microbial nanowires: A new paradigm for biological electron transfer and bioelectronics. *ChemSusChem*. 5. 1039–1046. 10.1002/cssc.201100733.

**Marsili, E.**; **Baron, D. B.**; **Shikhare, I. D.**; **Coursolle, D.**; **Gralnick, J. A.**; **Bond, D. R.** (2008). *Shewanella* secretes flavins that mediate extracellular electron transfer. *Proceedings of the National Academy of Sciences USA*. 105. 3968–3973. 10.1073/pnas.0710525105.

**Martinez, C. M.**; **Zhu, X.**; **Logan, B. E.** (2017). AQDS immobilized solid-phase redox mediators and their role during bioelectricity generation and RR2 decolorization in air-cathode single-chamber microbial fuel cells. *Bioelectrochemistry*. 118. 123–130. 10.1016/j.bioelechem.2017.07.007.

**Martínez-García, E.**; **Lorenzo, V.** de (2017). Molecular tools and emerging strategies for deep genetic/genomic refactoring of *Pseudomonas*. *Current Opinion in Biotechnology*. 47. 120–132. 10.1016/j.copbio.2017.06.013.

**McMillan, J. D.**; **Beckham, G. T.** (2017). Thinking big: Towards ideal strains and processes for large-scale aerobic biofuels production. *Microbial Biotechnology*. 10. 40–42. 10.1111/1751-7915.12471.

**Melin, F.**; **Hellwig, P.** (2020). Redox properties of the membrane proteins from the respiratory chain. *Chemical Reviews*. 120. 10244–10297. 10.1021/acs.chemrev.0c00249.

**Milliken, C. E.**; **May, H. D.** (2007). Sustained generation of electricity by the spore-forming, Gram-positive, *Desulfitobacterium hafniense* strain DCB2. *Applied Microbiology and Biotechnology*. 73. 1180–1189. 10.1007/s00253-006-0564-6.

**Morales, G.**; **Ugidos, A.**; **Rojo, F.** (2006). Inactivation of the *Pseudomonas putida* cytochrome o ubiquinol oxidase leads to a significant change in the transcriptome and to increased expression of the CIO and cbb3-1 terminal oxidases. *Environmental Microbiology*. 8. 1764–1774. 10.1111/j.1462-2920.2006.01061.x.

**Nandy, A.**; **Kumar, V.**; **Kundu, P. P.** (2013). Utilization of proteinaceous materials for power generation in a mediatorless microbial fuel cell by a new electrogenic bacteria *Lysinibacillus sphaericus* VA5. *Enzyme and Microbial Technology*. 53. 339–344. 10.1016/j.enzmictec.2013.07.006.

**Nelson, K. E.**; **Weinel, C.**; **Paulsen, I. T.**; **Dodson, R. J.**; **Hilbert, H.**; **Martins dos Santos, V. A. P.**; **Fouts, D. E.**; **Gill, S. R.**; **Pop, M.**; **Holmes, M.**; **Brinkac, L.**; **Beanan, M.**; **DeBoy, R. T.**; **Daugherty, S.**; **Kolonay, J.**; **Madupu, R.**; **Nelson, W.**; **White, O.**; **Peterson, J.**; **Khouri, H.**; **Hance, I.**; **Chris Lee, P.**; **Holtzapple, E.**; **Scanlan, D.**; **Tran, K.**; **Moazzez, A.**; **Utterback, T.**; **Rizzo, M.**; **Lee, K.**; **Kosack, D.**; **Moestl, D.**; **Wedler, H.**; **Lauber, J.**; **Stjepandic, D.**; **Hoheisel, J.**; **Straetz, M.**; **Heim, S.**; **Kiewitz, C.**; **Eisen, J. A.**; **Timmis, K. N.**; **Düsterhöft, A.**; **Tümmler, B.**; **Fraser, C. M.** (2002). Complete genome sequence and comparative analysis of the metabolically versatile *Pseudomonas putida* KT2440. *Environmental Microbiology*. 4. 799–808. 10.1046/j.1462-2920.2002.00366.x.

**Nevin, K. P.**; **Hensley, S. A.**; **Franks, A. E.**; **Summers, Z. M.**; **Ou, J.**; **Woodard, T. L.**; **Snoeyenbos-West, O. L.**; **Lovley, D. R.** (2011). Electrosynthesis of organic compounds from carbon dioxide is catalyzed by a diversity of acetogenic microorganisms. *Applied and Environmental Microbiology*. 77. 2882–2886. 10.1128/AEM.02642-10.

**Nguyen, A. V.**; **Lai, B.**; **Adrian, L.**; **Krömer, J. O.** (2021). The anoxic electrode-driven fructose catabolism of *Pseudomonas putida* KT2440. *Microbial Biotechnology*. 14. 1784–1796. 10.1111/1751-7915.13862.

Nguyen Anh Vu (2024). Investigating anaerobic metabolism of *Pseudomonas putida* using bioelectrochemical cultivation. 10.25673/116712.

**Nielsen, L. P.**; **Risgaard-Petersen, N.** (2015). Rethinking sediment biogeochemistry after the discovery of electric currents. *Annual Review of Marine Science*. 7. 425–442. 10.1146/annurev-marine-010814-015708.

**Nikel, P. I.**; **Chavarría, M.**; **Fuhrer, T.**; **Sauer, U.**; **Lorenzo, V.** de (2015). *Pseudomonas putida* KT2440 strain metabolizes glucose through a cycle formed by enzymes of the Entner-Doudoroff, Embden-Meyerhof-Parnas, and pentose phosphate pathways. *The Journal of Biological Chemistry*. 290. 25920–25932. 10.1074/jbc.M115.687749.

**Nikel, P. I.**; **Chavarría, M.**; **Martínez-García, E.**; **Taylor, A. C.**; **Lorenzo, V.** de (2013). Accumulation of inorganic polyphosphate enables stress endurance and catalytic vigour in *Pseudomonas putida* KT2440. *Microbial Cell Factories*. 12. 50. 10.1186/1475-2859-12-50.

**Nikel, P. I.**; **Lorenzo, V.** de (2013). Engineering an anaerobic metabolic regime in *Pseudomonas putida* KT2440 for the anoxic biodegradation of 1,3-dichloroprop-1-ene. *Metabolic Engineering*. 15. 98–112. 10.1016/j.ymben.2012.09.006.

**Nimje, V. R.**; **Chen, C.-Y.**; **Chen, C.-C.**; **Jean, J.-S.**; **Reddy, A. S.**; **Fan, C.-W.**; **Pan, K.-Y.**; **Liu, H.-T.**; **Chen, J.-L.** (2009). Stable and high energy generation by a strain of *Bacillus subtilis* in a microbial fuel cell. *Journal of Power Sources*. 190. 258–263. 10.1016/j.jpowsour.2009.01.019.

**Nogales, J.**; **Mueller, J.**; **Gudmundsson, S.**; **Canalejo, F. J.**; **Duque, E.**; **Monk, J.**; **Feist, A. M.**; **Ramos, J. L.**; **Niu, W.**; **Palsson, B. O.** (2020). High-quality genome-scale metabolic modelling of *Pseudomonas putida* highlights its broad metabolic capabilities. *Environmental Microbiology*. 22. 255–269. 10.1111/1462-2920.14843.

**Noinaj, N.**; **Guillier, M.**; **Barnard, T. J.**; **Buchanan, S. K.** (2010). TonB-dependent transporters: regulation, structure, and function. *Annual Review of Microbiology*. 64. 43–60. 10.1146/annurev.micro.112408.134247.

**Noori, M. T.**; **Rossi, R.**; **Logan, B. E.**; **Min, B.** (2024). Hydrogen production in microbial electrolysis cells with biocathodes. *Trends in Biotechnology*. 42. 815–828. 10.1016/j.tibtech.2023.12.010.

**Okuyama, H.**; **Sasaki, S.**; **Higashi, S.**; **Murata, N.** (1990). A trans-unsaturated fatty acid in a psychrophilic bacterium, *Vibrio* sp. strain ABE-1. *Journal of Bacteriology*. 172. 3515–3518. 10.1128/jb.172.6.3515-3518.1990.

**Paliwal, V.**; **Raju, S. C.**; **Modak, A.**; **Phale, P. S.**; **Purohit, H. J.** (2014). *Pseudomonas putida* CSV86: A candidate genome for genetic bioaugmentation. *PLOS One*. 9. e84000. 10.1371/journal.pone.0084000.

**Palleroni, N.** (1984). Family I. Pseudomonadaceae. *Bergey's Manual of Systematic Bacteriology*. 1. 141–199.

**Pandey, P.**; **Shinde, V. N.**; **Deopurkar, R. L.**; **Kale, S. P.**; **Patil, S. A.**; **Pant, D.** (2016). Recent advances in the use of different substrates in microbial fuel cells toward wastewater treatment and simultaneous energy recovery. *Applied Energy*. 168. 706–723. 10.1016/j.apenergy.2016.01.056.

**Pankratova, G.**; **Hederstedt, L.**; Lo Gorton (2019). Extracellular electron transfer features of Gram-positive bacteria. *Analytica Chimica Acta*. 1076. 32–47. 10.1016/j.aca.2019.05.007.

**Paquete, C. M.** (2020). Electroactivity across the cell wall of Gram-positive bacteria. *Computational and Structural Biotechnology Journal*. 18. 3796–3802. 10.1016/j.csbj.2020.11.021.

**Parameswaran, P.**; **Bry, T.**; **Popat, S. C.**; **Lusk, B. G.**; **Rittmann, B. E.**; **Torres, C. I.** (2013). Kinetic, electrochemical, and microscopic characterization of the thermophilic, anode-respiring bacterium *Thermincola ferriacetica*. *Environmental Science & Technology*. 47. 4934–4940. 10.1021/es400321c.

**Park, D. H.**; **Zeikus, J. G.** (1999). Utilization of electrically reduced neutral red by *Actinobacillus succinogenes*: physiological function of neutral red in membrane-driven fumarate reduction and energy conservation. *Journal of Bacteriology*. 181. 2403–2410. 10.1128/JB.181.8.2403-2410.1999.

**Park, D. H.**; **Zeikus, J. G.** (2000). Electricity generation in microbial fuel cells using neutral red as an electronophore. *Applied and Environmental Microbiology*. 66. 1292–1297. 10.1128/AEM.66.4.1292-1297.2000.

**Pause, L.**; **Weimer, A.**; **Wirth, N. T.**; **Nguyen, A. V.**; **Lenz, C.**; **Kohlstedt, M.**; **Wittmann, C.**; **Nikel, P. I.**; **Lai, B.**; **Krömer, J. O.** (2024). Anaerobic glucose uptake in *Pseudomonas putida* KT2440 in a bioelectrochemical system. *Microbial Biotechnology*. 17. e14375. 10.1111/1751-7915.14375.

**Pfeffer, C.**; **Larsen, S.**; **Song, J.**; **Dong, M.**; **Besenbacher, F.**; **Meyer, R. L.**; **Kjeldsen, K. U.**; **Schreiber, L.**; **Gorby, Y. A.**; **El-Naggar, M. Y.**; **Leung, K. M.**; **Schramm, A.**; **Risgaard-Petersen, N.**; **Nielsen, L. P.** (2012). Filamentous bacteria transport electrons over centimetre distances. *Nature*. 491. 218–221. 10.1038/nature11586.

**Phani, K.**; **Pitchumani, S.**; **Muralidharan, S.**; **Ravichandran, S.**; **Iyer, S.** (1993). Electrosynthesis of polyamino-benzoquinone (PAQ) polymers. *Journal of Electroanalytical Chemistry*. 353. 315–322. 10.1016/0022-0728(93)80308-5.

**Potter, M. C.** (1911). Electrical effects accompanying the decomposition of organic compounds. *Proceedings of the Royal Society of London*. 84. 260–276. 10.1098/rspb.1911.0073.

**Prévoteau, A.**; **Carvajal-Arroyo, J. M.**; **Ganigué, R.**; **Rabaey, K.** (2020). Microbial electrosynthesis from $CO_2$: Forever a promise? *Current Opinion in Biotechnology*. 62. 48–57. 10.1016/j.copbio.2019.08.014.

**Rabaey, K.**; **Boon, N.**; **Höfte, M.**; **Verstraete, W.** (2005). Microbial phenazine production enhances electron transfer in biofuel cells. *Environmental Science & Technology*. 39. 3401–3408. 10.1021/es048563o.

**Racki, L. R.**; **Tocheva, E. I.**; **Dieterle, M. G.**; **Sullivan, M. C.**; **Jensen, G. J.**; **Newman, D. K.** (2017). Polyphosphate granule biogenesis is temporally and functionally tied to cell cycle exit during starvation in *Pseudomonas aeruginosa*. *Proceedings of the National Academy of Sciences USA*. 114. 10.1073/pnas.1615575114.

**Ramírez-Vargas, C. A.**; **Arias, C. A.**; **Carvalho, P.**; **Zhang, L.**; **Esteve-Núñez, A.**; **Brix, H.** (2019). Electroactive biofilm-based constructed wetland (EABB-CW): A mesocosm-scale test of an innovative setup for wastewater treatment. *The Science of the Total Environment*. 659. 796–806. 10.1016/j.scitotenv.2018.12.432.

**Ramos, J. L.**; **Duque, E.**; **Gallegos, M.-T.**; **Godoy, P.**; **Ramos-Gonzalez, M. I.**; **Rojas, A.**; **Teran, W.**; **Segura, A.** (2002). Mechanisms of solvent tolerance in gram-negative bacteria. *Annual Review of Microbiology*. 56. 743–768. 10.1146/annurev.micro.56.012302.161038.

**Rao, N. N.**; **Gómez-García, M. R.**; **Kornberg, A.** (2009). Inorganic polyphosphate: Essential for growth and survival. *Annual Review of Biochemistry*. 78. 605–647. 10.1146/annurev.biochem.77.083007.093039.

**Rau, J.**; **Knackmuss, H.-J.**; **Stolz, A.** (2002). Effects of different quinoid redox mediators on the anaerobic reduction of azo dyes by bacteria. *Environmental Science & Technology*. 36. 1497–1504. 10.1021/es010227+.

**Read, S. T.**; **Dutta, P.**; **Bond, P. L.**; **Keller, J.**; **Rabaey, K.** (2010). Initial development and structure of biofilms on microbial fuel cell anodes. *BMC Microbiology*. 10. 98. 10.1186/1471-2180-10-98.

**Regenhardt, D.**; **Heuer, H.**; **Heim, S.**; **Fernandez, D. U.**; **Strömpl, C.**; **Moore, E. R. B.**; **Timmis, K. N.** (2002). Pedigree and taxonomic credentials of *Pseudomonas putida* strain KT2440. *Environmental Microbiology*. 4. 912–915. 10.1046/j.1462-2920.2002.00368.x.

**Renninger, N.**; **Knopp, R.**; **Nitsche, H.**; **Clark, D. S.**; **Keasling, J. D.** (2004). Uranyl precipitation by *Pseudomonas aeruginosa* via controlled polyphosphate metabolism. *Applied and Environmental Microbiology*. 70. 7404–7412. 10.1128/AEM.70.12.7404-7412.2004.

**Repetto, G.**; **Del Peso, A.**; **Zurita, J. L.** (2008). Neutral red uptake assay for the estimation of cell viability/cytotoxicity. *Nature Protocols*. 3. 1125–1131. 10.1038/nprot.2008.75.

**Rhoads, A.**; **Beyenal, H.**; **Lewandowski, Z.** (2005). Microbial fuel cell using anaerobic respiration as an anodic reaction and biomineralized manganese as a cathodic reactant. *Environmental Science & Technology*. 39. 4666–4671. 10.1021/es048386r.

**Rismani-Yazdi, H.**; **Carver, S. M.**; **Christy, A. D.**; **Tuovinen, O. H.** (2008). Cathodic limitations in microbial fuel cells: An overview. *Journal of Power Sources*. 180. 683–694. 10.1016/j.jpowsour.2008.02.074.

**Riveros-Rosas, H.**; **Julián-Sánchez, A.**; **Moreno-Hagelsieb, G.**; **Muñoz-Clares, R. A.** (2019). Aldehyde dehydrogenase diversity in bacteria of the *Pseudomonas* genus. *Chemico-Biological Interactions*. 304. 83–87. 10.1016/j.cbi.2019.03.006.

**Rojo, F.** (2010). Carbon catabolite repression in *Pseudomonas*: Optimizing metabolic versatility and interactions with the environment. *FEMS Microbiology Reviews*. 34. 658–684. 10.1111/j.1574-6976.2010.00218.x.

**Roller, S. D.**; **Bennetto, H. P.**; **Delaney, G. M.**; **Mason, J. R.**; **Stirling, J. L.**; **Thurston, C. F.** (1984). Electron‐transfer coupling in microbial fuel cells: 1. comparison of redox‐mediator reduction rates and respiratory rates of bacteria. *Journal of Chemical Technology and Biotechnology*. 34. 3–12. 10.1002/jctb.280340103.

**Rousseau, R.**; **Etcheverry, L.**; **Roubaud, E.**; **Basséguy, R.**; **Délia, M.-L.**; **Bergel, A.** (2020). Microbial electrolysis cell (MEC): Strengths, weaknesses and research needs from electrochemical engineering standpoint. *Applied Energy*. 257. 113938. 10.1016/j.apenergy.2019.113938.

**Sakhtah, H.**; **Koyama, L.**; **Zhang, Y.**; **Morales, D. K.**; **Fields, B. L.**; **Price-Whelan, A.**; **Hogan, D. A.**; **Shepard, K.**; **Dietrich, L. E. P.** (2016). The *Pseudomonas aeruginosa* efflux pump MexGHI-OpmD transports a natural phenazine that controls gene expression and biofilm development. *Proceedings of the National Academy of Sciences USA*. 113. E3538-47. 10.1073/pnas.1600424113.

**Schmitz, S.**; **Nies, S.**; **Wierckx, N.**; **Blank, L. M.**; **Rosenbaum, M. A.** (2015). Engineering mediator-based electroactivity in the obligate aerobic bacterium *Pseudomonas putida* KT2440. *Frontiers in Microbiology*. 6. 284. 10.3389/fmicb.2015.00284.

**Schröder, U.**; **Harnisch, F.**; **Angenent, L. T.** (2015). Microbial electrochemistry and technology: Terminology and classification. *Energy & Environmental Science*. 8. 513–519. 10.1039/c4ee03359k.

**Schultz, S. G.** (1968). Biological membranes: The movement of molecules across cell membranes. *Science*. 161. 1337. 10.1126/science.161.3848.1337.

**Seeliger, S.**; **Cord-Ruwisch, R.**; **Schink, B.** (1998). A periplasmic and extracellular c-type cytochrome of *Geobacter sulfurreducens* acts as a ferric iron reductase and as an electron carrier to other acceptors or to partner bacteria. *Journal of Bacteriology*. 180. 3686–3691. 10.1128/JB.180.14.3686-3691.1998.

**Seidel, K.**; **Kühnert, J.**; **Adrian, L.** (2018). The complexome of *Dehalococcoides mccartyi* reveals its organohalide respiration-complex is modular. *Frontiers in Microbiology*. 9. 1130. 10.3389/fmicb.2018.01130.

**Sevilla, E.**; **Alvarez-Ortega, C.**; **Krell, T.**; **Rojo, F.** (2013). The *Pseudomonas putida* HskA hybrid sensor kinase responds to redox signals and contributes to the adaptation of the electron transport chain composition in response to oxygen availability. *Environmental Microbiology Reports*. 5. 825–834. 10.1111/1758-2229.12083.

**Sharfstein, S. T.**; **Keasling, J. D.** (1994). Polyphosphate metabolism in *Escherichia coli*. *Annals of the New York Academy of Sciences*. 745. 77–91. 10.1111/j.1749-6632.1994.tb44365.x.

**Shaw, D. R.**; **Ali, M.**; **Katuri, K. P.**; **Gralnick, J. A.**; **Reimann, J.**; **Mesman, R.**; **van Niftrik, L.**; **Jetten, M. S. M.**; **Saikaly, P. E.** (2020). Extracellular electron transfer-dependent anaerobic oxidation of ammonium by anammox bacteria. *Nature Communications*. 11. 2058. 10.1038/s41467-020-16016-y.

**Simon, J.**; **van Spanning, R. J. M.**; **Richardson, D. J.** (2008). The organisation of proton motive and non-proton motive redox loops in prokaryotic respiratory systems. *Biochimica et Biophysica Acta*. 1777. 1480–1490. 10.1016/j.bbabio.2008.09.008.

**Stegmüller, J.**; **Rodríguez Estévez, M.**; **Shu, W.**; **Gläser, L.**; **Myronovskyi, M.**; **Rückert-Reed, C.**; **Kalinowski, J.**; **Luzhetskyy, A.**; **Wittmann, C.** (2024). Systems metabolic engineering of the primary and secondary metabolism of *Streptomyces albidoflavus* enhances production of the reverse antibiotic nybomycin against multi-resistant *Staphylococcus aureus*. *Metabolic Engineering*. 81. 123–143. 10.1016/j.ymben.2023.12.004.

**Steidl, R. J.**; **Lampa-Pastirk, S.**; **Reguera, G.** (2016). Mechanistic stratification in electroactive biofilms of *Geobacter sulfurreducens* mediated by pilus nanowires. *Nature Communications*. 7. 12217. 10.1038/ncomms12217.

**Stouthamer, A. H.**; **Bettenhaussen, C.** (1973). Utilization of energy for growth and maintenance in continuous and batch cultures of microorganisms. A reevaluation of the method for the determination of ATP production by measuring molar growth yields. *Biochimica et Biophysica Acta*. 301. 53–70. 10.1016/0304-4173(73)90012-8.

**Sun, J.**; **Cai, B.**; **Xu, W.**; **Huang, Y.**; **Zhang, Y.**; **Peng, Y.**; **Chang, K.**; **Kuo, J.**; **Chen, K.**; **Ning, X.**; **Liu, G.**; **Wang, Y.**; **Yang, Z.**; **Liu, J.** (2017). Enhanced bioelectricity generation and azo dye treatment in a reversible photo-bioelectrochemical cell by using novel anthraquinone-2,6-disulfonate (AQDS)/MnOx-doped polypyrrole film electrodes. *Bioresource Technology*. 225. 40–47. 10.1016/j.biortech.2016.11.038.

**Suresh, R.**; **Rajendran, S.**; **Kumar, P. S.**; **Dutta, K.**; **Vo, D.-V. N.** (2022). Current advances in microbial fuel cell technology toward removal of organic contaminants - A review. *Chemosphere*. 287. 132186. 10.1016/j.chemosphere.2021.132186.

**Sweet, W. J.**; **Peterson, J. A.** (1981). The respiratory system of *Pseudomonas putida*: Participation of cytochromes in electron transport. *Archives of Biochemistry and Biophysics*. 209. 256–265. 10.1016/0003-9861(81)90279-4.

**Sydow, A.**; **Krieg, T.**; **Mayer, F.**; **Schrader, J.**; **Holtmann, D.** (2014). Electroactive bacteria - molecular mechanisms and genetic tools. *Applied Microbiology and Biotechnology*. 98. 8481–8495. 10.1007/s00253-014-6005-z.

**Tang, X.**; **Li, H.**; **Du, Z.**; **Ng, H. Y.** (2014). Spontaneous modification of graphite anode by anthraquinone-2-sulfonic acid for microbial fuel cells. *Bioresource Technology*. 164. 184–188. 10.1016/j.biortech.2014.05.010.

**Taylor, I. J.**; **Anthony, C.** (1976). Acetyl-CoA production and utilization during growth of the facultative methylotroph *Pseudomonas* AM1 on ethanol, malonate and 3-hydroxybutyrate. *Journal of General Microbiology*. 95. 134–143. 10.1099/00221287-95-1-134.

**Tempest, D. W.**; **Neijssel, O. M.** (1984). The status of YATP and maintenance energy as biologically interpretable phenomena. *Annual Review of Microbiology*. 38. 459–486. 10.1146/annurev.mi.38.100184.002331.

**Timmis, K. N.** (2002). *Pseudomonas putida*: A cosmopolitan opportunist par excellence. *Environmental Microbiology*. 4. 779–781. 10.1046/j.1462-2920.2002.00365.x.

**Turick, C. E.**; **Caccavo, F.**; **Tisa, L. S.** (2003). Electron transfer from *Shewanella algae* BrY to hydrous ferric oxide is mediated by cell-associated melanin. *FEMS Microbiology Letters*. 220. 99–104. 10.1016/S0378-1097(03)00096-X.

**Udaondo, Z.**; **Molina, L.**; **Daniels, C.**; **Gómez, M. J.**; **Molina-Henares, M. A.**; **Matilla, M. A.**; **Roca, A.**; **Fernández, M.**; **Duque, E.**; **Segura, A.**; **Ramos, J. L.** (2013). Metabolic potential of the organic-solvent tolerant *Pseudomonas putida* DOT-T1E deduced from its annotated genome. *Microbial Biotechnology*. 6. 598–611. 10.1111/1751-7915.12061.

**van Winden, W. A.**; **Wittmann, C.**; **Heinzle, E.**; **Heijnen, J. J.** (2002). Correcting mass isotopomer distributions for naturally occurring isotopes. *Biotechnology and Bioengineering*. 80. 477–479. 10.1002/bit.10393.

**Vargas, M.**; **Yuan, Z.**; **Pijuan, M.** (2013). Effect of long-term starvation conditions on polyphosphate- and glycogen-accumulating organisms. *Bioresource Technology*. 127. 126–131. 10.1016/j.biortech.2012.09.117.

**Vasiliadou, I. A.**; **Molina, R.**; **Pariente, M. I.**; **Christoforidis, K. C.**; **Martinez, F.**; **Melero, J. A.** (2019). Understanding the role of mediators in the efficiency of advanced oxidation processes using white-rot fungi. *Chemical Engineering Journal*. 359. 1427–1435. 10.1016/j.cej.2018.11.035.

**Vassilev, I.**; **Averesch, N. J. H.**; **Ledezma, P.**; **Kokko, M.** (2021). Anodic electro-fermentation: Empowering anaerobic production processes via anodic respiration. *Biotechnology Advances*. 48. 107728. 10.1016/j.biotechadv.2021.107728.

**Vassilev, I.**; **Gießelmann, G.**; **Schwechheimer, S. K.**; **Wittmann, C.**; **Virdis, B.**; **Krömer, J. O.** (2018). Anodic electro-fermentation: Anaerobic production of L-lysine by recombinant *Corynebacterium glutamicum*. *Biotechnology and Bioengineering*. 115. 1499–1508. 10.1002/bit.26562.

**Wackett, L. P.**; **Gibson, D. T.** (1988). Degradation of trichloroethylene by toluene dioxygenase in whole-cell studies with *Pseudomonas putida* F1. *Applied and Environmental Microbiology*. 54. 1703–1708. 10.1128/aem.54.7.1703-1708.1988.

**Wang, C. C.**; **Newton, A.** (1971). An additional step in the transport of iron defined by the tonB locus of *Escherichia coli*. *The Journal of Biological Chemistry*. 246. 2147–2151.

**Ward, P. G.**; **O'Connor, K. E.** (2005). Bacterial synthesis of polyhydroxyalkanoates containing aromatic and aliphatic monomers by *Pseudomonas putida* CA-3. *International Journal of Biological Macromolecules*. 35. 127–133. 10.1016/j.ijbiomac.2005.01.001.

**Weimer, A.**; **Kohlstedt, M.**; **Volke, D. C.**; **Nikel, P. I.**; **Wittmann, C.** (2020). Industrial biotechnology of *Pseudomonas putida*: Advances and prospects. *Applied Microbiology and Biotechnology*. 104. 7745–7766. 10.1007/s00253-020-10811-9.

**Weimer, A.**; **Pause, L.**; **Ries, F.**; **Kohlstedt, M.**; **Adrian, L.**; **Krömer, J.**; **Lai, B.**; **Wittmann, C.** (2024). Systems biology of electrogenic *Pseudomonas putida* - multi-omics insights and metabolic engineering for enhanced 2-ketogluconate production. *Microbial Cell Factories*. 23. 246. 10.1186/s12934-024-02509-8.

**Weusthuis, R. A.**; **Lamot, I.**; **van der Oost, J.**; **Sanders, J. P. M.** (2011). Microbial production of bulk chemicals: Development of anaerobic processes. *Trends in Biotechnology*. 29. 153–158. 10.1016/j.tibtech.2010.12.007.

**Wierckx, N. J. P.**; **Ballerstedt, H.**; **Bont, J. A. M.** de; **Wery, J.** (2005). Engineering of solvent-tolerant *Pseudomonas putida* S12 for bioproduction of phenol from glucose. *Applied and Environmental Microbiology*. 71. 8221–8227. 10.1128/AEM.71.12.8221-8227.2005.

**Wittmann, C.**; **Heinzle, E.** (2005). Metabolic activity profiling by $^{13}C$ tracer experiments and mass spectrometry in *Corynebacterium glutamicum*. 10.1385/1-59259-847-1:191.

**Wordofa, G. G.**; **Kristensen, M.**; **Schrübbers, L.**; **McCloskey, D.**; **Forster, J.**; **Schneider, K.** (2017). Quantifying the metabolome of *Pseudomonas taiwanensis* VLB120: Evaluation of hot and cold combined quenching/extraction approaches. *Analytical Chemistry*. 89. 8738–8747. 10.1021/acs.analchem.7b00793.

**Wu, S.**; **Li, H.**; **Zhou, X.**; **Liang, P.**; **Zhang, X.**; **Jiang, Y.**; **Huang, X.** (2016). A novel pilot-scale stacked microbial fuel cell for efficient electricity generation and wastewater treatment. *Water Research*. 98. 396–403. 10.1016/j.watres.2016.04.043.

**Xin, X.**; **Pang, H.**; **She, Y.**; **Hong, J.** (2020). Insights into redox mediators-resource harvest/application with power production from waste activated sludge through freezing/thawing-assisted anaerobic acidogenesis coupling microbial fuel cells. *Bioresource Technology*. 311. 123469. 10.1016/j.biortech.2020.123469.

**Yang, Y.**; **Xu, M.**; **Guo, J.**; **Sun, G.** (2012). Bacterial extracellular electron transfer in bioelectrochemical systems. *Process Biochemistry*. 47. 1707–1714. 10.1016/j.procbio.2012.07.032.

**Yates, M. D.**; **Cusick, R. D.**; **Logan, B. E.** (2013). Extracellular palladium nanoparticle production using *Geobacter sulfurreducens*. *ACS Sustainable Chemistry & Engineering*. 1. 1165–1171. 10.1021/sc4000785.

**Yonei, S.**; **Noda, A.**; **Tachibana, A.**; **Akasaka, S.** (1986). Mutagenic and cytotoxic effects of oxygen free radicals generated by methylviologen (paraquat) on *Escherichia coli* with different DNA-repair capacities. *Mutation Research*. 163. 15–22. 10.1016/0027-5107(86)90053-9.

**Yong, X.-Y.**; **Yan, Z.-Y.**; **Shen, H.-B.**; **Zhou, J.**; **Wu, X.-Y.**; **Zhang, L.-J.**; **Zheng, T.**; **Jiang, M.**; **Wei, P.**; **Jia, H.-H.**; **Yong, Y.-C.** (2017). An integrated aerobic-anaerobic strategy for performance enhancement of *Pseudomonas aeruginosa*-inoculated microbial fuel cell. *Bioresource Technology*. 241. 1191–1196. 10.1016/j.biortech.2017.06.050.

**Yu, S.**; **Lai, B.**; **Plan, M. R.**; **Hodson, M. P.**; **Lestari, E. A.**; **Song, H.**; **Krömer, J. O.** (2018). Improved performance of *Pseudomonas putida* in a bioelectrochemical system through overexpression of periplasmic glucose dehydrogenase. *Biotechnology and Bioengineering*. 115. 145–155. 10.1002/bit.26433.

**Zahid, M.**; **Savla, N.**; **Pandit, S.**; **Thakur, V. K.**; **Jung, S. P.**; **Gupta, P. K.**; **Prasad, R.**; **Marsili, E.** (2022). Microbial desalination cell: Desalination through conserving energy. *Desalination*. 521. 115381. 10.1016/j.desal.2021.115381.

**Zhang, L.**; **Zhou, S.**; **Zhuang, L.**; **Li, W.**; **Zhang, J.**; **Lu, N.**; **Deng, L.** (2008). Microbial fuel cell based on *Klebsiella pneumoniae* biofilm. *Electrochemistry Communications*. 10. 1641–1643. 10.1016/j.elecom.2008.08.030.

**Zhang, T.**; **Zhang, L.**; **Su, W.**; **Gao, P.**; **Li, D.**; **He, X.**; **Zhang, Y.** (2011). The direct electrocatalysis of phenazine-1-carboxylic acid excreted by *Pseudomonas alcaliphila* under alkaline condition in microbial fuel cells. *Bioresource Technology*. 102. 7099–7102. 10.1016/j.biortech.2011.04.093.

**Zhang, Z. R.**; **Bao, W. F.**; **Liu, C. C.** (1994). Electrochemical properties of benzoquinone and ferrocene monocarboxylic acid at a polyaniline coated platinum electrode for glucose sensing. *Talanta*. 41. 875–879. 10.1016/0039-9140(94)E0050-2.

**Zhao, J.**; **Li, F.**; **Cao, Y.**; **Zhang, X.**; **Chen, T.**; **Song, H.**; **Wang, Z.** (2021). Microbial extracellular electron transfer and strategies for engineering electroactive microorganisms. *Biotechnology Advances*. 53. 107682. 10.1016/j.biotechadv.2020.107682.

# 6. Appendix

**Table S1. Key process parameters of anaerobic glucose conversion of *P. putida* KT2440 mutants in BES.** FeCN was used as the electron transfer mediator and the anode potential poised at +0.5 V vs SHE.

| | WT | KT-G* | KT-GL | KT-KG |
|---|---|---|---|---|
| CB [%] | 100.0 | 26.7 | 101.3 | 103.9 |
| EB [%] | 101.1 | 19.2 | 102.2 | 104.8 |
| **Yield [mmol/mmol_glucose]** | | | | |
| Y2kga/glc | -0.93 ± 0.04 | | | -0.92 ± 0.04 |
| Yga/glc | 0.08 ± 0.04 | | -0.98 ± 0.05 | 0.31 ± 0.12 |
| | -0.12 ± 0.03 | | | -0.34 ± 0.04 |
| Yace/glc | -0.07 ± 0.01 | -0.48 ± 0.06 | -0.07 ± 0.01 | -0.18 ± 0.01 |
| Yco2/glc ** | -0.07 ± 0.01 | -0.48 ± 0.06 | -0.07 ± 0.01 | -0.18 ± 0.01 |
| Ypyr/glc | | -0.06 ± 0.02 | | |
| Yelectrons/glc | -4.37 ± 0.08 | -0.22 ± 0.17 | -2.44 ± 0.12 | -4.69 ± 0.10 |
| **Rate [mmol/$g_{CDW}$/h]** | | | | |
| $r_{glc}$ | -0.12 ± 0.02 | -0.01 ± 0.01 | -0.18 ± 0.01 | -0.08 ± 0.01 |
| $r_{2kga}$ | 0.11 ± 0.02 | | | 0.08 ± 0.01 |
| $r_{ga}$ | -0.01 ± 0.01 | | 0.18 ± 0.01 | -0.03 ± 0.01 |
| | 0.01 ± 0.01 | | | 0.03 ± 0.01 |
| $r_{ace}$ | 0.01 ± 0.01 | -0.01 ± 0.01 | 0.01 ± 0.01 | 0.02 ± 0.01 |
| $r_{pyr}$ | | -0.0007 ± 0.0003 | | |
| $r_{electrons}$ | 0.51 ± 0.10 | 0.003 ± 0.002 | 0.45 ± 0.01 | 0.39 ± 0.03 |

*Note: The extremely low turnover rate for KT-G strain makes the systematic error (e.g. analytic resolution, etc) plays a determining role in these values.

** the $CO_2$ yield was estimated based on the biochemical coefficient that one acetate would correspond to one $CO_2$ release.

The yields were calculated using the linear regression functions as shown in the figure S4-S7 below. The glucose consumption rate was calculated by plotting the glucose quantity against the time normalized to the integrated averaged biomass quantity over the batches. The rates of the metabolic products and electrons were then calculated by the equation: $r_{product} = r_{glucose} * Y_{product/glucose}$ [mmol_product/$g_{CDW}$/h].

The carbon balance and electron balance were calculated used the equations below:

$$CB\ [\%] = \left(Y_{2kga} * 6 + Y_{ga} * 6 + Y_{ace} * 2 + Y_{CO2} * 1\right)/6 * 100$$

$$EB\ [\%] = \left(Y_{2kga} * 6 * DoR_{2kga} + Y_{ga} * 6 * DoR_{2kga} + Y_{ace} * 2 * DoR_{2kga} + Y_{electrons}\right)/(6 * DoR_{glc}) * 100$$

DoR: degree of reduction, calculated for chemical $C_aH_bO_cN_d$ as: DoR = (a*4 + b*1 + c*(-2) + d*(-3))/a.

The numbers in the CB and ED equations are the carbon atom number in the respective chemicals.

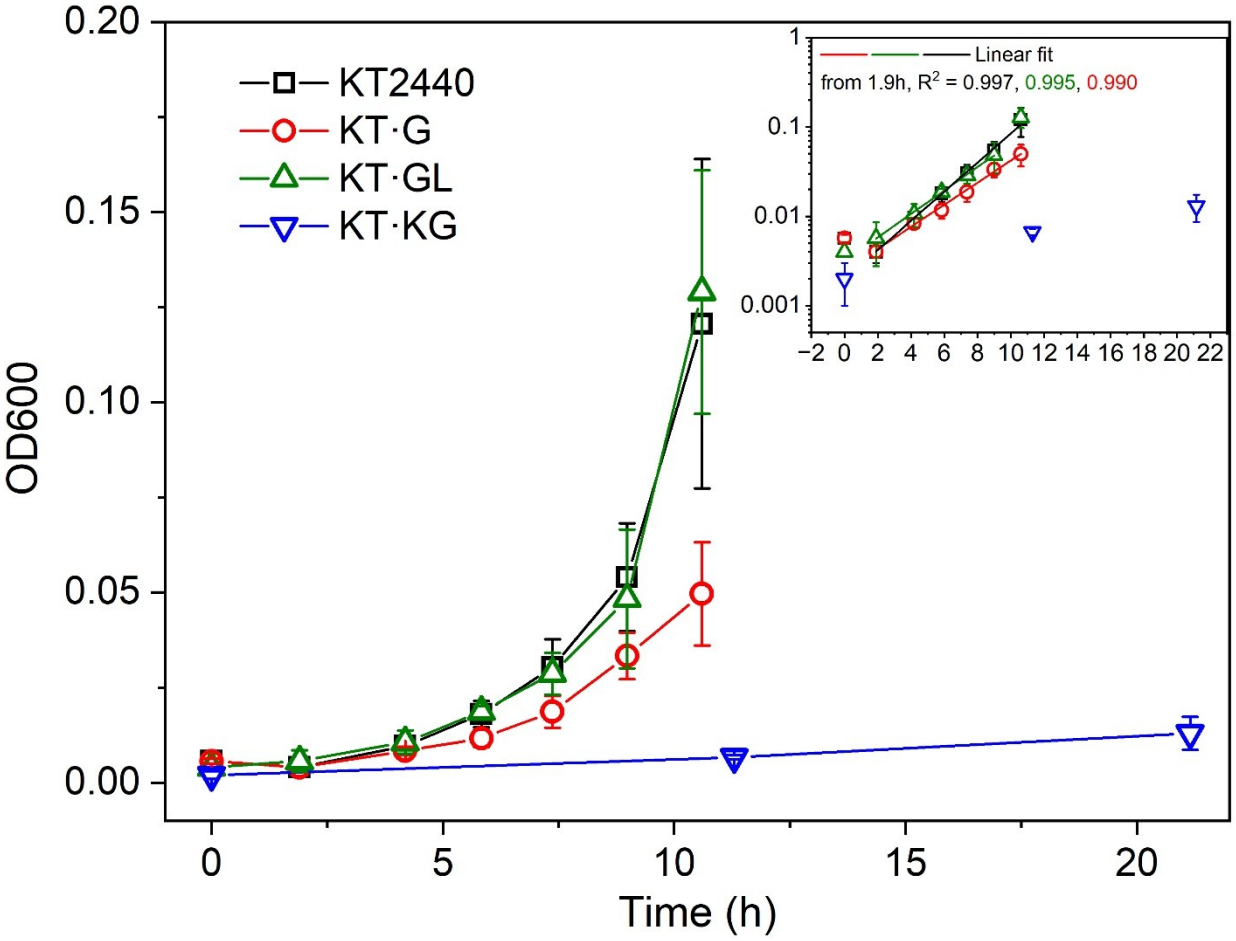


**Figure S1. Growth profiles of the *P. putida* KT2440 WT and the three gene deletion mutants.** All the strains were reactivated from cryo-stocks on LB agar plate and then the colonies were picked up and inoculated into DM9 medium with 5g/L glucose. Each strain was done with 3 biological replicates.

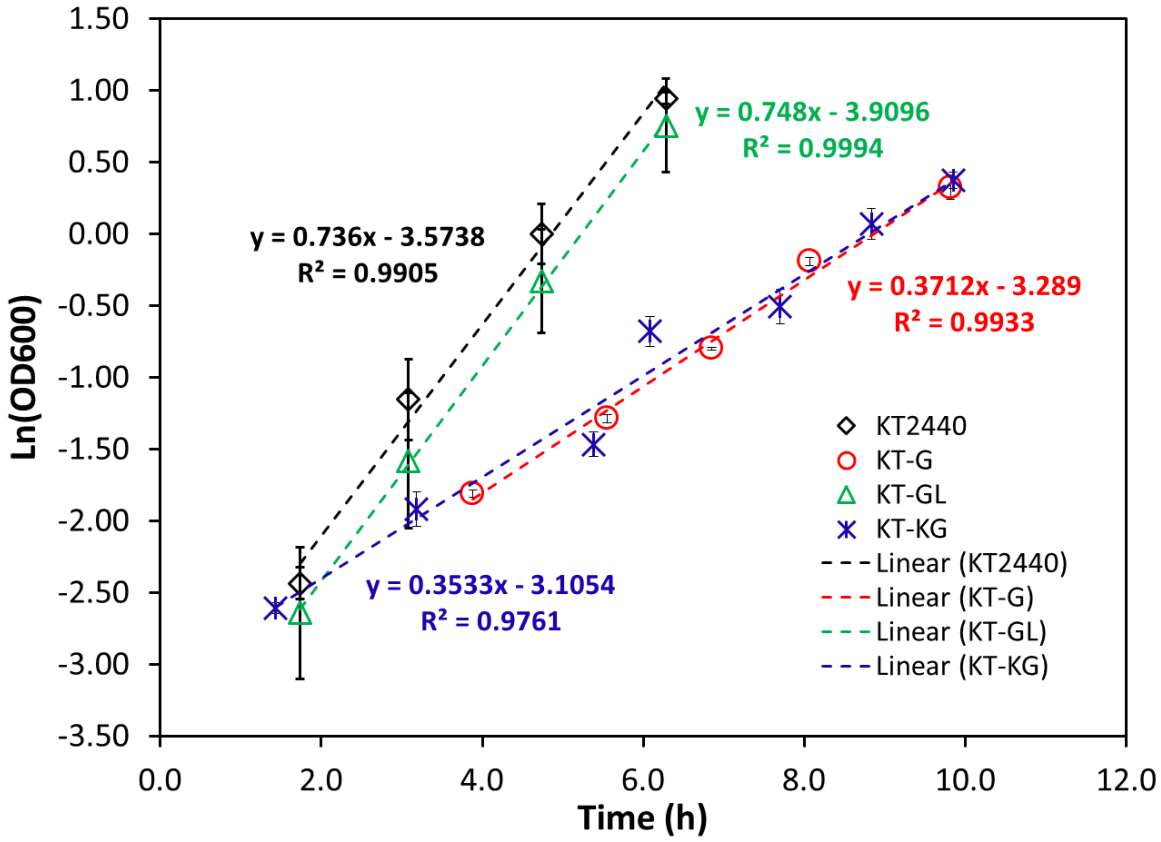


**Figure S2. Semi-logarithmic plot of the growth data in Figure 2A.** The linear range indicates exponential growth, the slope represents the maximal growth rate. The growth test was conducted by using DM9 liquid preculture, rather than the single colony used for Figure S1 above. Three biological replicates were used.

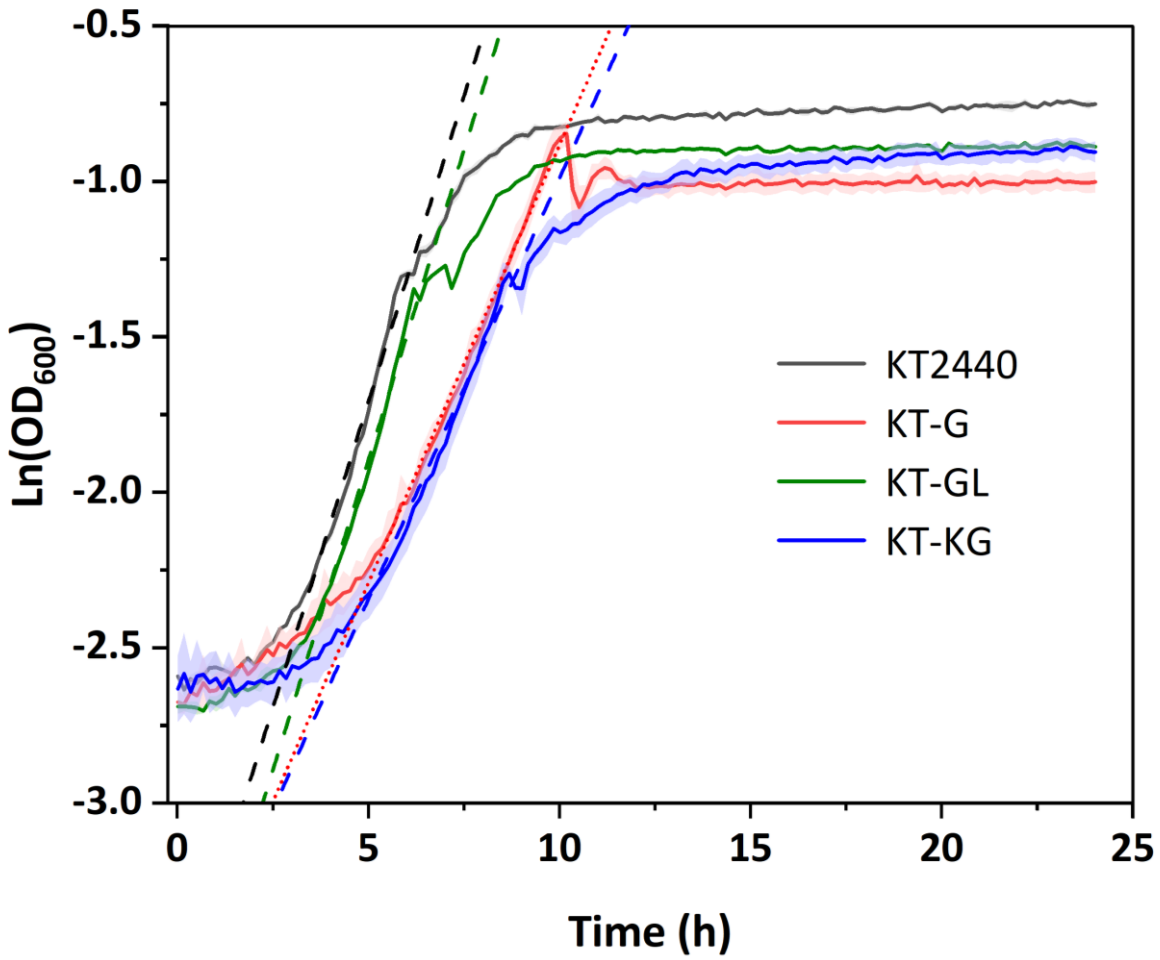


**Figure S3. Growth patterns of the wild-type and gene deletion mutants of *P. putida* KT2440 determined using a high-throughput parallel cultivation system (BioLector, Beckman).** Precultures were prepared as for the growth test for Figure 10 A and Figure S2 (i.e. Single colony on LB plate -> DM9 liquid culture -> BioLector cultivation) . Each well contained 1200 µL DM9 medium with 5 g/L glucose. Each strain was done with 3 biological replicates, and the lines show the average data.

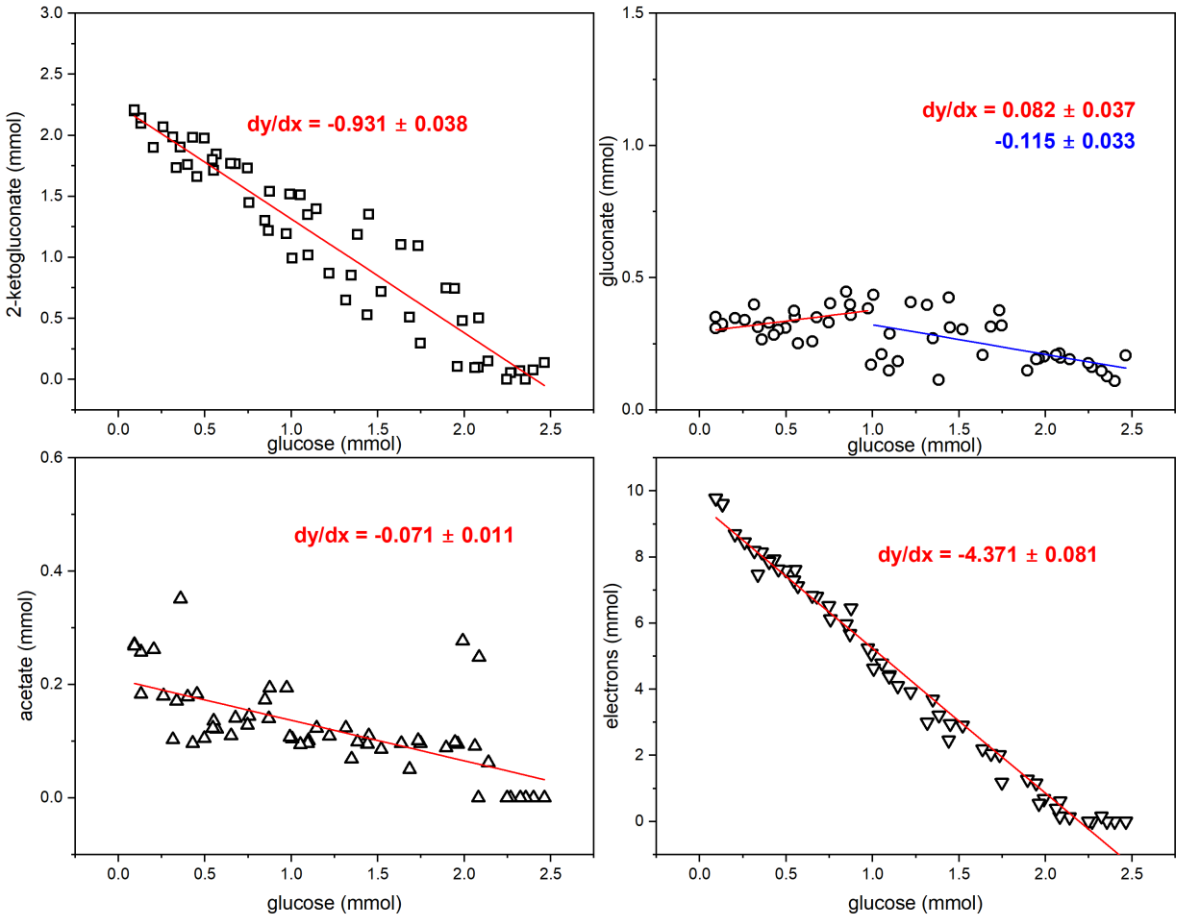


**Figure S4. Regression analysis for the determination of product/glucose yield coefficients for the strain *P. putida* KT2440 WT.** The analysis was done using OriginPro 2022b with 55 data points from 6 biological replicates.

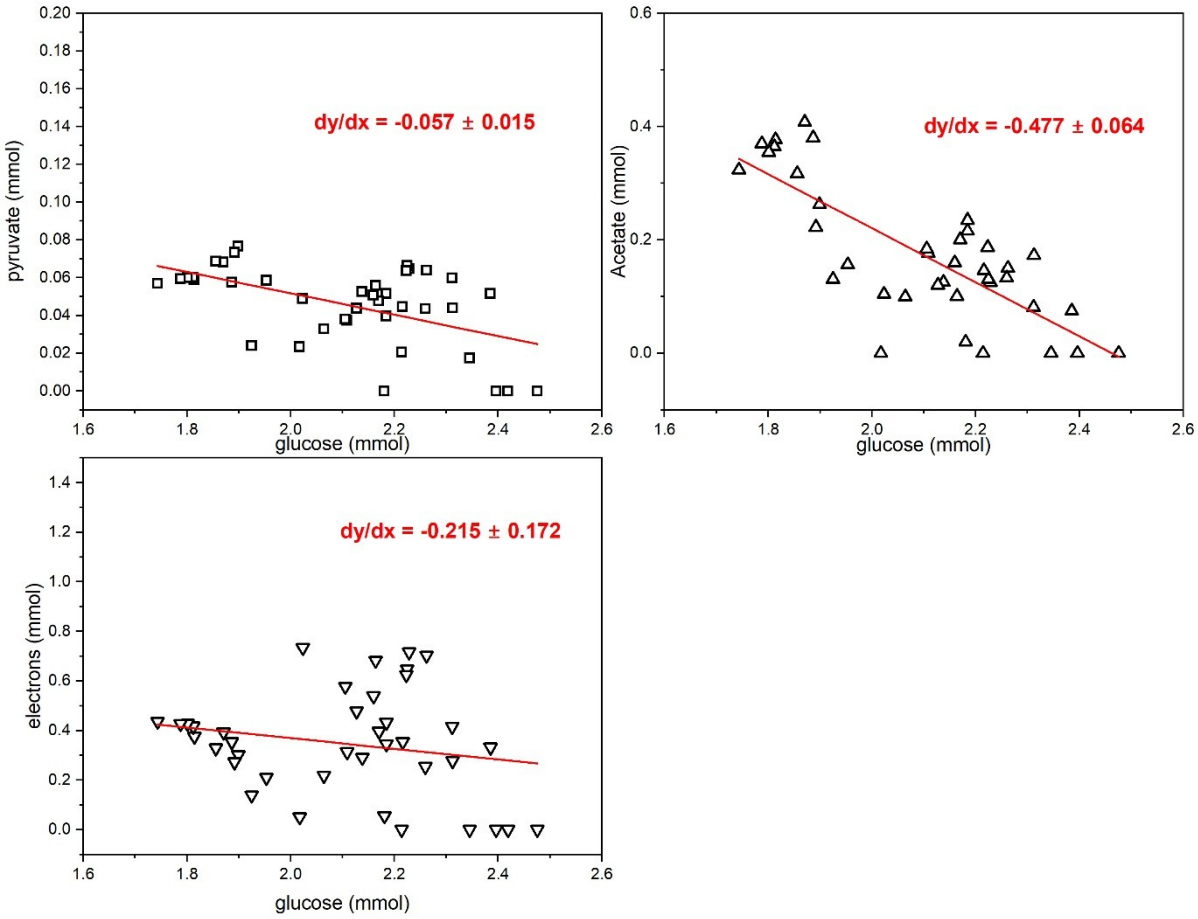


**Figure S5. Regression analysis for the determination of product/glucose yield coefficients for the strain KT-G**. The analysis was done using OriginPro 2022b with 51 data points from 6 biological replicates (except 37 data points from 4 biological replicates).

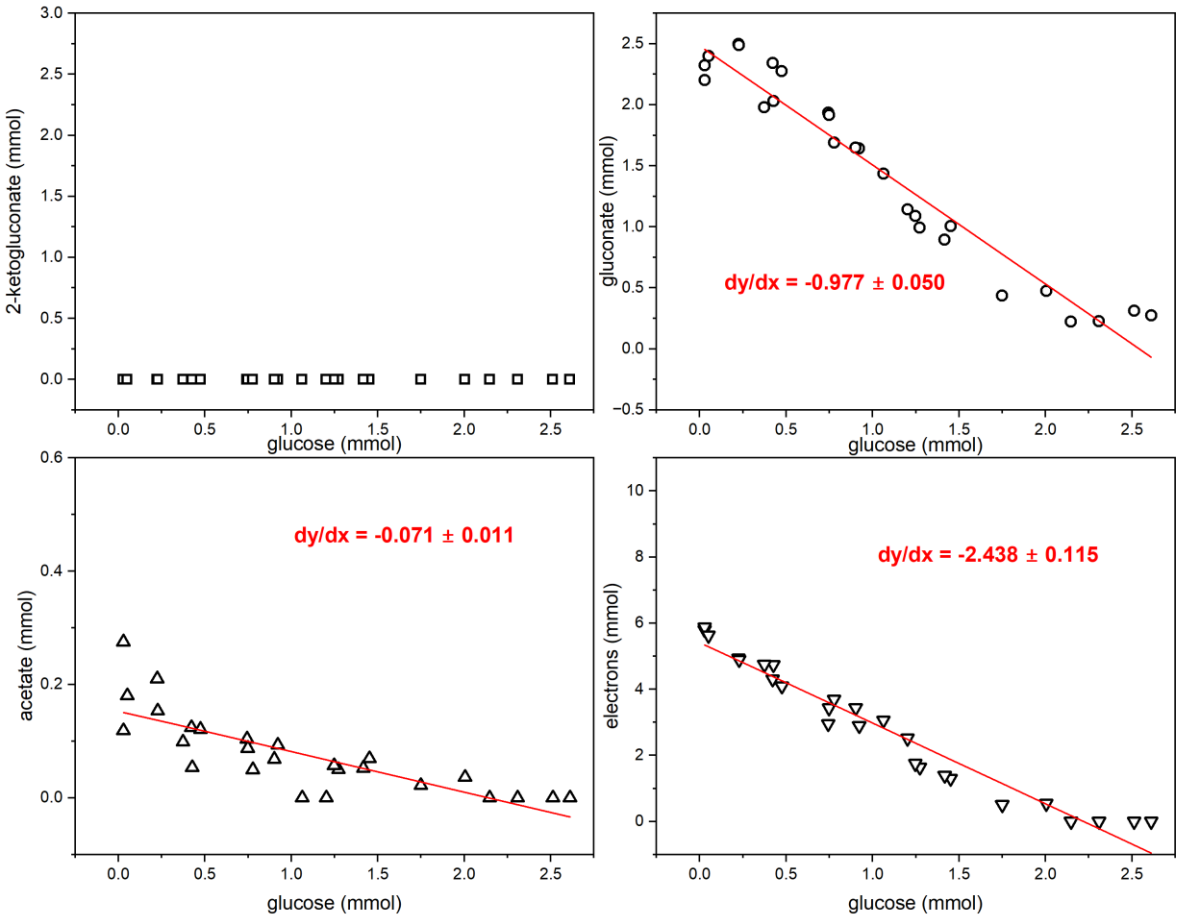


**Figure S6. Regression analysis for the determination of product/glucose yield coefficients for the strain KT-GL.** The analysis was done using OriginPro 2022b with 26 data points from 4 biological replicates.

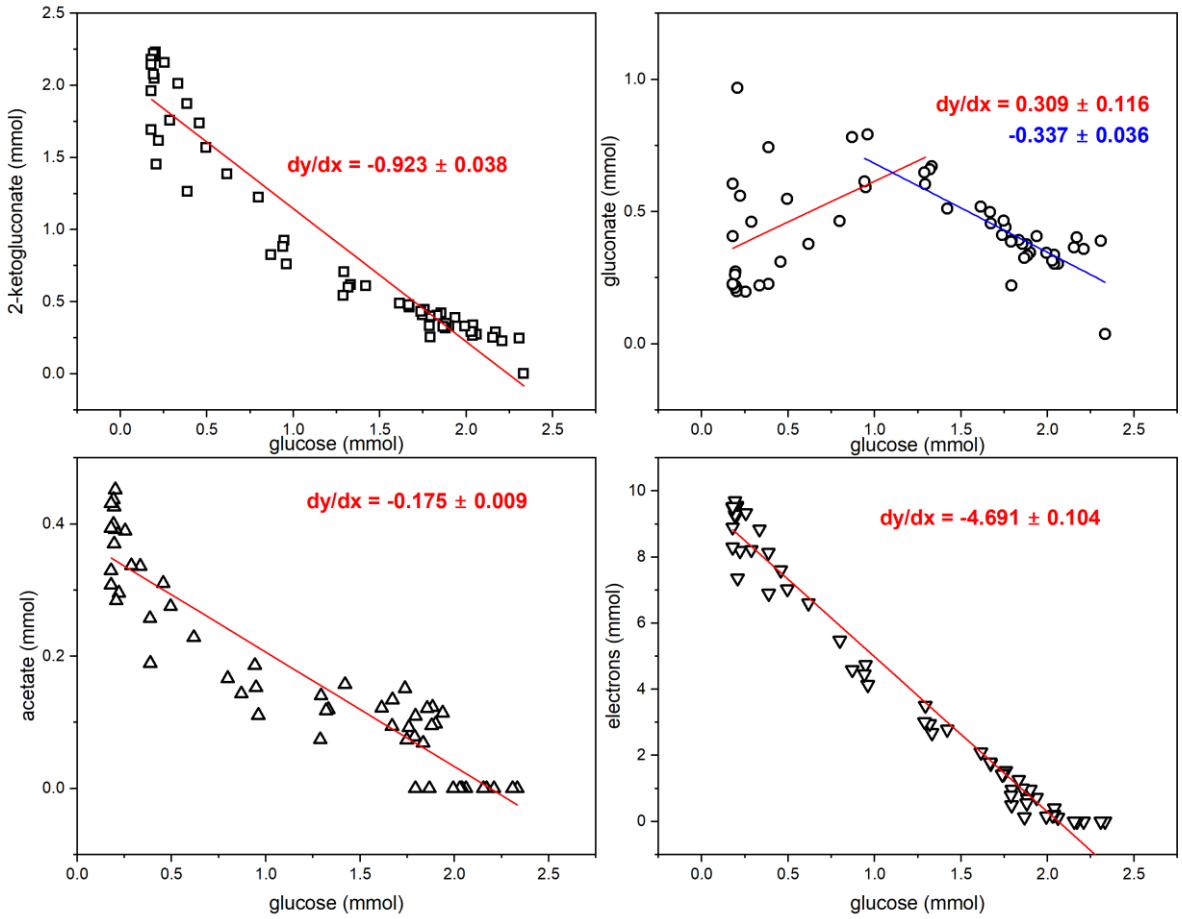


**Figure S7. Regression analysis for the determination of product/glucose yield coefficients for the strain KT-KG**. The analysis was done using OriginPro 2022b with 56 data points from 6 biological replicates.

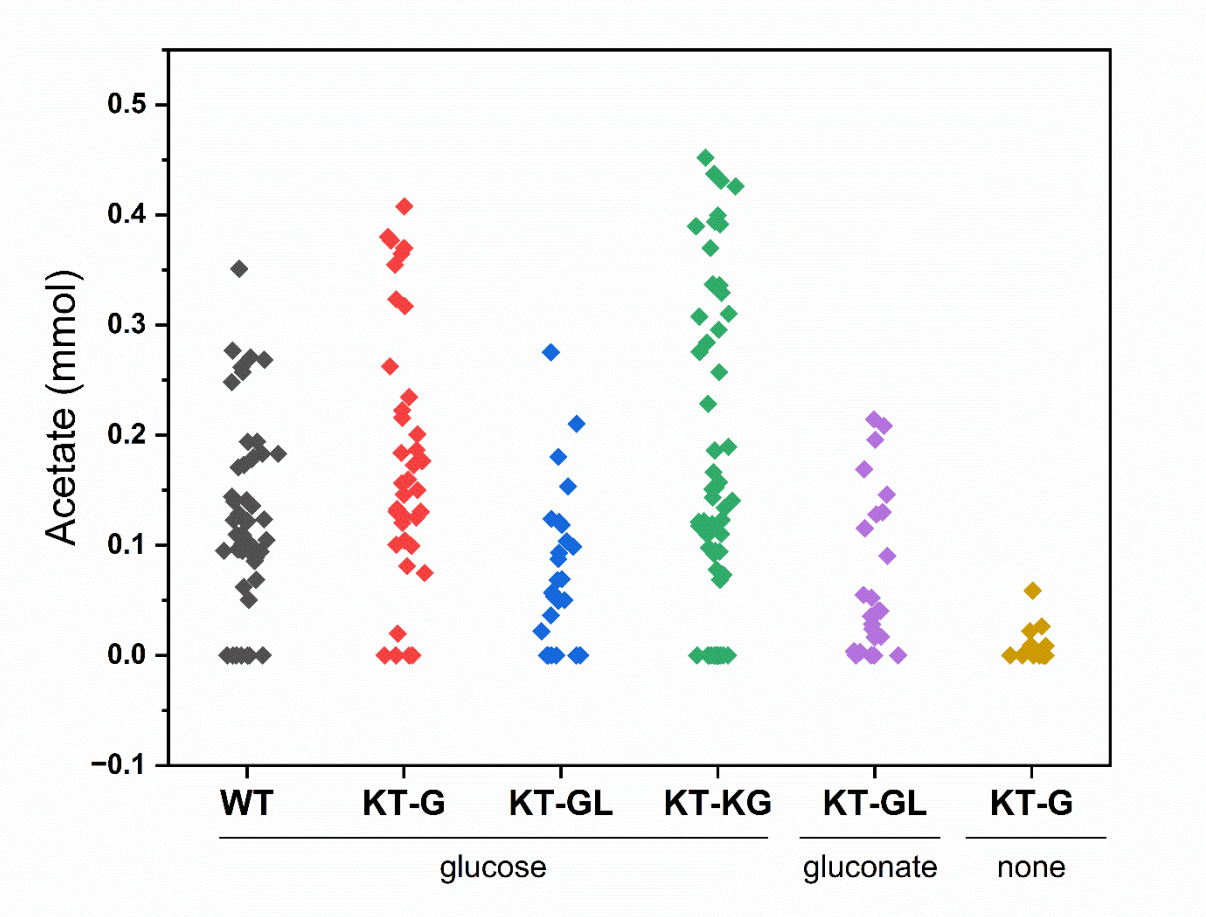


**Figure S8. The secreted acetate concentrations of different strains in BES.** The data points present the acetate concentrations during the fermentation batches from inoculation to the end of the batch. KT-GL (gluconate): BES fermentation of the KT-GL strain with gluconate as the sole carbon source. KT-G (none): KT-G strain without added carbon source. The released acetate represents basal acetate formation from biomass components.

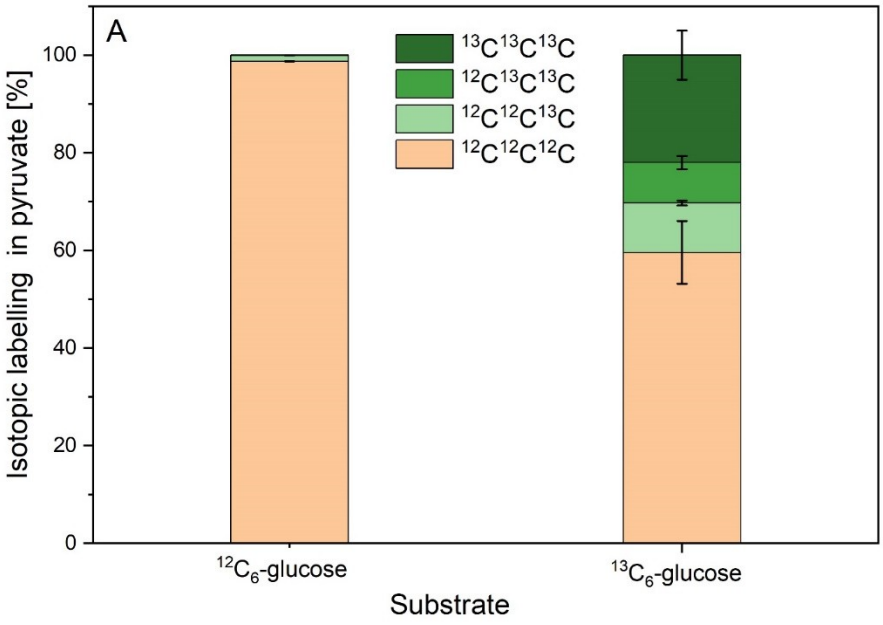


**Figure S9. The isotopic labelling in pyruvate produced by the KT-G strain in BES fed with $^{12}C_6$-glucose or $^{13}C_6$-glucose.** The error bar represents the deviation of 3 biological replicates.

The mass isotopomer distribution of pyruvate was determined using gas chromatography coupled to mass spectrometry (GC-MS). Briefly, 200µL of fermentation supernatant were dried under nitrogen stream. Derivatization was done in a two-step procedure: First, dried samples were dissolved in 50µL methoxyamine hydrochloride in pyridine (20mg/mL), and incubated at 80 °C for 30 min. Afterwards, 50µL MSTFA (Macherey-Nagel, Düren, Germany) were added, and incubated likewise. Mass fragment distribution of pyruvate was determined by GC/MS (Agilent 7890A, Quadrupole Mass Selective Detector 5975C, Agilent Technologies) using the following oven program: 30 °C (0-1 min), 10 °C $min^{-1}$ increase (1-10 min), and 40 °C $min^{-1}$ increase (10-15.125 min). Selected ion monitoring (SIM) targeting m/z 174 was performed to quantify the mass isotopomer fractions *m+0*, *m+1*, *m+2*, *m+3* of a fragment ion containing all carbon atoms of pyruvate. The obtained $^{13}C$ enrichment was corrected for natural abundance of stable isotopes (van Winden*, et al.* 2002), and was expressed as summed fractional labelling (Wittmann; Heinzle 2005).

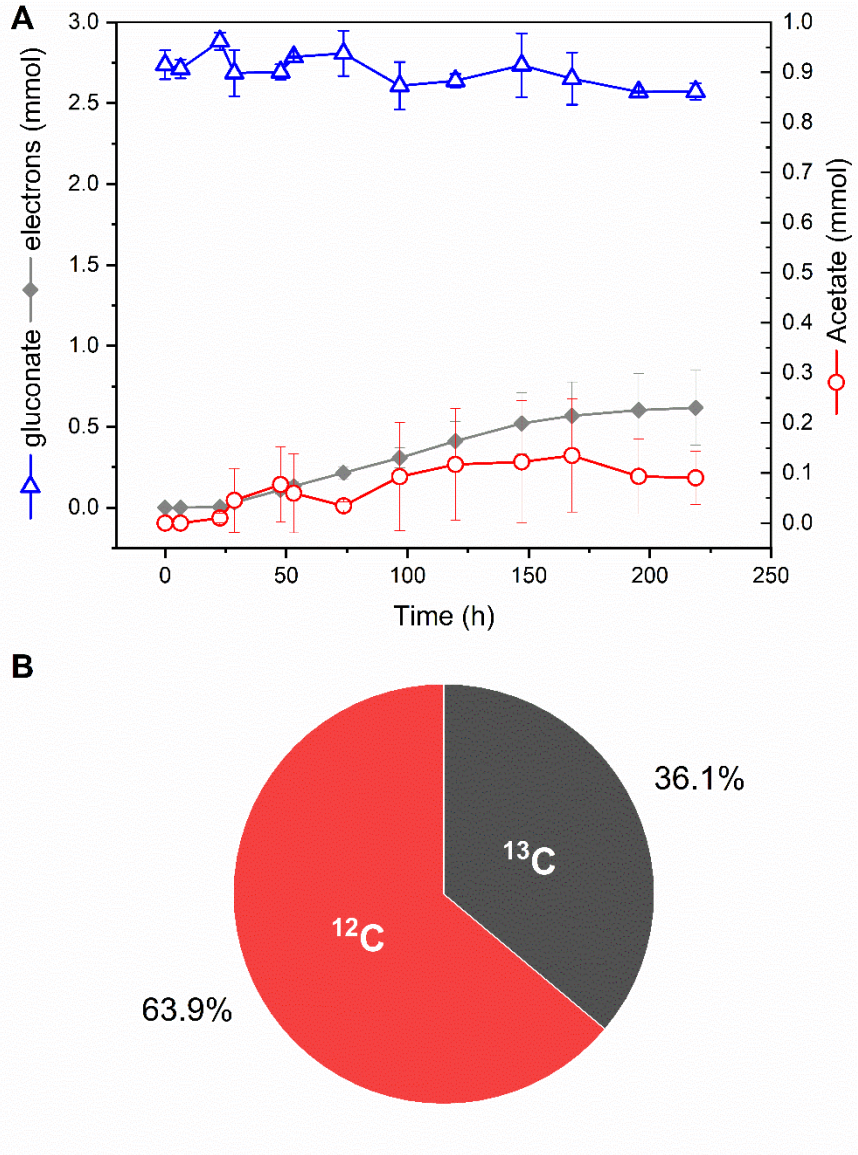


**Figure S10. BES fermentation of KT-GL strain with gluconate as the sole carbon source.** A - fermentation profile. B - the isotopic analysis of secreted acetate in the BES medium. Error bar represents the deviation of biological replicates.

Labeled gluconate was not available for this experiment. Instead, the preculture of KT-GL was prepared in shake-flasks using $^{13}C_6$-glucose as the substrate. After overnight cultivation, the fully labeled biomass was harvested and inoculated into BES reactors with unlabelled gluconate as the sole carbon source. This yields an inverse labeling ratio compared to the situation with unlabeled biomass and $^{13}C$-glucose as substrate. Here, the fraction of $^{12}C$ indicates the carbon originating from the carbon source in the BES reactor, while the $^{13}C$ shows the biomass fraction of acetate.

# Curriculum Vitae

| | |
|---|---|
| *Persönliche Daten* | |
| Name | Laura Pause |
| *Ausbildung* | |
| Seit 06/2021 | Promotion |
| | Helmholtz-Zentrum für Umweltforschung – UFZ, Leipzig |
| | Department: SOMA/ UMB/ MIBITECH |
| | Arbeitsgruppe: System Biotechnology, Prof. Jens O. Krömer |
| 10/2017 – 06/2020 | Studium Biochemie |
| | Universität Leipzig |
| | Abschluss: Master of Science |
| 10/2013 – 09/2017 | Studium Biochemie |
| | Universität Leipzig |
| | Abschluss: Bachelor of Science |
| 08/2004 – 06/2013 | Abitur |
| | Pestalozzi Gymnasium Heidenau/ Berufsschulzentrum für Technik Pirna |